

The role of the proinflammatory cytokines IL-17, IL-6 and IL-1 in (IMQ-induced) psoriasis

Dissertation
Zur Erlangung des Grades
Doktor der Naturwissenschaften

Am Fachbereich Biologie
Der Johannes Gutenberg-Universität Mainz

vorgelegt von
Sabrina Klebow
geb. am 04. Juni 1985
in Mainz, Deutschland

Mainz, 2016

1. Berichterstatter:

2. Berichterstatter:

Tag der mündlichen Prüfung: 21.06.2016

Table of Contents

1	Introduction	1
1.1	Psoriasis	1
1.1.1	<i>The skin: The largest organ in the body and the first defense barrier</i>	1
1.1.2	<i>Differences in the skin of mice and human</i>	2
1.1.3	<i>Clinical and histological appearance of psoriasis</i>	3
1.1.4	<i>Immune defense in psoriasis</i>	6
1.1.5	<i>Animal models of psoriasis</i>	9
1.2	IMQ-induced psoriasis-like skin disease	11
1.2.1	<i>Toll-like receptor signaling induced by IMQ</i>	11
1.2.2	<i>Signaling cascades activated by Aldara™ cream independent of TLR7/8</i>	13
1.2.3	<i>IL-23/IL-17 axis in (IMQ-induced) psoriasis</i>	15
1.3	IL-6 signaling	17
1.4	IL-1 signaling	19
1.5	Monoclonal antibodies as a treatment option for psoriasis	20
1.6	Objectives	22
2	Materials and Methods	24
2.1	Chemicals and biological materials	24
2.2	Molecular Biology	25
2.2.1	<i>Preparation of genomic DNA</i>	25
2.2.2	<i>Polymerase chain reaction (PCR)</i>	26
2.2.3	<i>RNA isolation and Quantitative Real Time PCR</i>	28
2.2.4	<i>Agarose gel electrophoresis</i>	29
2.2.5	<i>Quantification of RNA and DNA</i>	29
2.3	Cell biology	29
2.3.1	<i>Preparation of single cell suspensions from mouse organs</i>	29
2.3.2	<i>Sorting of cells by magnetic beads and FACS</i>	30
2.3.3	<i>Stimulation of MACS purified splenocytes</i>	31
2.3.4	<i>Cell counting</i>	31
2.3.5	<i>Flow Cytometry</i>	31
2.3.6	<i>pSTAT3 staining</i>	33
2.3.7	<i>Histological analysis and immunohistochemistry</i>	33
2.4	Biochemistry	34
2.4.1	<i>Preparation of total protein extracts</i>	34
2.4.2	<i>Western Blot</i>	34
2.5	Immunohistochemistry	35
2.5.1	<i>Enzyme-linked Immunosorbent Assay</i>	35

2.6	Mouse experiments.....	35
2.6.1	<i>Mice</i>	36
2.6.2	<i>Imiquimod treatment.....</i>	36
2.6.3	<i>PASI score</i>	36
2.6.4	<i>Anti-IL-17A treatment</i>	37
2.6.5	<i>Injection of Diphtheria Toxin.....</i>	37
2.7	Statistics and Software.....	37
3	Results.....	39
3.1	Neutralization of IL-17A in <i>K14-IL-17A^{ind/+}</i> mice	39
3.1.1	<i>Reduced clinical scores in anti-IL-17A treated <i>K14-IL-17A^{ind/+}</i> mice.....</i>	39
3.1.2	<i>Anti-IL-17A treatment of <i>K14-IL-17A^{ind/+}</i> mice shows influence on myelomonocytic cells in the spleen.....</i>	40
3.1.3	<i>Repetition of anti-IL-17A treatment in <i>K14IL17A^{ind/+}</i> mice shows no improvement in terms of infiltrating myelomonocytic cells and T cells</i>	44
3.1.4	<i>Repetition of anti-IL-17A treatment in <i>K14IL17A^{ind/+}</i> mice shows no improvement in terms of infiltrating myelomonocytic cells and T cells</i>	46
3.2	Anti-IL-17A treatment of <i>wt</i> mice in IMQ-induced psoriasis-like skin disease	50
3.2.1	<i>Neutralization of IL-17A shows an impact on clinical scores with high dose of 0.6mg/treatment.....</i>	50
3.2.2	<i>Anti-IL-17A treatment with low dose antibody treatment shows a mild effect on infiltrating myelomonocytic cells into the skin.....</i>	52
3.2.3	<i>Neutralization of IL-17A with high dose antibody treatment has an impact on myeloid cell populations of skin and secondary lymphoid organs.....</i>	54
3.3	IMQ-induced psoriasis-like skin disease in <i>IL-6Rα^{Δmyel}</i> mice	56
3.3.1	<i><i>IL-6Rα^{Δmyel}</i> show reduced expression of <i>IL-6Rα</i> in myelomonocytic cells.....</i>	56
3.3.2	<i>Distribution of immune cell populations is similar in <i>IL-6Rα^{Δmyel}</i> and <i>wt</i> mice.....</i>	58
3.3.3	<i>Myelomonocytic deletion of <i>IL-6Rα</i> does not ameliorate IMQ-induced psoriasis-like skin disease.....</i>	63
3.3.4	<i>Distribution of myelomonocytic cells in <i>IL-6Rα^{Δmyel}</i> mice is not influenced by IMQ treatment.....</i>	65
3.3.5	<i>Diminished <i>IL-6</i> signaling <i>IL-6Rα^{Δmyel}</i> mice has no influence on populations of $\gamma\delta$ T cells during IMQ treatment.....</i>	66
3.3.6	<i>Analysis of <i>STAT3</i> activation in <i>IL-6Rα^{Δmyel}</i> mice compared to <i>wt</i> mice.....</i>	70
3.4	<i>IL-1</i> signaling in IMQ-induced psoriasis-like skin disease	71
3.4.1	<i><i>Il1r2^{-/-}</i> mice reveal an impact on myelomonocytic cells in steady state conditions.....</i>	71
3.4.2	<i><i>Il1r2^{-/-}</i> mice show higher susceptibility to IMQ-induced psoriasis</i>	74
3.4.3	<i>Neutrophil specific deletion of <i>Il1r2</i> has no influence on myelomonocytic cells.....</i>	78

3.4.4	<i>IMQ-induced psoriasis in Il1r2^{ΔN} mice has no effect on cells of the myelomonocytic compartment.....</i>	81
3.4.5	<i>T cell specific deletion of Il1r2 shows no effect on clinical scores in IMQ-induced psoriasis.....</i>	83
3.5	Depletion of neutrophils via the iDTR system	84
4	Discussion	88
4.1	Neutralizing antibodies as a treatment option for psoriasis.....	88
4.2	Signaling of IL-6 and its role in (IMQ-induced) psoriasis.....	91
4.3	IL-17 producing cells in (IMQ-induced) psoriasis	94
4.4	IL-1 and its family members in (IMQ-induced) psoriasis	97
9	Summary	102
10	Zusammenfassung	104
11	References	106
12	Acknowledgements	128
13	Versicherung.....	129
14	Lebenslauf.....	130
15	Publications	131

List of Figures

Figure 1: Cells and structure of the skin in mice and human	3
Figure 2: Characteristics of psoriasis vulgaris	6
Figure 3: The loop of innate and adaptive immunity in psoriasis.....	8
Figure 4: Structural formula of Imiquimod	12
Figure 5: <i>Aldara</i> TM cream and its mode of action.....	14
Figure 6: The two forms of IL-6 signaling.....	19
Figure 7: Neutralization of IL-17A in <i>K14-IL-17A^{ind/+}</i> mice leads to milder clinical scores.....	40
Figure 8: <i>K14-IL-17A^{ind/+}</i> mice treated with anti-IL-17A show no effect on infiltrating myelomonocytic cells	42
Figure 9: Treatment with anti-IL-17A shows no effect on T cell populations in <i>K14-IL-17A^{ind/+}</i> mice.....	44
Figure 10: 2 nd experiment shows no effect on clinical scores after neutralization of IL-17A in <i>K14-IL-17A^{ind/+}</i> mice	45
Figure 11: anti-IL-17A treatment of <i>K14-IL-17A^{ind/+}</i> mice shows no effect on infiltrating myelomonocytic cells in 2 nd experiment.....	48
Figure 12: anti-IL-17A treatment of <i>K14-IL-17A^{ind/+}</i> mice shows no effect on T cell populations in 2 nd experiment	49
Figure 13: Neutralization of IL-17A with high dose of antibody shows decreased clinical scores in IMQ-induced psoriasis of <i>wt</i> mice	52
Figure 14: Neutralization of IL-17A with low dose of antibody shows mild effect on infiltrating myelomonocytic cells in the skin of <i>wt</i> mice.....	53
Figure 15: Neutralization of IL-17A with high dose of antibody shows strong effect on infiltrating myelomonocytic cells in the skin and mild effect on secondary lymphoid organs of <i>wt</i> mice.....	55
Figure 16: Myelomonocytic cell-specific inactivation of <i>Il6ra</i> gene in mice (<i>Il6ra^{Δmyel}</i>).....	57
Figure 17: IL-6Ra deletion in myelomonocytic cells has no effect on splenic T cell populations in <i>Il6ra^{Δmyel}</i> mice	58
Figure 18: IL-6Ra deletion in myelomonocytic cells has no effect on splenic B cell subpopulations in <i>Il6ra^{Δmyel}</i> mice	59
Figure 19: <i>Il6ra^{Δmyel}</i> mice show no differences in myelomonocytic cell compartments compared to <i>wt</i>	61
Figure 20: IL-6 α deletion in myelomonocytic cells has no effect on $\gamma\delta$ T cell subpopulations in <i>Il6ra^{Δmyel}</i> mice.....	62
Figure 21: <i>Il6ra^{Δmyel}</i> mice show no effect in clinical scores and histology in IMQ-induced psoriasis compared to <i>wt</i> mice	64
Figure 22: IMQ treatment leads to same differentiation of myelomonocytic cells in <i>Il6ra^{Δmyel}</i> and <i>wt</i> mice	66
Figure 23: $\gamma\delta$ TCR sub-populations in the spleen of <i>Il6ra^{Δmyel}</i> mice and <i>wt</i> are comparable in the model of IMQ-induced psoriasis	67
Figure 24: $\gamma\delta$ TCR sub-populations of ears in <i>Il6ra^{Δmyel}</i> mice are not affected during the treatment with IMQ.....	69
Figure 25: Analysis of STAT3 activation in myelomonocytic cells of <i>Il6ra^{Δmyel}</i> mice	71
Figure 26: Generation of <i>Il1r2^{-/-}</i> mice and distribution of myelomonocytic cells in naïve mice.....	74

Figure 27: <i>Il1r2</i> ^{-/-} mice show higher clinical scores compared to <i>wt</i> mice in IMQ-induced psoriasis	75
Figure 28: Deletion of <i>Il1r2</i> leads to an increase of infiltrating myelomonocytic cells in IMQ-induced psoriasis.....	76
Figure 29: $\gamma\delta$ T cells of <i>Il1r2</i> ^{-/-} mice are not altered in IMQ-induced psoriasis	77
Figure 30: Deletion of <i>IL1r2</i> leads to an increase of pro-inflammatory cytokines in IMQ-induced psoriasis.....	78
Figure 31: Generation of <i>Il1r2</i> ^{ΔN} mice and impact of neutrophil specific deletion of <i>IL1r2</i> on myelomonocytic cells under basal conditions	80
Figure 32: <i>Il1r2</i> ^{ΔN} mice show no effect in clinical scores in IMQ-induced psoriasis	81
Figure 33: Myelomonocytic cells of <i>Il1r2</i> ^{ΔN} mice are not altered in IMQ-induced psoriasis	82
Figure 34: <i>Il1r2</i> ^{ΔN} and <i>Il1r2</i> ^{ΔT} mice show no effect in clinical scores in IMQ-induced psoriasis	84
Figure 35: Depletion of Ly6G ⁺ via the iDTR system and experiment setup	85
Figure 36: <i>Ly6G</i> ^{iDTR} mice show a reduction in Ly6G ⁺ cells after DT injection	87

List of Tables

Table 1: List of Chemicals.....	25
Table 2: List of primers used for genotyping.....	27
Table 3: List of PCR programs.....	28
Table 4: List of qRT-Primers.....	29
Table 5: List of antibodies used for flow cytometry.....	33

1 Introduction

1.1 Psoriasis

1.1.1 *The skin: The largest organ in the body and the first defense barrier*

The average human skin comprises a total area of about 1.8 m² and is thereby the largest organ, interacting between body and environment (Di Meglio et al., 2011; Nestle et al., 2009a). It functions as physical and biochemical barrier, but also regulates hydration. Further, the skin is also able to synthesize vitamins and hormones, and serves as an immune protective organ with the ability to defend deeper body tissues (Di Meglio et al., 2011). The immunological barrier of the skin (skin-associated lymphoid tissue (SALT)) contains cellular and humoral components of the immune system (Perera et al., 2012). To act as a physical and biochemical barrier with the ability to maintain tissue homeostasis, a perfect interplay of different factors is required. Terminally differentiated keratinocytes (KCs) (corneocytes) interplay with the acidic and hydrolipidic properties of the skin (Di Meglio et al., 2011; Pasparakis et al., 2014). This comprises a combination of sweat, sebum, lipids and antimicrobial peptides (AMPs), which are present on the skin surface (Di Meglio et al., 2011). Dysregulation of tissue homeostasis can lead to inflammatory skin diseases, like psoriasis (Pasparakis et al., 2014).

The skin consists of different layers: epidermis, dermis and the subcutaneous fatty region (Heath and Carbone, 2013), whereby the epidermis is the outermost compartment. Epidermis and dermis contain many different cell types, which support the initial process of immunological defense against infection and invading pathogens (Heath and Carbone, 2013; Pasparakis et al., 2014). The epidermis is further subdivided into four layers (Fig. 1): stratum basale (basal layer), stratum spinosum (spinous cell layer), stratum granulosum and stratum corneum (Nestle et al., 2009a). In the stratum basale epidermal cells are constantly renewed. It consists of one layer undifferentiated KCs, which after differentiation move to the stratum spinosum (Nestle et al., 2009a). Here the KCs start their maturation process and synthesize keratin (Nestle et al., 2009a). In the stratum granulosum tight junctions are located (Heath and Carbone, 2013)

and the KCs are visible as dark clumps of cytoplasmic material; they produce high amounts of keratin protein and lipids (Nestle et al., 2009a). The tight junctions of the stratum granulosum in combination with the stratum corneum build the physical barrier to the environment and its pathogens (Heath and Carbone, 2013; Nestle et al., 2009a). Moreover, in the stratum corneum, corneocytes are the predominant population, which are dead enucleated KCs (Di Meglio et al., 2011; Nestle et al., 2009a).

On the other hand, only few cell types comprise the epidermis. Besides KCs, also melanocytes are resident in the epidermis with the ability to produce melanin (Nestle et al., 2009a) and protect from UV light (Heath and Carbone, 2013). Also Langerhans cells (LCs) and CD8⁺ T cells can be found here (Fig. 1), predominantly in the strata basale and spinosum (Di Meglio et al., 2011; Nestle et al., 2009a). Finally, nerve-ending cells (Merkel cells) populate the epidermis (Di Meglio et al., 2011). The dermis has greater cell diversity than the epidermis (Fig. 1) (Nestle et al., 2009a). Here also dendritic cells (DCs), CD4⁺ T cells, $\gamma\delta$ T cells, natural killer T cells (NKT cells), macrophages, mast cells, innate lymphoid cells (ILCs) and fibroblasts are present (Di Meglio et al., 2011; Nestle et al., 2009a). The fibroblasts mainly produce elastin and collagen fibres, as well as extracellular matrix (Di Meglio et al., 2011; Heath and Carbone, 2013). Moreover, the dermis contains blood- and lymphatic vessels, allowing the cells to traffic (Heath and Carbone, 2013; Nestle et al., 2009a). The adipose tissue is also crossed by blood vessels (Pasparakis et al., 2014).

1.1.2 Differences in the skin of mice and human

Although the strata of mouse and human skin are quite similar, these two species present some differences in the anatomy and cellular components. The human skin has a thicker dermis with only rarely spread hair follicles (Pasparakis et al., 2014) (Lowes et al., 2007) following an asynchronous hair cycle (Khavari, 2006), whereas in mice the hair follicles are very dense (Khavari, 2006). Here they undergo a synchronous hair cycle (Khavari, 2006). Moreover, the interfollicular regions in humans take up large areas, in contrast to mice, where these regions are small (Khavari, 2006).

Also the epidermis of the human skin (>100 μm) consisting of 6-10 cell layers is thicker than the murine epidermis (<25 μm) with only 3 layers (Khavari, 2006) (Lowes et al., 2007) (Fig. 1). Further, the mouse skin has a faster epidermal turnover (Berking et al., 2002). As a consequence of that, mouse skin can regenerate without scar formation (Khavari, 2006).

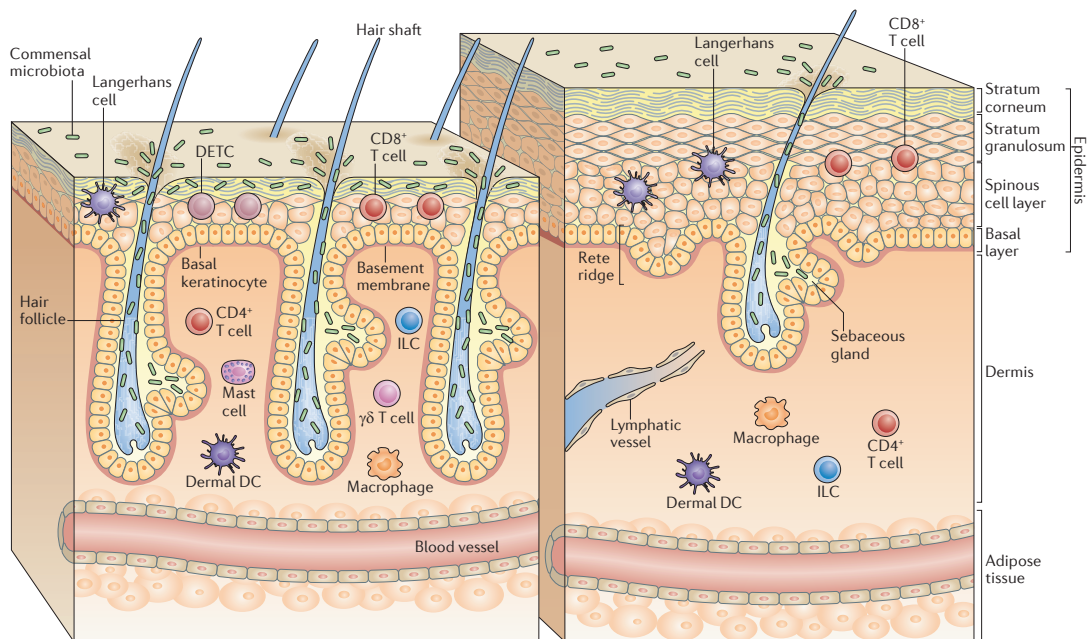


Figure 1: Cells and structure of the skin in mice and human

The skin of mice and humans displays some major differences. Human skin (right panel) has a thicker epidermis (consisting of more layers) and dermis than mouse skin (left panel). Hair follicles are dense in the skin of mice, whereas in humans only few hair follicles exist. The epidermis of mice consists of KCs, LCs, CD8⁺ T cells and V γ 5⁺ dendritic epidermal T cells (DETCs), which are completely absent in human skin. Macrophages, mast cells, CD4⁺ T cells, NKT cells, fibroblasts and ILCs populate the dermis of mice and human. In contrast to human dermis, the dermis of mice contains recruited $\gamma\delta$ T cells with the ability to produce IL-17. The figure is adapted from Pasparakis et al., 2014.

The cellular components differ insofar, as humans completely lack DETCs (Fig. 1) (Nestle et al., 2009a; Pasparakis et al., 2014). Moreover, melanocytes of the human skin are situated between follicles of the epidermis, whereas in mice the melanocytes are follicular (Khavari, 2006).

1.1.3 Clinical and histological appearance of psoriasis

Psoriasis is a chronic autoimmune skin disease affecting 2-4% of the worldwide population (Danilenko, 2008; Lowes et al., 2014). It develops over time, mostly in

late adolescence or early adulthood (Lowes et al., 2007). Triggers of the disease are genetic and environmental factors (Di Cesare et al., 2009) as well as immunological events (Perera et al., 2012). Environmental triggers can be streptococcal infection, physical trauma, certain medications (e.g. anticytokine therapies), as well as alcohol and smoking (Perera et al., 2012). Related to genetic elements, several loci with connection to this disease have been identified. A well-known locus is psoriasis susceptibility 1 (*PSORS1*), but also other members of this family (*PSORS2-10*) are linked to this disease (Nestle et al., 2009b; Perera et al., 2012). Moreover, the human leukocyte antigen (HLA)-Cw6 allele in the *PSORS1* locus was found to be strongly associated with psoriasis (Nestle et al., 2009b), as 60% of all psoriasis patients carry this allele (Perera et al., 2012). This is supported by the fact that patients, who are homozygous for the HLA-Cw6 allele, have a 2.5 fold increased chance to develop psoriasis compared to patients carrying this allele heterozygously (Gudjonsson et al., 2003). Further, SNPs in genes of the IL-23/IL-17 pathway (Nestle et al., 2009b), nuclear factor kappa-light-chain-enhancer of activated B cells (NF- κ B) or epidermal differentiation complex (EDC) were observed to be psoriasis-associated, indicating an important role in the pathogenesis of this disease (Perera et al., 2012).

The common form of psoriasis is psoriasis vulgaris, affecting 90% of the patients (Raychaudhuri et al., 2014) manifested by red, scaly plaques in certain areas (knees, elbows and the scalp) (Fig. 2A). Another form of psoriasis is guttate psoriasis, which can occur after the remission of a streptococcal infection (see above). Patients, who had suffered from a streptococcal infection, also have a higher risk to develop chronic plaque psoriasis (Raychaudhuri et al., 2014). In line with this, both forms of psoriasis are associated with the *PSORS1* gene locus (see above) (Raychaudhuri et al., 2014). Psoriasis is also manifested histologically. This includes retention of nuclei in cells of the stratum corneum (parakeratosis), thickening of the epidermis, including a KC turnover (acanthosis), and loss of the granular layer (hypogranulosis) (Fig. 2B) (Lowes et al., 2014; Perera et al., 2012; Raychaudhuri et al., 2014). During the process of acanthosis KCs move through the epidermis for 4-5 days, ten times faster than in healthy skin (Lowes et al., 2014). Further, the skin of psoriatic patients displays

exaggerated vascularity (new vessel formation) (Perera et al., 2012), which results in erythema (Lowes et al., 2014). The scaling of the skin processes through corneocytes, which lose their ability to stack normally and which have lost their ability to secrete lipids (Lowes et al., 2007). By this the skin loses its ability to function as a protective barrier (Lowes et al., 2007). Besides, immune cells infiltrate into the skin, such as DCs and CD4⁺ T helper cells into the dermis and CD8⁺ T cells in the epidermis (Danilenko, 2008; Perera et al., 2012). Neutrophils gather in the epidermis and the stratum corneum, which are known as Kogoj pustules or Munro's microabscesses, respectively (Lowes et al., 2014). To score the clinical severity, the Psoriasis Area/Activity and Severity Index (PASI) is used. Here erythema, induration (thickness) and desquamation (scale) are scored, with the maximal number of 72 (Lowes et al., 2014). Patients, who participate in clinical trials, need a score of at least 12 (Lowes et al., 2014). In most of the cases only 1% of the whole body skin is involved, but in one third of the patients 10% or more of the skin is covered with scaly plaques (Lowes et al., 2014). Psoriasis often occurs with different comorbidities. 30% of psoriasis patients develop arthritis (Lowes et al., 2007; Raychaudhuri et al., 2014) and they also have a higher risk for cardiovascular disease, diabetes or metabolic syndrome (Karbach et al., 2014; Lowes et al., 2014). Moreover, patients suffering from a severe psoriasis have a decreased expectation of life (Gelfand et al., 2007).

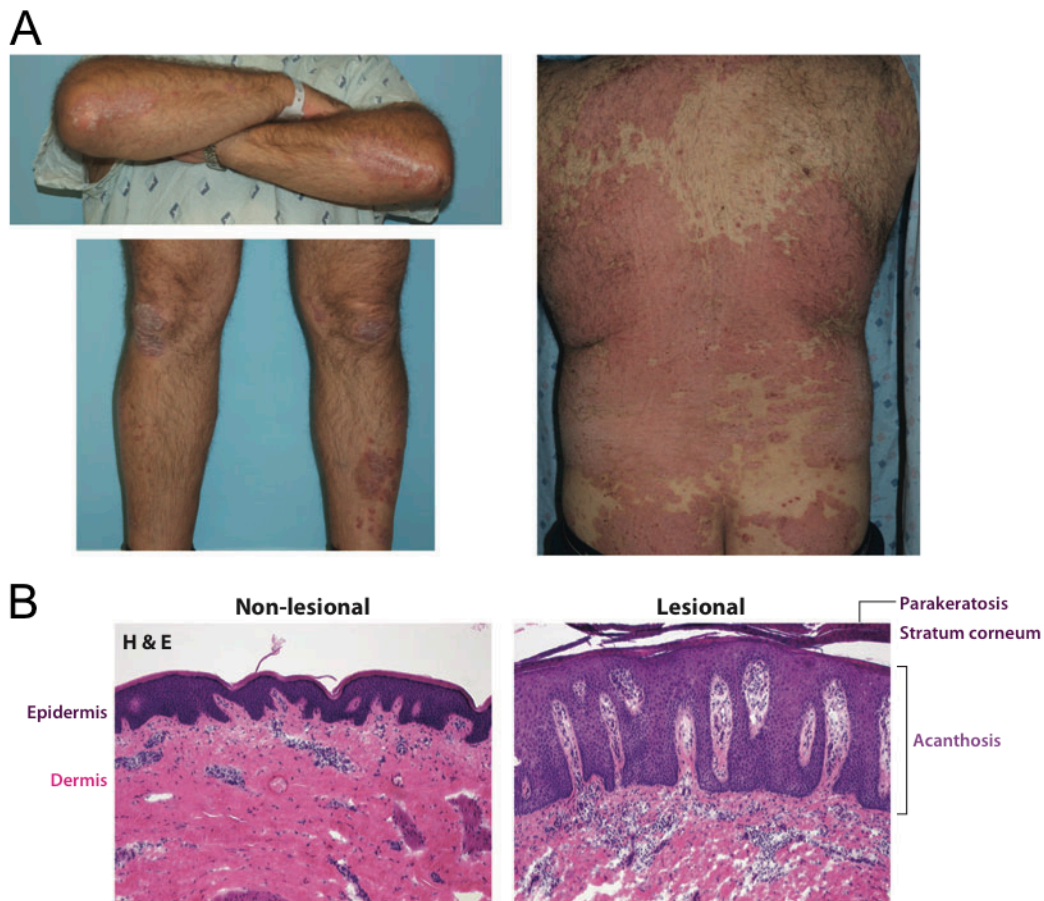


Figure 2: Characteristics of psoriasis vulgaris

(A) Psoriatic patient(s) with red and scaly plaques at knees, elbows and the back. **(B)** Hematoxylin and Eosin staining (H&E) of a non-lesional and lesional skin biopsy. The epidermis (dark layer) shows KC nuclei and the dermis is depicted in pink. Lesional psoriatic skin shows thickened epidermis (acanthosis), which spreads into the dermis. Retention of nuclei (parakeratosis) is seen as thickened stratum corneum. The dermis of the lesional biopsy displays an increase of infiltrating immune cells. The figure is adapted and modified from Lowes et al., 2014.

1.1.4 Immune defense in psoriasis

The surface of the skin is inhabited by 10^2 - 10^7 microorganism/cm² nevertheless they rarely cause infections, demonstrating the very efficient protection mechanism of this organ. (Schauber and Gallo, 2008; Schroder and Harder, 2006). This is due to the constitutive production of AMPs, which represent the chemical barrier of the skin (Schroder and Harder, 2006). These cationic peptides (Gallo and Nakatsuji, 2011) protect the skin with their antimicrobial activity and participate in the initiation of a host defense (Schauber and Gallo, 2008). Moreover, AMPs are responsible for a healthy composition of microbial communities in the skin (Gallo and Nakatsuji, 2011) (Trivedi, 2012). Many

different cell types have the ability to produce AMPs, just as KCs, sebocytes, eccrine glands, mast cells and neutrophils (Gallo and Nakatsuji, 2011) (Schauber and Gallo, 2008). There are some AMPs known to be overexpressed in psoriatic skin, like β -defensins, members of the S100 protein family (S100A7-9) or cathelicidin LL-37 (Buchau and Gallo, 2007). However, S100A8 and S100A9 have chemotactic activity and play a role in KC maturation and proliferation (Buchau and Gallo, 2007). LL-37 is also able to induce proliferation and migration of KCs and by this also activates signal transducer and activator of transcription 1 and 3 (STAT1 and STAT3) (Schauber and Gallo, 2007). Further, it induces the expression of proinflammatory cytokines in KCs (Schauber and Gallo, 2008).

Dying cells release RNA and DNA, which can build complexes with LL-37 (Ganguly et al., 2009). The complex of LL-37 with self-DNA activates plasmacytoid dendritic cells (pDCs) and subsequently toll-like receptor 9 (TLR9) signaling (Nestle et al., 2009b; Schauber and Gallo, 2008). pDCs are present in high numbers already in an early stage of disease (Nestle et al., 2009b). By their activation by self-DNA/LL-37 complexes, production of type I interferons IFN α and IFN β is initiated (Lowes et al., 2014), whereas Interferon α (IFN α) is the initial driver of psoriasis (Nestle et al., 2009b). Further, complexes consisting of self-RNA and LL-37 lead to TLR7/8 activation in DCs (Ganguly et al., 2009) and monocytes (Chamilos et al., 2012). Probably, initiated signaling by host DNA and is the key for breaking immunologic tolerance in psoriasis (Nestle et al., 2009b). This is supported by the fact that extracellular DNA can be found in psoriatic skin in form of neutrophil extracellular traps (NETs) (Lowes et al., 2014). The formation of NETs is a kind of specific cell death where chromatin structures are released in the extracellular space (Grayson and Kaplan, 2016). However, LL-37 was also identified as an autoantigen for circulating T cells in psoriasis patients (Lande et al., 2014). This was the first study showing that AMPs have a role in innate and adaptive immune response of psoriasis (Lande et al., 2014).

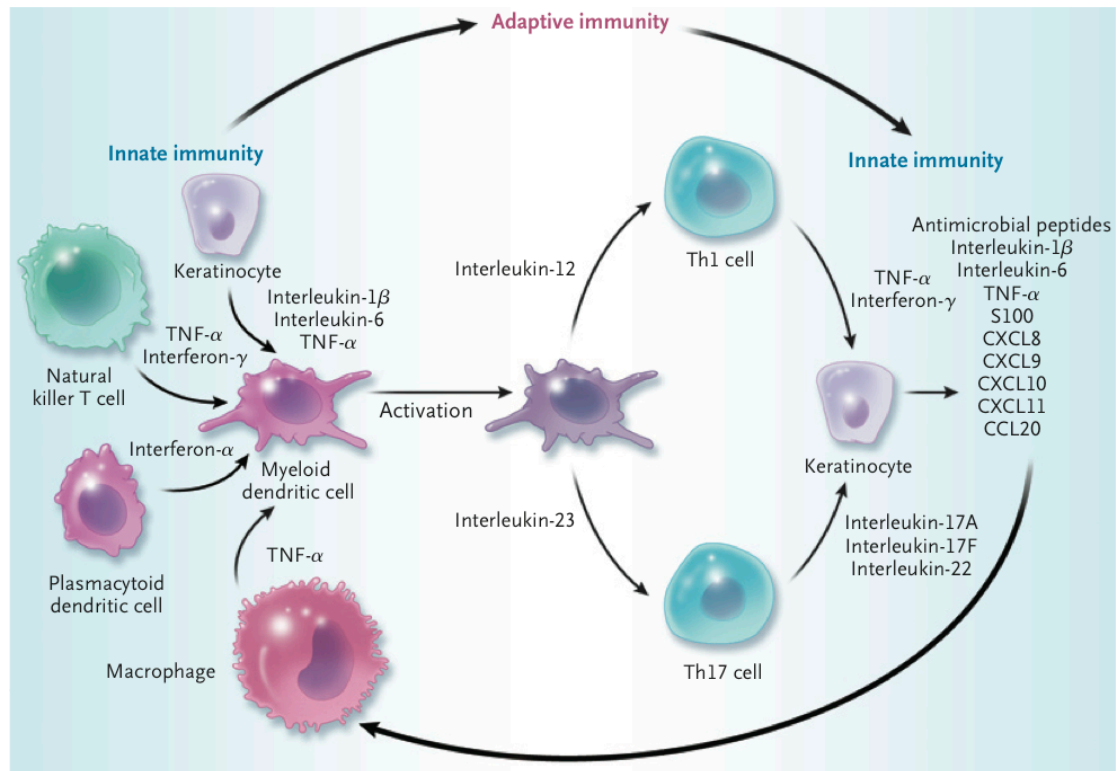


Figure 3: The loop of innate and adaptive immunity in psoriasis

Innate immune cells, like keratinocytes, NKT cells, pDCs and macrophages produce cytokines to activate myeloid DCs. As a consequence they migrate into the draining lymph nodes (LNs) for antigen presentation to T cells. Differentiated T cells (Th1 or Th17 cells) act on KCs by releasing different cytokines (IL-17 and IL-22). Subsequent production of chemokines, proinflammatory cytokines and antimicrobial peptides initiates the feed back loop of this inflammatory process. The figure is adapted from Nestle et al., 2009.

The release of IFN α by pDCs leads to the activation of myeloid DCs (Nestle et al., 2009a), which migrate as DCs to the draining LNs (Platt and Randolph, 2013). Further, DCs can be directly activated by stressed cells, which release IL-1 β , IL-6 or tumor necrosis factor α (TNF α) (Perera et al., 2012). In the draining LNs, these activated DCs present antigens to naïve T cells and initiate the secretion of cytokines like IL-12 or IL-23 (Fig. 3). Dependent on the secreted cytokine, naïve T cells differentiate into type 1 or type 17 helper T cells (Th1 and Th17), which are subsequently directed into the antigen-derived tissue (Nestle et al., 2009b). There they release cytokines, like IL-17 and IL-22 and consequently activate keratinocytes to proliferate and produce chemokines (C-X-C motif chemokine ligand 8 (CXCL8), CXCL1, CXCL10 and CC-chemokine ligand 20 (CCL20)), proinflammatory cytokines (IL-1 β , IL-6 and TNF α) as well as antimicrobial peptides (Fig. 1). Further, these chemokines (CXCL1, CXCL2 and CXCL8) (Lowe et al., 2014) attract neutrophils in the epidermis (Nestle et al., 2009b). The whole

process raises the immune response in the skin (Lowes et al., 2014). Through the production of IL-1 β , IL-6 and TNF α the feed back loop of the proinflammatory disease psoriasis is initiated (Nestle et al., 2009b). A very important event is the migration of T cells from the dermis to the epidermis, (Conrad et al., 2007), which is mediated by type I cytotoxic T cells (Tc1) (Nestle et al., 2009b) expressing the very-late antigen 1 (VLA1) (Nestle et al., 2009a). They bind to collagen IV and can enter the epidermis where they produce IFN γ (Nestle et al., 2009a). Like this, CD8⁺ T cells contribute to the crosstalk between immune and epithelial cells in the skin (Nestle et al., 2009a).

Besides Th17 cells, also CD8⁺ T cells are able to produce IL-17 (Di Cesare et al., 2009). Psoriatic lesions show high numbers of CD8⁺ T cells producing IL-17 and other cytokines, like IL-22 (Hijnen et al., 2013; Res et al., 2010). This strongly indicates their contribution to the adaptive immune response and thereby playing an important role in the pathogenesis of psoriasis.

1.1.5 *Animal models of psoriasis*

Psoriasis is an inflammatory skin disease and naturally only occurs in humans (Gudjonsson et al., 2007). Over the years, different animal models have been developed to examine the pathogenesis of this disease and its consequent influence on cellular and molecular processes. There are different kinds of models, transgenic and induced mouse models (Danilenko, 2008). Also, humanized mice display a model to study the pathogenesis of this disease. Here, skin biopsies of psoriasis patients are transplanted to immunodeficient mice, which don't reject skin grafts (Raychaudhuri and Raychaudhuri, 2010). Common mice strains used for this method are severe combined immunodeficient (SCID) mice (lack of B and T cells), Prkdc^{scid} mice (Raychaudhuri and Raychaudhuri, 2010), nude mice (Hafttek et al., 1981) and AGR129 mice (lack of type I+II IFN receptors on RAG-2^{-/-} background). A few weeks after transplantation of lesional skin grafts, murine skin develops clinical and histological features of psoriasis (Boehncke et al., 1994; Boyman et al., 2004; Hafttek et al., 1981; Raychaudhuri and Raychaudhuri, 2010). However, SCID mice needed an injection of activated peripheral blood mononuclear cells (PBMCs) into the graft to achieve this effect

(Boehncke et al., 1994). A huge disadvantage of this model is the lack of systemic effects, so only the skin phenotype can be analyzed.

Further, there are some transgenic mouse strains used to investigate the pathogenesis of psoriasis. As the IL-23/IL-17 axis plays a critical role in this disease (Di Cesare et al., 2009), different mouse strains addressed the involvement of these cytokines. The keratinocyte specific overexpression of members of the IL-17 family (K5-IL-17C and K14-IL-17A^{ind/+} mice) led to a severe psoriasis-like phenotype in mice (Croxford et al., 2014; Johnston et al., 2013), confirming a strong contribution of IL-17 to this disease. The same is also true for IL-23: mice, where the p40 subunit of IL-12 and IL-23 is expressed in keratinocytes, under the human K14 promoter (K14-p40 mice), show a high release of IL-23 by epidermal cells, but not IL-12 (Kopp et al., 2003). This resulted in an inflammatory skin disease, similar to psoriasis.

Also other signaling pathways, like nuclear factor kappa-light-chain-enhancer of activated B cells (NF- κ B) and STAT3, were shown to be involved in the pathogenesis of psoriasis (Andres et al., 2013). An overexpression of constitutively active STAT3 in keratinocytes (K5-STAT3C mice) had a similar effect as described above (Sano et al., 2005). Here the psoriatic characteristics appeared spontaneously or after tape - stripping. The specific deletion of IKK2, which is an inhibitor of the NF- κ B kinase subunit beta, in keratinocytes (K-14-IKK2 mice) also resulted in skin inflammation with hallmarks of human psoriasis, and was found to be dependent on TNF- α (Pasparakis et al., 2002). As the mice die very early (day P7-P9), it is difficult to perform detailed analysis, but on the other hand it strongly indicates the importance of NF- κ B signaling in the pathogenesis of psoriasis.

However, also other cytokines besides IL-23 and IL-17 play a critical role in the pathogenesis of psoriasis, including IL-1 and IL-6. IL-6 was shown to be highly upregulated in the skin of psoriasis patients (Grossman et al., 1989). Another study, where IL-6 is expressed in the epidermis (K14-IL-6 mice), revealed a thicker stratum corneum, but it had no influence on cell infiltrations (Turksen et al., 1992). This suggests that IL-6 does not only have proinflammatory properties (Turksen et al., 1992), but also induces an imbalance of the cellular composition in the skin. Besides, an injection of IL-1 α induced cutaneous inflammation (Dowd

et al., 1988). In line with these findings, keratinocyte specific overexpression of IL-1 α (K14-IL-1 α) also resulted in an inflammatory skin disease (Groves et al., 1995).

As already mentioned before, the injection of recombinant cytokines (e.g. IL-1 α (Dowd et al., 1988)) to mouse skin can result in skin inflammation, displaying another mouse model of psoriasis. Similarly, subcutaneous injection of IL-23 displays this effect (Kopp et al., 2003; Lindroos et al., 2011).

Recently, a new model was introduced by van der Fits et al. Here, topical application of *Aldara*TM cream for some consecutive days, leads to a psoriasis-like skin inflammation also involving the IL-23/IL-17 axis (van der Fits et al., 2009). *Aldara*TM cream contains 5% of Imiquimod (IMQ), which is a TLR 7/8 agonist (Flutter and Nestle, 2013) and an immune activator. In humans it is used to treat genital warts caused by the human papillomavirus (Beutner and Ferenczy, 1997) and skin irritations like basal cell carcinoma (Geisse et al., 2004) or keratosis (Szeimies et al., 2004). The specific mode of action and the involved immune cells in this model will be described in more detail in the next paragraph (1.2).

1.2 IMQ-induced psoriasis-like skin disease

1.2.1 Toll-like receptor signaling induced by IMQ

IMQ is a nucleoside analogue belonging to the family of imidazoquinoline (Fig. 4). Originally it was developed to serve as an antiviral agent (Schon and Schon, 2007), but it was discovered that its topical application to the skin in form of *Aldara*TM cream enhances disease in psoriasis patients (Fanti et al., 2006; Rajan and Langtry, 2006). Also in mice its application to the skin results in a psoriasis-like disease (Cai et al., 2011; El Malki et al., 2013; Pantelyushin et al., 2012; van der Fits et al., 2009; Wohn et al., 2013).

As already mentioned, IMQ is a TLR7/8 agonist and activates cells expressing these receptors, including monocytes, macrophages, DCs and pDCs (Gilliet et al., 2004; Stanley, 2002), whereby viral ssRNA serves as its natural ligand (Gilliet et al., 2004; Schon and Schon, 2007). The psoriatic plaque formation as a consequence of IMQ treatment is accompanied by high production of type I interferons (IFN α/β) (Gilliet et al., 2004). pDCs are known to be the main

producers of IFN α/β in the blood of humans as a response to TLR7/8 stimulation (Gibson et al., 2002). Also in the skin of IMQ treated patients high numbers of pDCs are visible (Gilliet et al., 2004; Urosevic et al., 2005). Moreover, mice that are deficient for TLR7 or its signaling pathway (MyD-88 dependent) do not produce IFNs in response to IMQ (Hemmi et al., 2002). This clearly shows that the IMQ-induced psoriasis is a viable model to study the disease, as it also induces the innate immune response through the activation of TLR7/8 (Gilliet et al., 2004; Stanley, 2002).

Further, IMQ induces migration of LCs to draining lymph nodes for antigen-presentation to naïve T cells (Stanley, 2002; Suzuki et al., 2000). Interestingly, keratinocytes respond to IMQ by producing different cytokines, such as IL-8, IL-6, IFN α and TNF α (Fujisawa et al., 1996; Kono et al., 1994), although they do not express TLR7/8, at least in humans (Kollisch et al., 2005; Lebre et al., 2007).

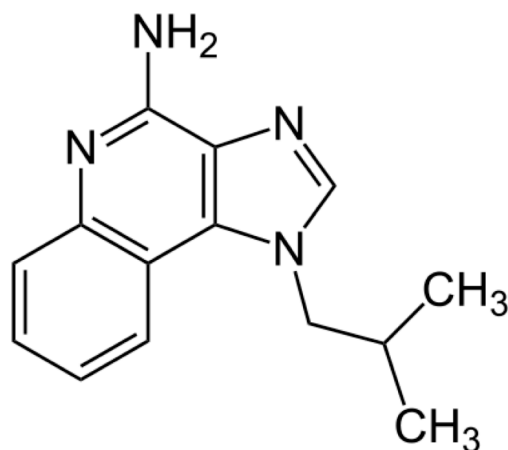


Figure 4: Structural formula of Imiquimod

The figure was adapted and modified from Stanley et al., 2002.

In humans, the entire family of TLRs consists of 10 members (1-10) while in mice there are 12 members (1-9, 11-13) (Kaisho and Akira, 2006). For the majority of TLRs signaling is initiated on the cell surface (TLR1-2, TLR4-6 and TLR11), but some of them are located intracellular (TLR3, TLR7-9). TLRs belong to the group of pattern recognition receptors (PRRs), which are receptors of the innate immune system (Stanley, 2002), recognizing conserved molecular patterns (motifs of microorganisms), named pathogen-associated molecular patterns (PAMPs) (Schon and Schon, 2007) (Medzhitov, 2001). They are membrane glycoproteins with a leucine-rich extracellular domain and an

intracellular Toll-IL-1-receptor (Gudjonsson et al.) domain, mediating the recognition and binding of ligands, and initiating intracellular signaling cascades respectively (Feng and Chao, 2011; Kawai and Akira, 2006). Except for TLR3, all TLRs activate myeloid differentiation primary response protein (MyD88) dependent pathways (Fig. 5A) (Feng and Chao, 2011). MyD88 recruits different IL-1 receptor associated kinases (IRAK), which leads to the activation of certain signaling pathways such as NF- κ B (Fig. 5A) and Mitogen-activated protein kinases (MAPKs) (Feng and Chao, 2011). This results in the nuclear translocation of transcription factors (activator protein 1 (AP-1), p50/p65) and subsequent production of inflammatory cytokines (Feng and Chao, 2011) and chemokines, like IL-6, IL-8, IL-12, CCL2 or TNF α (Kawai and Akira, 2006; Schon and Schon, 2007), but also IL-17, IL-23 and CXCL1 (Flutter and Nestle, 2013). Furthermore, TLR7-9 also induces the interferon regulatory transcription factor 7 (IRF7). Its translocation into the nucleus results in the activation of type I IFN genes (Feng and Chao, 2011; Kawai and Akira, 2010).

1.2.2 Signaling cascades activated by AldaraTM cream independent of TLR7/8

Besides the TLR7/8 dependent responses, IMQ also acts on other signaling pathways (Fig. 5).

For instance, in adenosine receptor (AR) signaling (Fig. 5C), IMQ serves as a receptor antagonist (Flutter and Nestle, 2013). Receptor binding leads to suppression of the anti-inflammatory cyclic adenosine monophosphate (cAMP) formation (Flutter and Nestle, 2013), which consequently results in a higher production of pro-inflammatory mediators (Schon and Schon, 2007).

Moreover, IMQ was also shown to activate the nucleotide-binding domain, leucine-rich repeat-containing receptor protein 3 (NLRP3) inflammasome (Fig. 5B) (Kanneganti et al., 2006).

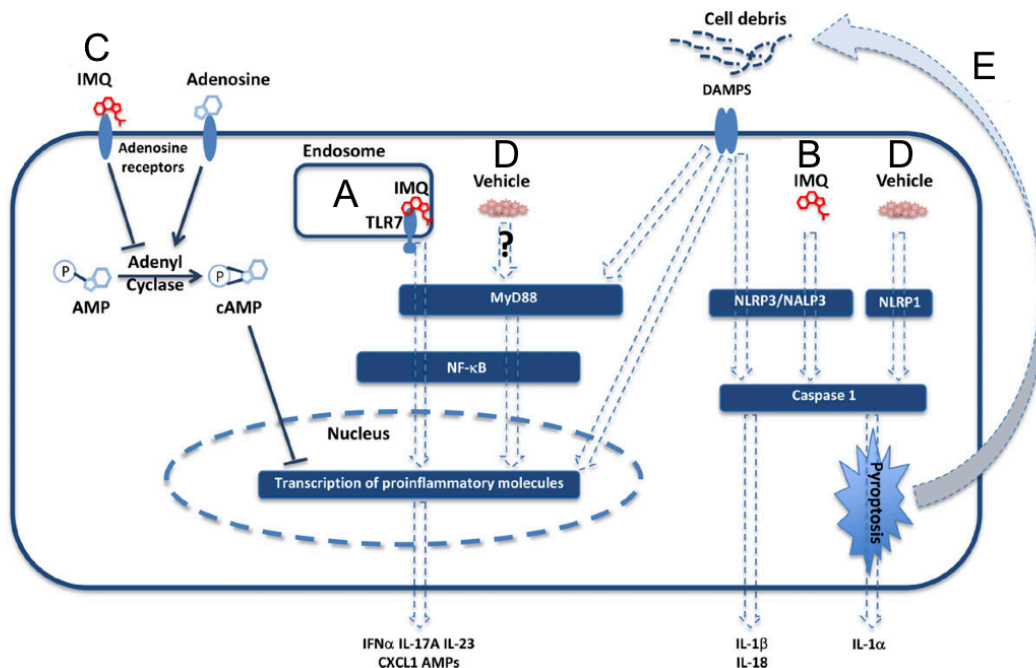


Figure 5: Aldara™ cream and its mode of action

The active compound IMQ can activate signaling pathways either via TLR7 (A), by activating the NLRP3 inflammasome (B) or as an antagonist of the adenosine receptor (C). Isostearic acids (also an ingredient of Aldara™ cream) can activate the NLRP1 inflammasome (D) and possibly other cells by cell death of KCs (E). The figure was adapted and modified from Nestle et al., 2009.

Inflammasomes are complexes, which consist of many different proteins responsible for the activation of inflammatory caspases (Martinon and Tschopp, 2007). Hereby, for example, NLRP1 and 3 inflammasomes activate caspase-1, which in turn activates proIL-1β and -18 (Feldmeyer et al., 2010). As a consequence of this, the mature forms of the cytokines are secreted and induce inflammation (Feldmeyer et al., 2010).

However, the study of Walter et al. observed that isostearic acids, which are a component of Aldara™ cream can already induce an immune response. They showed an activation of the NLRP1 inflammasome, release of IL-1 and apoptosis of KCs independent of IMQ (Walter et al., 2013). Based on their data, caspase-1 activity leads to cell death of KC (pyroptosis) and subsequent release of IL-1α (Fig. 5D) as well as pro-IL-1β (Walter et al., 2013). It is known, that IL-1α released by KCs is able to induce an inflammatory response (Feldmeyer et al., 2010), but in healthy skin, pro-IL-1α and pro-IL-1β synthesized by KCs cannot be processed (Nestle et al., 2009a). Therefore it is very likely that release of IL-1α and cellular debris as a consequence of pyroptosis induces signaling pathways in surrounding cells (Fig. 5E) (Flutter and Nestle, 2013). The release of pro-IL-1α

by keratinocytes and macrophages being dependent on caspase-1 activity was already observed in an earlier investigation (Keller et al., 2008). Interestingly, fatty acids have the ability to activate inflammasomes (Vandanmagsar et al., 2011) (Wen et al., 2011). However, vehicle treatment has not the same effects on the skin as IMQ, suggesting that IMQ and the isostearic acids have additional effects (Walter et al., 2013). Nonetheless, signaling via MyD88 is needed at some point during disease progression, as Myd88 deficient mice are resistant to IMQ-induced psoriasis (Wohn et al., 2013).

1.2.3 IL-23/IL-17 axis in (IMQ-induced) psoriasis

Many different cytokines are involved in the pathogenesis of psoriasis, but especially the IL-23/IL-17 axis seems to play a crucial role. IL-23 is a heterodimer consisting of a p19 and a p40 subunit. The latter is also part of IL-12 (Teng et al., 2015), whereas the p19 subunit (discovered in 2000) has no additional biological activity (Oppmann et al., 2000). Originally IL-23 was noted to induce IFN γ production of memory T cells (Oppmann et al., 2000). Furthermore, IL23 is required for the differentiation and expansion of Th17 cells (Aggarwal et al., 2003; Harrington et al., 2005), which subsequently secrete cytokines such as IL-17A, IL-17F and IL-22 (Iwakura et al., 2011; Teng et al., 2015). Furthermore, IL-23 is increased in the skin of psoriatic patients (Lee et al., 2004; Piskin et al., 2006) and genetically modified mice, constitutively expressing the p19 subunit, which leads to multiorgan inflammation, including the skin (Wiekowski et al., 2001). Intradermal injection of IL-23 causes erythema and infiltration of inflammatory cells (Chan et al., 2006; Zheng et al., 2007).

The importance of IL-22 in the pathogenesis of a psoriasis-like disease was shown by another study. IMQ treated IL-22^{-/-} mice exhibit a strongly reduced disease severity compared to *wt* mice (Van Belle et al., 2012).

The involvement of IL-17 in psoriasis was already detected in the late 1990's. Teunissen et al. presented elevated IL-17 mRNA levels in lesional skin compared to non-lesional skin (Teunissen et al., 1998). Therefore it is not surprising that the IL-23/IL-17 axis also has a prominent role in the model of IMQ-induced psoriasis. Van der Fits et al. demonstrated in their study higher mRNA levels of

IL-23p19, IL-17A and IL-17F in the back skin of IMQ treated mice (van der Fits et al., 2009) Further, they observed a significant milder IMQ-induced psoriasis-like disease in IL-17RA deficient mice as well as in IL-23p19 deficient mice when compared to *wt* mice (van der Fits et al., 2009). The importance of IL-17 was further confirmed by an investigation from our lab. IL-17RA deficient mice displayed an ameliorated IMQ-induced skin disease (El Malki et al., 2013). Furthermore, also here *wt* mice demonstrated a more severe disease after IL-23 injection (El Malki et al., 2013).

The early inflammation caused by IMQ is probably driven by Langerin^{neg} conventional DCs (cDCs). Upon treatment with IMQ (within hours), Langerin^{neg} DCs are the only cells producing IL-23, which subsequently activates IL-17/IL-22 producing innate lymphocytes (Wohn et al., 2013). Interestingly, the same study also showed that this was independent of pDCs and type I IFN production (Wohn et al., 2013). However, it seems as if specific nociceptors, which are in close proximity with the IL-23 producing dermal DCs interact with those and by this control the immune response of the skin (Riol-Blanco et al., 2014). The IL-17 production by innate lymphocytes was also shown by the work of Mabuchi et al., who showed that upon IL-23 injection into the mouse skin, CCR6⁺ $\gamma\delta$ TCR^{int} cells infiltrate the epidermis and highly expressed mRNA transcripts of IL-17A and IL-22 (Mabuchi et al., 2011). Strikingly, the dependence of $\gamma\delta$ T cells on IL-23 and IL-1 β to produce IL-17 was shown by other studies (Cai et al., 2011; Gray et al., 2011; Sutton et al., 2009).

Recent findings suggested the dermal $\gamma\delta$ T cells to be the main producers of IL-17 in psoriasis-like disease (Cai et al., 2011; Pantelyushin et al., 2012; Shibata et al., 2015), in contrast to CD4⁺ and CD8⁺ T cells (1.1.4). The skin harbors two populations of $\gamma\delta$ T cells: dermal and epidermal. They can be distinguished by their expression of V γ TCR segments. Dermal $\gamma\delta$ T cells express V γ 4 (Cai et al., 2011; Sumaria et al., 2011), whereas epidermal $\gamma\delta$ T cells are V γ 5⁺ and are exclusively located in the epidermis (Gray et al., 2011; Havran and Jameson, 2010). They are termed dendritic epidermal T cells (DETCs). Cai et al. observed that the IL-17 production is very dependent on the V γ 4 TCR segment as a V γ 4 depleting antibody decreased the IL-17 production of dermal $\gamma\delta$ T cells significantly (Cai et al., 2011). The theory that $\gamma\delta$ T cells are the main producers

of IL-17 in IMQ-induced psoriasis is strongly supported by the fact, that ablation of those resulted in less IL-17 production (Cai et al., 2011). Also skin inflammation induced by IL-23 injection is decreased in *Tcrd*^{-/-} mice (Cai et al., 2011) (Mabuchi et al., 2011).

Interestingly, Hartwig et al. discovered an IL-17A/F producing V γ 4⁺V δ 4⁺ T cell population in the dermis of IMQ treated mice with a memory effect (Hartwig et al., 2015). They could show that these T cells stay in the dermis for a long time after the initial challenge with IMQ (up to 180 days). Upon a 2nd period of treatment with IMQ, these cells respond much faster (Hartwig et al., 2015; Prinz and Sandrock, 2015), underlining an important role of innate cells in this model. However, without $\gamma\delta$ T cells, the production of IL-17 in IMQ-induced skin inflammation, can be balanced by IL-17 production of CD4⁺ T cells (Cai et al., 2011; Pantelyushin et al., 2012; Tortola et al., 2012). Also in humans an IL-17 producing population of $\gamma\delta$ T cells was observed in the skin of psoriasis patients (Laggner et al., 2011).

Moreover, neutrophils are associated to IL-17 signaling. For example, mice with a deletion of the IL17RA displayed less Gr-1⁺ cells under IMQ treatment (van der Fits et al., 2009). Recently, two studies in the context of human skin inflammation revealed neutrophils and mast cells to be the main producers of IL-17 (Keijsers et al., 2014; Lin et al., 2011). Further, this was also connected to the formation of NETs.

1.3 IL-6 signaling

As already mentioned above, IL-6 is strongly involved in the pathogenesis of psoriasis. Besides its high expression in human psoriatic skin (Grossman et al., 1989), it was also shown to have an important role in psoriasis-like disease in different mouse models of (Croxford et al., 2014; El Malki et al., 2013; Hvid et al., 2008; van der Fits et al., 2009). Further, intradermal injection of IL-23, which results in skin inflammation, showed reduced ear swelling in IL-6^{-/-} mice (Lindroos et al., 2011).

IL-6 belongs to a family of cytokines, which all share gp130 as receptor subunit (β receptor) (Wolf et al., 2014). Other members of this family are IL-11, IL-27,

oncostatin M (OSM), ciliary neurotrophic factor (CNTF), leukemia inhibitory factor (LIF), cardiotrophin-1 (CT-1) and cardiotrophin like cytokine (CLC) (Heinrich et al., 2003; Jones et al., 2011).

The signaling of IL-6 can occur in two different forms: signaling of IL-6 via the membrane bound receptor (mIL-6R α) and the so-called IL-6 trans-signaling, which is the soluble form of IL-6R α (sIL-6R α) (Fig. 6) (Rose-John, 2012). For activating the mIL-6R α signaling, IL-6 binds the mIL-6R α . Moreover, two gp130 molecules are needed, which serve as the co-receptor (β receptor) (Fig. 6) (Levy and Darnell, 2002; Rose-John, 2012). Building this complex is indispensable for the activation of intracellular signaling cascades, like the JAK/STAT pathways (Camporeale and Poli, 2012). Binding of IL-6 to the IL-6R leads to the phosphorylation of gp130 associated tyrosine residues by Janus kinases (JAKs) (Wang et al., 2013). Recruited STAT3 binds to these phosphorylated tyrosines and subsequent dimerization of STAT3 leads to its translocation to the nucleus inducing gene transcription (Levy and Darnell, 2002; Wang et al., 2013). Gp130 on its own is not able to initiate signaling, as it has no affinity to IL-6 (Rose-John, 2012). However, the classical signaling can only occur in cells expressing the mIL-6R α , like neutrophils, monocytes/macrophages, hepatocytes and other leukocytes (Rose-John et al., 2006; Rose-John et al., 2007; Scheller and Rose-John, 2006; Wolf et al., 2014). sIL-6R α accrues after the proteolytic cleavage of mIL-6R α which is mediated by a disintegrin and metalloproteinase (Paul et al.) 10 or 17 (Schumacher et al., 2015). This process enables trans-signaling allowing cells with no mIL-6R α expression to respond to IL-6, as long as they express the co-receptor gp130 (Wolf et al., 2014). Hence, this is true for all body cells, as gp130 is expressed universally (Rose-John et al., 2007; Wolf et al., 2014).

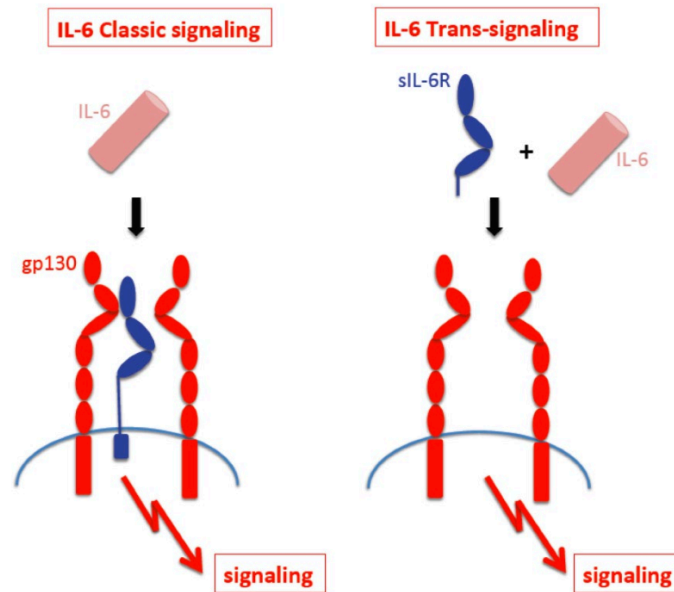


Figure 6: The two forms of IL-6 signaling

Classical signaling via the mIL-6R α on myelomonocytic cells, hepatocytes and leukocytes (left). IL-6 trans-signaling via the sIL-6R α (Hueber et al.) can occur on all body cells, due to the universal expression of gp130. The figure was adapted from Rose-John, 2012.

Recent studies revealed that IL-6 is a cytokine with pleiotropic effects, as the classical signaling of IL-6 via the mIL-6R α has the potential to act anti-inflammatory, whereas sIL-6R α functions in a more pro-inflammatory manner (Rose-John, 2012; Scheller et al., 2011; Wolf et al., 2014).

The natural inhibitor of the trans-signaling is soluble gp130, which only recognizes IL-6 bound to the sIL-6R α (IL-6/ sIL-6R α complex) (Barkhausen et al., 2011; Rose-John et al., 2006). Taking advantage of this finding, soluble gp130Fc (sgp130Fc) was developed to serve as a potential treatment option for inflammatory diseases, e.g. Morbus Chron (Jostock et al., 2001). For the generation of sgp130Fc two monomers of the sgp130 protein were fused through the Fc region of human immunoglobulin G1 (IgG1) (Rose-John et al., 2006; Wolf et al., 2014). The trials for phase I of clinical studies for sgp130Fc started in 2013 (Scheller et al., 2014).

1.4 IL-1 signaling

The proinflammatory cytokine IL-1 contributes to the development of skin inflammations, as the skin of psoriatic patients shows a high expression level of

IL-1R1, IL-1RA and IL-1 α (Groves et al., 1994; Hammerberg et al., 1992). Furthermore, intradermal application of IL-1 α induces skin inflammation (Dowd et al., 1988). Strikingly, mice with a deletion of IL-1R1 developed a milder form of IMQ-induced psoriasis compared to *wt* mice (Rabeony et al., 2015; Uribe-Herranz et al., 2013), underlining the importance of IL-1 in the pathogenesis of psoriasis-like disease. In line with this, mice lacking the IL-1 receptor antagonist (IL-1Ra) suffer under a psoriasis-like skin inflammation (Nakajima et al., 2010; Shepherd et al., 2004).

The IL-1 family consists of many different members: seven ligands (IL-1 α , IL-1 β , IL-18, IL-33, IL-36 α , IL-36 β and IL-36 γ), three receptor antagonists (IL-1Ra, IL-36Ra and IL-38), four signaling receptors and two decoy receptors (IL-1R2 and IL-18BP) (Garlanda et al., 2013). Moreover, the inflammatory cytokine IL-37 as well as the two negative regulators TIR8 and IL-1RAcPb belong to the family of IL-1 (Garlanda et al., 2013). The decoy receptor IL-1R2 can bind IL-1 β , IL-1Ra and also IL-1 α , but with less affinity (Boraschi and Tagliabue, 2013). Due to its missing intracellular TIR domain, IL-1R2 cannot transmit a signal (Garlanda et al., 2013). Besides the membrane bound receptor also a soluble form of IL-1R2 exists both acting as inhibitors (Boraschi and Tagliabue, 2013). The soluble form of IL-1R2 arises by cleavage from the membrane, mediated by ADAM17 (Lorenzen et al., 2012; Uchikawa et al., 2015). Signaling through IL-1R1 can initiate the inflammatory response by binding its ligands IL-1 α and IL-1 β (Boraschi and Tagliabue, 2013). After the recruitment of the receptor subunit (IL-1RAcP) NF- κ B and MAPK pathways are activated, which induce gene transcription mediating the inflammatory response (Sims and Smith, 2010).

1.5 Monoclonal antibodies as a treatment option for psoriasis

Since the IL-23/IL-17 axis was demonstrated to be critically involved in psoriasis (1.2.3), monoclonal antibodies (mAb`s) targeting these cytokines represent a good treatment option.

Ustekinumab (*Stelara*[®]; Janssen) is a human mAb, which binds the p40 subunit of IL-12/IL-23 (Campa et al., 2016). Its efficiency was shown by different phase III clinical trails (Leonardi et al., 2008; Papp et al., 2008) and also in long-term

treatments (Papp et al., 2013). 2009 it was approved for the treatment of psoriasis patients (Campa et al., 2016). Further, Ustekinumab is also applied in psoriatic arthritis (PsA) (Campa et al., 2016; Elyoussfi et al., 2016). Moreover, there are two promising mAb targeting specifically IL-23 by binding the p19 subunit: Gruselumab (Janssen) and Tildrakizumab (Merck). Currently, for both antibodies are tested in an ongoing phase III of clinical studies (accessed in August and September 2015, respectively) (Campa et al., 2016).

Secukinumab (*Cosentyx*[®]; Novartis) is a human anti-IL-17A mAb, which was recently approved by the Food and Drug Administration (FDA) for the treatment of moderate-to-severe plaque psoriasis (Ritchlin and Krueger, 2016) (Campa et al., 2016). It is well tolerated (Ritchlin and Krueger, 2016) and can also be applied in patients who suffer from PsA (McInnes et al., 2015). However, the application of Secukinumab in Crohn's disease resulted in side effects (Hueber et al., 2012). With another anti-IL-17A antibody, Ixekizumab (Eli Lilly), the majority of the patients reached a reduction in the clinical response (between PASI 75 and PASI 100) (Griffiths et al., 2015). Strikingly, it is also successfully applied for the treatment of PsA (Ritchlin and Krueger, 2016). Currently the clinical studies are in phase III (Campa et al., 2016). Brodalumab (Amgen) (Campa et al., 2016) blocks the signaling of IL-17A/F and IL-23 receptors (Elyoussfi et al., 2016; Farahnik et al., 2016; Jinna and Strober, 2016) and has the potential to suppress and/or reverse the expression of genes that are associated with psoriasis (Ritchlin and Krueger, 2016). However, due to increased rates of suicides or suicidal ideations of patients participating in the trials the studies with Brodalumab have been stopped (Ritchlin and Krueger, 2016).

Besides the blocking of IL-17 or IL-23 also inhibitors of TNF α exist. Adalimumab (*Humira*[®]; AbbVie) and Infliximab (Janssen) are anti-TNF α mAb's (Lowes et al., 2013), which are used for the treatment of psoriasis. However, Adalimumab is only used in psoriasis patients, where common treatment options had no effect, although it is also applied efficiently in other joint and skin diseases (Elyoussfi et al., 2016). Besides this, also Etanercept (Amgen) as a soluble TNF α receptor fused to the Fc region of human IgG1 (Lowes et al., 2013) has a positive effect on skin diseases, but is less efficient than other TNF α inhibitors (Elyoussfi et al., 2016).

Altogether mAb`s display a promising treatment option in psoriasis, successfully reducing cardinal symptoms of disease (Campa et al., 2016; Elyoussfi et al., 2016).

1.6 Objectives

The inflammatory skin disease psoriasis displays a strong interplay of immune cells, such as monocytes, macrophages and neutrophils, but also T cells. Besides other disease typical characteristics, one important hallmark of psoriasis is also the formation of neutrophil abscesses in the epidermis, called Munro's Microabscesses. Many inflammatory cytokines are known to be upregulated during this disease, including IL-6, IL-1, IL-17, IL-22 and IL-23.

The aim of this thesis is to investigate the role of myelomonocytic cells in different models of psoriasis-like skin disease.

A previous publication from our lab demonstrated that the keratinocyte specific overexpression of IL-17A (*K14-IL-17A^{ind/+}*) results in an inflammation of the skin with many hallmarks of human psoriasis. Here it was shown, that an anti-IL-6 treatment of those mice resulted in a strong reduction of neutrophil microabscesses. An anti-IL-17A treatment (in cooperation with Novartis) of those mice should explore if the neutralization of IL-17A also had the potential to improve the disease severity, as well in the model of IMQ-induced psoriasis applied on C57Bl/6 mice.

Further, with the model of IMQ-induced psoriasis different mouse lines were analyzed for changes in the composition of the myelomonocytic compartment.

IL-6 is critically involved in psoriasis and important for general neutrophil recruitment. So, in this work it was addressed how IL-6 signaling in myelomonocytic cells affects the disease severity during IMQ treatment. For this purpose, the membrane bound IL-6R α was deleted in myelomonocytic cells (*IL-6R α ^{Am α myel}*), and mice were analyzed in terms of infiltrating cells and clinical scores. Moreover, also IL-1 is critically involved in the pathogenesis of IMQ-induced psoriasis. Linking to previous reports, showing *Il1r1^{-/-}* mice develop less Munros's abscesses during IMQ treatment, *Il1r2^{-/-}*, *Il1r2^{ΔT}* (T cell specific deletion of IL-1R2) and *Il1r2^{ΔN}* (neutrophil specific deletion of IL-1R2) mice were

examined in this model. Here, it was evaluated which cell type is influenced by altered IL-1 signaling in the psoriasis-like disease.

To address the question if the disease severity of psoriasis would be influenced by total ablation of neutrophils, Ly6G-Cre mice were crossed to iDTR mice to achieve a full depletion of neutrophils.

2 Materials and Methods

2.1 Chemicals and biological materials

Chemicals (Table 1) were purchased from Sigma (Steinheim, Germany), Fluka Chemie (Switzerland), Merck (Darmstadt, Germany) or AppliChem (Darmstadt, Germany) unless stated otherwise. Solutions were prepared with double distilled water (ddH₂O). Sterility of solutions and chemicals used in cell culture was maintained by working under a sterile hood (Heraeus, Germany).

Name of Chemical	Supplier
3-(N-morpholino)propanesulfonic acid (MOPS)	Roth, Karlsruhe
Agarose, electrophoresis grade	AppliChem, Darmstadt
Ammonium chloride	Sigma-Aldrich, Steinheim
Bovine serum albumin (BSA)	Sigma-Aldrich, Steinheim
Bradford	Bio-Rad, Germany
Brefeldin A	Sigma-Aldrich, Steinheim
Diphtheria Toxin	Calbiochem, USA
Dithiothreitol (DTT)	Boehringer GmbH, Mannheim
dNTPs	Pharmacia Biotech, USA
ECL	GE Healthcare, UK
Eosin Y	Thermo Fisher Scientific, USA
Ethanol, abs.	AppliChem, Darmstadt
Ethidium bromide	Sigma-Aldrich, Steinheim
Ethylendiamine tetraacetate (EDTA)	Fluka Chemie GmbH, Switzerland
Evans Blue	Sigma-Aldrich, Steinheim
Fetal calf serum (FCS)	Boehringer GmbH, Mannheim
Formaldehyde	Sigma-Aldrich, Steinheim
Glacial acetic acid	Fluka Chemie GmbH, Switzerland
Hematoxylin	Thermo Fisher Scientific, USA
HEPES	Roth, Karlsruhe
Hydrochloric acid (37%)	Merck, Darmstadt
Ionomycin	Thermo Fisher Scientific, USA
Isoflourane	Abbvie, Ludwigshafen
Isopropanol	AppliChem, Darmstadt
L-glutamine	Sigma-Aldrich, Steinheim
Liberase TM	Roche, Switzerland
Methanol	Roth, Karlsruhe
Milk powder	Fluka Chemie GmbH, Switzerland

Non essential amino acids	Thermo Fisher Scientific, USA
Paraformaldehyde	Sigma-Aldrich, Steinheim
Penicillin/streptomycin	Sigma-Aldrich, Steinheim
Phosphatase inhibitor	Sigma-Aldrich, Steinheim
Phosphate buffered saline	Sigma-Aldrich, Steinheim
PMA	PromoCell, Heidelberg
Protease inhibitor	Sigma-Aldrich, Steinheim
Proteinase K	Roche, Switzerland
Red Taq Readymix	Sigma-Aldrich, Steinheim
RIPA buffer	Cell Signaling, USA
Roti-Histofix 4%	Roth, Karlsruhe
RPMI medium	Thermo Fisher Scientific, USA
Saponin	Sigma-Aldrich, Steinheim
Sodium bicarbonate	Sigma-Aldrich, Steinheim
Sodium carbonate	Merck, Darmstadt
Sodium chloride	AppliChem, Darmstadt
Sodium dodecyl sulfate	AppliChem, Darmstadt
Sodium hydrogen carbonate	Roth, Karlsruhe
Sodium hydrogen phosphate	Fluka Chemie GmbH, Switzerland
Sodium hydroxide	Fluka Chemie GmbH, Switzerland
Sodium pyruvate	Sigma-Aldrich, Steinheim
Tris base	Fluka Chemie GmbH, Switzerland
Trypan blue 0,4%	Thermo Fisher Scientific, USA
Tween 20	Sigma-Aldrich, Steinheim
β -Mercaptoethanol (β -ME)	Fluka Chemie GmbH, Switzerland

Table 1: List of Chemicals

2.2 Molecular Biology

2.2.1 Preparation of genomic DNA

Tail biopsies (0,2cm) or toes were lysed overnight (o/n) at 56°C in lysis buffer (10mM Tris-HCl, pH 8; 10mM EDTA; 150mM NaCl; 0.2% (w/v) SDS; 400mg/ml proteinase K (PNK)). Undigested tissue was pelleted by centrifugation (14800 rpm, 10-15 min, room temperature (RT)). Supernatant was transferred into a new tube and mixed with an equal volume of isopropanol to precipitate the DNA. Subsequently, DNA was pelleted by centrifugation (see above), washed in 70% (v/v) EtOH, dried at RT, and resuspended in ddH₂O.

2.2.2 Polymerase chain reaction (PCR)

Mice were screened for the presence of targeted alleles or transgenes by applying tail or toe tip DNA with specific primer pairs (primers shown in table 2) to PCR (Mullis and Faloona, 1987; Saiki et al., 1985). Reactions were performed in T3000 Thermo cycler (Biometra, Göttingen, Germany). Genotyping was generally performed in a total volume of 24µl in one of the following reaction mix: 10pmol of each primer and 10µl of RedTaq Readymix (Sigma, Steinheim, Germany) and 14µl of PCR water (Sigma, Steinheim, Germany), according to manufacture instructions. Amplification was performed as shown in table 3.

Name of primer	Sequence (5'-3')	T _{ann.} °C	Direction
Aktin fwd	TGT TAC CAA CTG GGA CGA CA	58	sense
Aktin rev	GAC ATG CAA GGA GTG CAA GA	58	anti-sense
Allg Cre fwd	GCA CTG ATT TCG ACC AGG TT	58	sense
Allg Cre rev	CCC GGC AAA ACA GGT AGT TA	58	anti-sense
CD4cre forw.	CCC AAC CAA CAA GAG CTC	58	sense
CD4cre rev.	CCC AGA AAT GCC AGA TTA	58	anti-sense
Cre8	CCC AGA AA TGCC AG ATTA CG	54	anti-sense
IL17_Aind F1	TCA GGG TCG AGA AGA TGC TGG	63	sense
IL1r2_3429_33	TGT CTC CAT CAG ACT GAC	60	sense
IL1r2_3429_34	ACC ATG TCT GCC TGT TCA	60	anti-sense
IL1r2_3430_29	GGA TAG TCT GTT ACA GCC	60	sense
IL6R1	CCA GAG GAG CCC AAG CTC TC	51	sense
IL6R2	CCG CGG GCG ATC GCC TAG G	51	anti-sense
IL6R3	AAT AAC TGA GAA TCA AAG C	51	anti-sense
K14Cre anti-sense	CGC ATA ACC AGT GAA ACA GCA	58	anti-sense
K14Cre sense	AGC ACC TTC TCCT TCA CTC AGC	58	sense
Ly6G 2240_31	ACGTCCAGACACAGCATAGG	60	sense
Ly6G 5064_61	GAG GTC CAA GAG ACT TTC TGG	60	anti-sense
Ly6G 5065_63	GGTTTTATCTGT GCA GCC C	60	sense
MLys1	CTT GGGCTG CCA GAA TTT CTC	54	sense
MLys2	TTA CAG TCG GCC AGG CTG AC	54	anti-sense
R26_IRES R	GTA AAG CAT GTG CAC CGA GG	63	anti-sense
Rosa FA	AAA GTC GCT CTG AGT TGT TAT	58	anti-sense
Rosa RA	GGA GCG GGA GAA ATG GAT ATG	58	anti-sense
Rosa26SpliAcB	CAT CAA GGA AAC CCT GGA CTA CTG	58	sense

Table 2: List of primers used for genotyping.

Sequences of oligonucleotide primers are shown in 5'- 3' and referred to as sense if the primer orientation is the same as the transcriptional direction, and anti-sense if otherwise.

A				
Step	Action	T°C	Time [s]	jump to step: X cycles
1	Denaturation	94	240	
2	Denaturation	94	30	
3	Annealing	58	30	
4	Amplification	72	45	2 x34
5	Amplification	72	300	
B				
Step	Action	T°C	Time [s]	jump to step: X cycles
1	Denaturation	95	300	
2	Denaturation	95	30	
3	Annealing	60	60	
4	Amplification	72	60	2 x 34
5	Amplification	72	600	
C				
Step	Action	T°C	Time [s]	jump to step: X cycles
1	Denaturation	94	300	
2	Denaturation	94	30	
3	Annealing	51	30	
4	Amplification	72	45	2 x 34
5	Amplification	72	420	
D				
Step	Action	T°C	Time [s]	jump to step: X cycles
1	Denaturation	94	240	
2	Denaturation	94	45	
3	Annealing	62	45	
4	Amplification	72	60	2 x 34
5	Amplification	72	600	
E				

Step	Action	T°C	Time [s]	jump to step: X cycles
1	Denaturation	95	300	
2	Denaturation	95	30	
3	Annealing	63	30	
4	Amplification	72	60	2 x 34
5	Amplification	72	600	

Table 3: List of PCR programs.

(A) Detection of K14-Cre allele, CD4-Cre allele, general Cre allele, and Rosa allele; **(B)** detection of Ly6G allele and IL1r2 allele; **(C)** detection of IL6R allele **(D)** detection of LysM-Cre allele and **(E)** detection of IL17Aind allele.

2.2.3 RNA isolation and Quantitative Real Time PCR

Small sections of frozen back skin of mice, MACS (see 2.3.2) purified CD11b⁺ bone marrow cells from mice or tomato positive sorted cells from bone marrow were taken and prepared using peqGOLD Total RNA Kit (Peqlab, Erlangen, Germany) according to manufacture instructions. Ly6G⁺ sorted cells from bone marrow (prior MACSed for CD11b) were prepared using the RNeasy Micro Kit (Qiagen, Hilden, Germany) according to manufacture instructions (without DNase digestion). Subsequently, RNA was reverse transcribed (Invitrogen, Darmstadt, Germany) into cDNA, using random primers and SuperScript II. cDNA was diluted 1:3 and used in an iCycler (Light Cycler 1.2; Roche, Switzerland) with a quantitative real-time PCR (qRT-PCR) SYBR Green PCR Kit according to manufacturer instructions. Primers for qRT-PCR analysis were purchased from Qiagen (qRT-primers shown in table 4) as described at their homepage:

<http://www.qiagen.com/products/pcr/quantitect/primerassays.aspx>

The expression level of certain genes was normalized by comparison to the expression level of the housekeeping gene hypoxanthine-guanine phosphoribosyltransferase (HPRT).

Specificity	Catalognumber	Supplier
Cntf1	QT00303478	Qiagen
Il1r2	QT00101157	Qiagen
Il17a	QT00103278	Qiagen
Il17f	QT00144347	Qiagen
Il22	QT00128324	Qiagen

Il6ra	QT00098168	Qiagen
Il6	QT00098875	Qiagen
Il1b	QT01048355	Qiagen
Osm1	QT00263193	Qiagen
Stat3	QT00148750	Qiagen
Tgf β	QT00145250	Qiagen

Table 4: List of qRT-Primers.

2.2.4 Agarose gel electrophoresis

Separation of PCR products was achieved by electrophoresis (Sambrook and Gething, 1989) on a 2% agarose gel (w/v). Agarose was diluted with 1xTAE (40mM Tris, 18mM acetic acid and 10mM EDTA pH 8) buffer. To visualize the amplified DNA fragments, ethidiumbromide (EtBr) (Fluka, Steinheim, Germany) was added to the diluted agarose, intercalating with the DNA and is visible under ultraviolet (UV) light, which was applied by an UV imager (Gel Doc™, Bio-Rad, Germany).

2.2.5 Quantification of RNA and DNA

The concentration of RNA and DNA was measured with a spectrophotometer, determining the absorption of the sample at 260 nm and 280 nm, respectively. Thereby absorption of 1 indicates to approximately 50 μ g/ml of double-stranded DNA and 40 μ g/ml in case of single-stranded DNA or RNA. Calculating the ratio between OD260 and OD280 (OD260/OD280) assessed purity of the sample. 1,8 and 2,0 is an optimum for pure DNA and pure RNA, respectively.

2.3 Cell biology

2.3.1 Preparation of single cell suspensions from mouse organs

Spleen, inguinal-, axillary- and submandibular lymph nodes (LN) were isolated from mice and pushed through a sterile sieve (40 μ m) to obtain single cell suspensions. Peritoneal cavity (PerC) and bones were flushed with a syringe containing 1x phosphate buffered saline (PBS) plus 2% (v/v) fetal calf serum (FCS) to extract cells from the peritoneum and bone marrow (BM), respectively. Syringe needles for cell isolation of PerC and BM had a size of 0.9mm x 40mm

and 0.55mm x 25mm, respectively. Red blood cells from spleen and bone marrow were lysed with 1x ACK buffer (140mM NH₄Cl, 17mM Tris-HCl pH 7,65) tris-ammonium chloride, pH 7.2 for 3min. at RT. Lysis was stopped by washing cells with 10ml PBS/FCS 2% (v/v), centrifuged (7min, 300g, 4°C), resuspended in an appropriate volume of PBS-FCS (2%) (v/v) and kept on ice for later analysis. For the purification of myeloid cells from the blood, blood was taken directly from the heart with a syringe (0.6mm x 30mm). Prior, 100µl heparin (Ratiopharm GmbH, Ulm, Germany; pre-diluted 1:5 with PBS) was injected into the heart.

Labelling of the cells with antibodies (see 2.3.4) was followed by blood lysis. Blood was lysed with BD FACS lysing solution according to the manufacture instructions.

Cells of the skin (back or ears) were digested with 0.25mg/ml Liberase TM (Roche, Switzerland) (diluted in PBS + CaCl₂ and MgCl₂) and subsequently homogenised with 0.6mm x 30mm needles. After homogenisation, cell suspension was pushed through a sterile sieve (70µm) to obtain single cell suspensions. Cells were washed once in PBS/FCS 2%, finally resuspended in an appropriate volume and kept on ice.

2.3.2 Sorting of cells by magnetic beads and FACS

For the magnetic activated cell sorting (MACS; Miltenyi Biotec, Bergisch Gladbach, Germany), a heterogeneous cell suspension was labeled with CD11b antibodies covalently linked to magnetic microbeads (5µl beads and 95µl MACS buffer (PBS, 0,5% BSA, 2mM EDTA per 1x10⁷ cells). Cell population (CD11b⁺ cells) bound by microbeads, was separated on a MACS separation column (LS) within a magnetic field. Tomato positive cells were sorted using FACSaria™ (Becton Dickinson, Franklin Lakes, USA). The purity of MACS purified CD11b⁺ cells was reviewed by FACS analysis.

FACS sorting was performed with the help of the Flow Cytometry Core Facility of the Institute of Molecular Biology (IMB) (Mainz, Germany).

2.3.3 Stimulation of MACS purified splenocytes

Total splenocytes were MACS sorted as described in 2.3.2. Cells (5×10^6) were kept in T cell medium (RPMI 1640 medium (Gibco, Long Island, NY, USA) supplemented with 10% FCS, 1mM sodium pyruvate (Gibco, Long Island, NY, USA), 2mM L-glutamine (Gibco, Long Island, NY, USA), 1x non-essential amino acids (Gibco, Long Island, NY, USA), 1% penicillin/streptomycin (Sigma, Steinheim, Germany), 10mM HEPES (Gibco, Long Island, NY, USA) and 0,1mM 2- β -mercaptoethanol (Fluka, Switzerland)) and stimulated with 20ng/ml IL-6 (Promocell, Heidelberg, Germany) for 30min. at 37°C and 200rpm. Afterwards cells were centrifuged (5min., 3000rpm, 4°C) and pellets shock frozen in liquid nitrogen (N₂).

2.3.4 Cell counting

Viable cells from single cell suspension were assessed using the trypan blue dye exclusion test. For counting of trypan blue negative cells a Neubauer chamber (Assistent, Sondheim, Germany) was used. Therefore, an aliquot of the cell suspension was diluted with physiological trypan blue solution (Gibco, Long Island, NY, USA), which stains dead cells because of their disrupted, porous cell membrane. Live cells do not take up the dye due to their intact membrane. The trypan blue negative counted cell number (N) of 16 single quadrants has to be multiplied by the dilution factor (V) and the 'chamber factor' (10^4), resulting in the number of living cells per ml ($N \times V \times 10^4 = \text{viable cell number/ml}$).

2.3.5 Flow Cytometry

Single cell suspensions were prepared from isolated organs as described in 2.3.1. 1×10^6 cells per sample were subsequently treated with Fc-Block (BioXcell, West Lebanon, NH, USA) and surface stained in 30 μ l PBS/FCS 2% (v/v) with combinations of fluoresceine isothiocyanate (FITC), phycoerythrine (PE), Peridinin-Chlorophyll (PerCP), tandem fluorochrome PE and cyanine dye Cy7 (Pe-Cy7), Allophycocyanin (APC), tandem fluorochrome APC and cyanine dye Cy7 (APC-Cy7), BD Horizon™ V450 and BD Horizon™ V500 or bio-conjugated

mAbs for 15min at 4°C (list of used antibodies see table ***). Stainings with biotinylated mAbs were followed by a secondary staining step with Streptavidin-APC-Cy7 (Pharmingen), Streptavidin-PE-Cy7 and Streptavidin-V500 (15min, 4°C). For intracellular staining, 3-5x10⁶ cells were stimulated in culture medium containing phorbol 12-myristate 13-acetate (50 ng/ml) (PMA) and ionomycin (500 ng/ml) (Iono), in the presence of Brefeldin A (1 µg/ml) (BrefA) at 37°C and 5% CO₂ for 4hrs. After staining of surface markers, cells were fixed and permeabilized (0.1% Saponin and 2% PFA), followed by intracellular staining of different cytokines (used antibodies see table ***. Intracellular antibodies are marked with a *). Labeled cells were acquired on a FACS CantoII (Becton Dickinson, Mountain View, USA) or LSRFortessa (BD, Heidelberg, Germany). Dead cells were excluded from analysis by pre-gating on cell viability dye negative cells (APC-Cy7 or V500) (for viability dyes see table 5).

Specificity	Clone	Supplier
CD11b	M1/70	eBioscience
CD126/ IL-6Ra	D7715A7	eBioscience
CD19	6D5	Biologend
CD21/35	eBio4E3	BD Bioscience
CD23	B3B4	BD Bioscience
CD3ε	145-2C11	BD Bioscience
CD4	RM4-5	BD Bioscience
CD44	IM7	eBioscience
CD45.2	104	BD Bioscience
CD45R/ B220	RA3-6B2	Biologend
CD62L	MEL-14	eBioscience
CD8	53-6.7	eBioscience
CD90.2	53-2.1	eBioscience
CD93/ AA4.1	AA4.1	eBioscience
F4/80	BM8	eBioscience
fixable viability dye		eBioscience
Gr-1/ Ly6C+Ly6G	RB6-8C5	BD Bioscience
IgD	11-26c	eBioscience
IgG2b isotype control (rat)	eB149/10H5	eBioscience
IgM	II/41	eBioscience
IL-17A*	eBio17B7	eBioscience
IL-1R2*	4E2	BD Bioscience

Ly6C	AL-21	BD Bioscience
Ly6G	1A8	Biolegend
pSTAT3 (pY705)*	4/P-STAT3	BD Bioscience
V γ 2 (V γ 4)	UC3-10A6	Biolegend
V γ 3 (V γ 5)	536	Biolegend
β TCR	H57-597	eBioscience
$\gamma\delta$ TCR	eBio GL3	eBioscience

Table 5: List of antibodies used for flow cytometry

2.3.6 *pSTAT3 staining*

Single cell suspensions were prepared from spleen as described in 2.3.1 and 1×10^6 cells per sample were surface stained as described in 2.3.5. Next, the cells were cultured for 2h 37°C in T cell medium. Cells were stimulated for 30min. at 37°C by adding the appropriate volume of IL-6 (Promocell, Heidelberg, Germany) to achieve a final concentration of 50ng/ml. The stimulation was stopped, by adding Formaldehyde with a final concentration of 1.5% to fix the cells. After the incubation time of 10min. at RT, cells were centrifuged with 500g for 5min. For permeabilization, cells were resuspended in 200 μ l of ice cold Methanol and incubated for 20min. at 4°C. Cells were centrifuged again (500g for 5min.) and then stained intracellular with pSTAT3 (2.3.5) for 30min. at 4°C in PBS/FCS 2%.

2.3.7 *Histological analysis and immunohistochemistry*

Tissues frozen in tissue freezing medium (Jung, Nussloch) (on dry ice and afterwards stored at -80°C) were sectioned in 8 μ m slices, air dried, and fixed with 4% PFA for 20min. at RT. Using a Pap pen, the tissue was outlined on a glass slide, placed in a wet chamber with tris buffer saline (TBS) was added for 5 min at RT. Slides were incubated with quenching buffer containing 0,3% (v/v) H₂O₂ for 30min. and washed once with TBS. The sections were incubated with avidin (Vector Kit SP-2001) and biotin solution (Vector Kit SP-2001) for 15min. each and subsequently washed three times with TBS containing 2% BSA. Afterwards the sections were incubated with different primary antibodies in a wet chamber over night at 4°C. The following primary antibodies were used: rat anti-mouse F4/80 (eBioscience BM8) or rabbit anti-mouse Myeloperoxidase (MPO) (Abcam ab15484). The next day, sections were washed 3 times with TBS and incubated

with secondary antibodies for 30min at RT. The following secondary antibodies were used: anti-rabbit biotin (DIANOVA, Hamburg, Germany) and anti-rat biotin (BD Pharmingen, Heidelberg, Germany). Immunofluorescence of cryosections was performed using the TSA Cy3 and TSA Fluorescein (PerkinElmer, Rodgau, Germany) and fluorescence microscope Olympus IX81. Nuclei were counterstained with Hoechst 33342 (Invitrogen, Darmstadt, Germany). Tissues were mounted in Vectashield H-1000.

2.4 Biochemistry

2.4.1 Preparation of total protein extracts

For total protein lysates, 5×10^6 cells from frozen cell pellets, were lysed in 40 μ l RIPA buffer (Invitrogen, Darmstadt, Germany) supplemented with protease inhibitor cocktail (Roche, Switzerland), phosphatase inhibitor (Roche, Switzerland) and 1mM Dithiothreitol (DTT). Cells were resuspended and kept on ice for 15min. During incubation time, cells were lysed by gently mixing up and down every 5 min. After spinning down at 14.800 rpm for 10min at 4°C, supernatant (total protein) was transferred into a fresh tube. Concentration of proteins was determined in duplicates by using Bradford assay (Bio-Rad, Germany).

2.4.2 Western Blot

Protein lysates were loaded in an equal amount and ran on 4-12% (gradient) SDS-PAGE gels from NUPAGE® Novex Gel Systems (Invitrogen, Darmstadt, Germany), using Bio-Rad gel electrophoresis chambers (Bio-Rad, Germany). Afterwards, gels were blotted with a semi-dry blot system (Bio-Rad, Germany) on a polyvinylidene fluoride membrane. Membranes were blocked for 1hr with 5% milk powder (MP) in TBS containing 0,1% Tween at RT and incubated o/n with different primary antibodies (pSTAT3 (clone 3E2, Cell Signaling, USA) and Actin (clone I-19, Santa Cruz). Secondary horseradish peroxidase (HRP) conjugated anti-rabbit and anti-mouse antibodies were purchased from SantaCruz or Bio-Rad. ECL Plus reagent from GE Healthcare was used as substrate for the HRP reaction and for blot developing.

2.5 Immunohistochemistry

2.5.1 Enzyme-linked Immunosorbent Assay

IL-17A or IL-6 serum concentrations were determined with an Enzyme-linked Immunosorbent Assay (ELISA). Flat bottom microtiter plates (Greiner, Frickenhausen, Germany) were coated with the capture antibody for IL-17A (rat anti-mouse IL-17A; TC11-8H4) diluted in coating buffer (0.1M Sodium Carbonate, 0.1M Sodium bicarbonate pH 9.5) at 4°C o/n. Next day, plates were blocked with blocking buffer (1xPBS/FCS, 10% (v/v) FCS) for 1h at RT. Subsequently, serially diluted (dilution buffer = blocking buffer) blood sera from mice and respective standards were applied to wells and incubated for 1h. This was followed by adding a secondary biotinylated antibody (IL-17A: biotin rat anti-mouse IL-17A; TC11-18H10) for 1h at RT. Afterwards an Avidin (AV)-HRP (in case of IL-6 directly coupled to biotin antibody) was incubated with the samples for 1h at RT. To determine the antibody binding, Tetramethylbenzidine (TMB) was used as a substrate solution. To stop the reaction phosphoric acid (H₃PO₄) was added to each well. Each incubation step was followed by three to five washing steps with washing buffer (1xPBS, 0,05% (w/v) Tween 20) to remove unbound antibodies or SA-conjugated HRP. To detect the cytokine levels of sIL-6R α , a DuoSet® ELISA from R&D systems (DY1830) was performed. All corresponding antibodies were used from R&D systems according to manufacture instructions.

The OD₄₅₀ for all cytokines was measured with an ELISA-photometer (Tecan Infinite M200, Pro Nano Quant). The standard curve demonstrated direct relationship between OD and secreted cytokine levels.

Determination of the relative antibody concentration was done using SoftMax Pro version 2.2.2.

2.6 Mouse experiments

Tail bleeding as well as the general handling of mice was performed according to Hogan (Hogan et al., 1987) and Silver (Silver et al., 1995).

2.6.1 Mice

The following mouse strains were used for experiments of this thesis:

LysM-Cre mice (Clausen et al., 1999) were crossed to IL-6R $\alpha^{FL/FL}$ mice (Wunderlich et al., 2010). K14-Cre mice (Hafner et al., 2004) were crossed to IL-17A^{ind/+} mice (Croxford et al., 2014). Furthermore, IL1r2^{fl/fl} (Taconic Biosciences, Cologne, Germany) were crossed to Ly6G-Cre (Catchup) mice (Hasenberg et al., 2015), CMV-Cre mice (Schwenk et al., 1995) or CD4-Cre mice (Wolfer et al., 2001) to achieve tissue specific deletion of the Il1r2 gene. Catchup mice were also crossed to iDTR^{fl/fl} mice (Buch et al., 2005) or analyzed just as heterozygous Ly6G^{+/-} (k.o.) mice.

C57Bl/6 were obtained from the Central Animal Facility Institution of the University of Mainz (ZVTE, University of Mainz), Janvier or Harlan. BALB/cj and CMV-Cre mice were obtained from ZVTE, Mainz. All mice were generated on C57Bl/6 genetic background or bred for at least 10 generations to this background and housed in specific pathogen-free conditions. All animal experiments were in accordance with the guidelines of the ZVTE, University of Mainz.

2.6.2 Imiquimod treatment

At the age of 7-8 weeks, female mice were treated with *Aldara*TM (5% IMQ; Meda AB, Solna, Sweden) or sham cream (van der Fits et al., 2009) on ears (each with 5mg) and the back skin (50mg) for 5-7 consecutive days. For treating only the ears, also male mice were used independent of the age. In this setup the same amount of *Aldara*TM was used as before (see above) for 5 consecutive days.

2.6.3 PASI score

To measure the severity of inflammation on the back, a scoring system similar to the human PASI (Psoriasis Area and Severity Index) score was used. In mice, this score considers the parameters of skin thickness, scaling and erythema. A cumulative PASI score or the individual score concerning one of the parameters (skin thickness, scaling, erythema) is shown. The measurement of the skin

thickness was performed in triplicates with a dial thickness gage (Mitutoyo, Kawasaki, Japan).

2.6.4 *Anti-IL-17A treatment*

To neutralize the cytokine IL-17A, mice were treated with an anti-IL-17A antibody (Novartis, Switzerland; BZN035) in different experimental setups:

K14-IL-17A^{ind/+} mice were treated for 6.5 weeks with two different batches of antibody starting with an age of 3 weeks. The applied amount of antibody was 60mg/kg body weight twice a week.

C57Bl/6 mice were injected with anti-IL-17A during IMQ treatment on day 0 and 4 with 0.2mg/mouse or on day 0, 3 and 6 with 0.6mg/mouse. Anti-Cyclosporine A was used as an Isotype control. Antibody and Isotype were diluted in PBS. The antibody was kindly provided by Novartis.

2.6.5 *Injection of Diphtheria Toxin*

To specifically deplete neutrophils, Catchup mice (Hasenberg et al., 2015) were crossed to the iDTR (Buch et al., 2005) strain. This crossing results in the removal of the STOP cassette and the expression of DTR on Ly6G positive cells. A subsequent injection of Diphtheria Toxin (DT) into the mice leads to a cell death in the specific tissue. Mice were injected with 25ng/g mouse weight of DT (Calbiochem, San Diego, USA) only once or for three consecutive days. After the last injection, mice were sacrificed the next day.

2.7 **Statistics and Software**

For analyzing data of fluorescence-activated cell sorting (FACS), FlowJo® Version 8.87 was used. For statistics, Prism® (GraphPad 5 Software Inc.) and Microsoft Excel were used. Values are typically as mean ± SEM (standard error of the mean). For statistical analysis first the Kolmogorov-Smirnov test was performed to test normal distribution. If this was given 2-tailed unpaired Student's *t*-test or 1-way ANOVA were applied. If there was no normal distribution, Mann-Whitney or Kruskal-Wallis was used as appropriate. P-values

< 0.05 were regarded significant, displayed by “*” in the figures (** = p-values < 0.005; *** = p-values < 0.001).

3 Results

3.1 Neutralization of IL-17A in *K14-IL-17A^{ind/+}* mice

3.1.1 *Reduced clinical scores in anti-IL-17A treated K14-IL-17A^{ind/+} mice*

The pro-inflammatory cytokine IL-17A is known to play a critical role in human psoriasis (Di Cesare et al., 2009; Lowes et al., 2013); up-regulation of IL-17 correlated with the cumulative Psoriasis Area and Severity Index (PASI) in psoriasis patients (Arican et al., 2005). As there is still a lack of mouse models to study this disease, our group developed a mouse strain where IL-17A is specifically over expressed by keratinocytes, resulting in a psoriasis-like phenotype (*K14-IL-17A^{ind/+}*) (Croxford et al., 2014). With these mice it could already be shown that an anti-IL-6 treatment reduced the accumulation of neutrophil microabscesses in the skin. However, antibodies targeting IL-17 are also successfully used for the treatment of psoriasis and related diseases (Elyoussfi et al., 2016; Ratner, 2015). We investigated an anti-IL-17A treatment in *K14-IL-17A^{ind/+}* mice in collaboration with Novartis, who developed an anti-IL-17A antibody with low immunogenicity to treat autoimmune diseases (Karle et al., 2016).

As described above, for this experiment, K14-Cre mice were crossed to IL-17A^{ind/+} mice to achieve the overexpression of IL-17A specifically in keratinocytes (Fig. 7A). The mice were treated at three weeks of age over a period of six weeks with a high dose of the anti-IL-17A antibody or isotype control (60mg/kg body weight). An ELISA of the blood sera after three weeks of treatment indicated a neutralization of IL-17A, as the sera levels of IL-17A in anti-IL-17A treated mice were significantly reduced compared to isotype treated mice (Fig. 7B). Furthermore, clinical scores of the PASI, which is adapted from the severity index used for psoriasis patients (El Malki et al., 2013), were slightly decreased in anti-IL-17A treated mice compared to isotype and PBS treatment (Fig. 7C), during the course and progression of psoriasis.

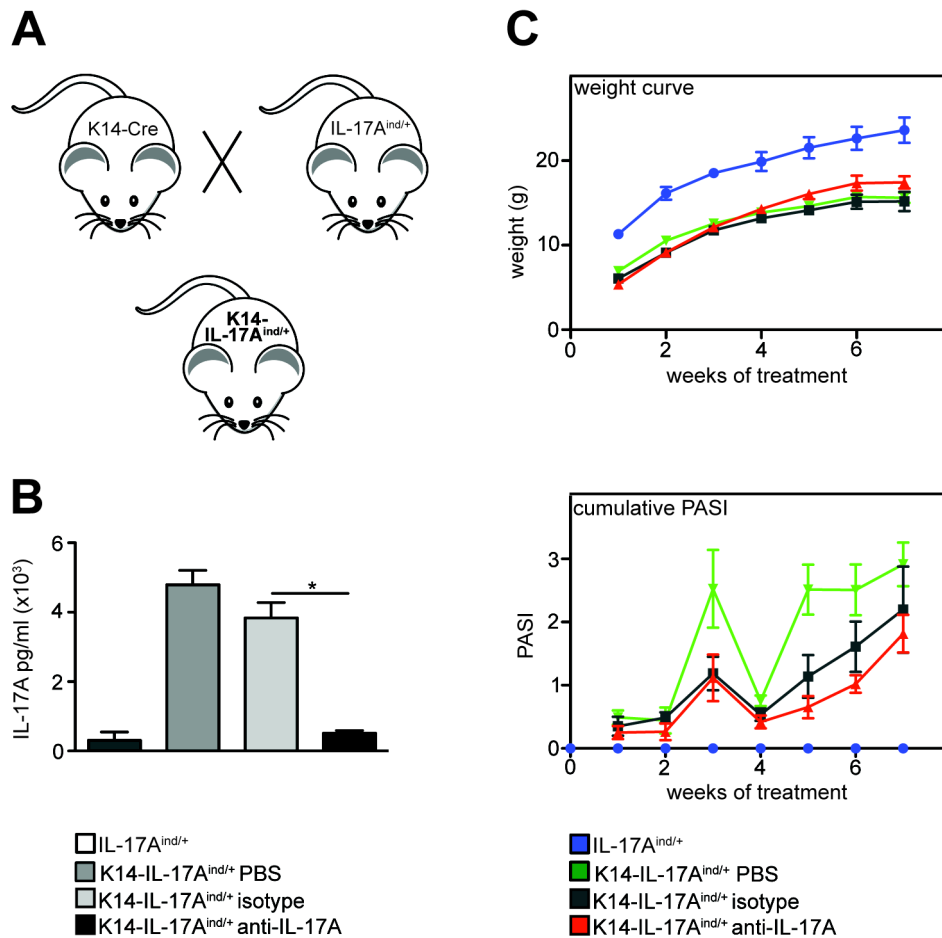


Figure 7: Neutralization of IL-17A in *K14-IL-17A^{ind/+}* mice leads to milder clinical scores

(A) Schematic representation of the crossing to obtain *K14-IL-17A^{ind/+}* mice. K14-Cre mice were crossed to IL-17A^{ind/+} mice to achieve an overexpression of IL-17A specifically in keratinocytes (*K14-IL-17A^{ind/+}* mice). (B) Serum Levels of IL-17A in untreated, PBS-, isotype- or anti-IL-17A treated mice after three weeks of treatment measured by ELISA. Data are shown as bar graphs with mean and SEM. * $p \leq 0,05$ Significance was calculated using Mann Whitney test between isotype- and anti-IL-17A treated groups (untreated group $n=2$, PBS group $n=2$; isotype group $n=4$; anti-IL-17A group $n=5$). (C) Weight and cumulative PASI (consistent of skin thickness, erythema, scaling and affected area) of indicated experimental groups. Modified PASI was scored twice a week (untreated group $n=2$, PBS group $n=2$; isotype group $n=4$; anti-IL-17A group $n=5$). Animals were treated twice a week with either isotype or anti-IL-17A (0.6mg/injection) over a period of 6.5 weeks.

3.1.2 Anti-IL-17A treatment of *K14-IL-17A^{ind/+}* mice shows influence on myelomonocytic cells in the spleen

Next, we wanted to determine if the antibody treatment had an influence on infiltrating cells in the skin and secondary lymphoid organs. As *K14-IL-17A^{ind/+}* mice show an increase of neutrophils and monocytes in different organs (Croxford et al., 2014), we first investigated the distribution of myelomonocytic cells.

Neutrophils and monocytes are increased in the skin of patients with psoriatic skin inflammation (Lowes et al., 2013; Terui et al., 2000).

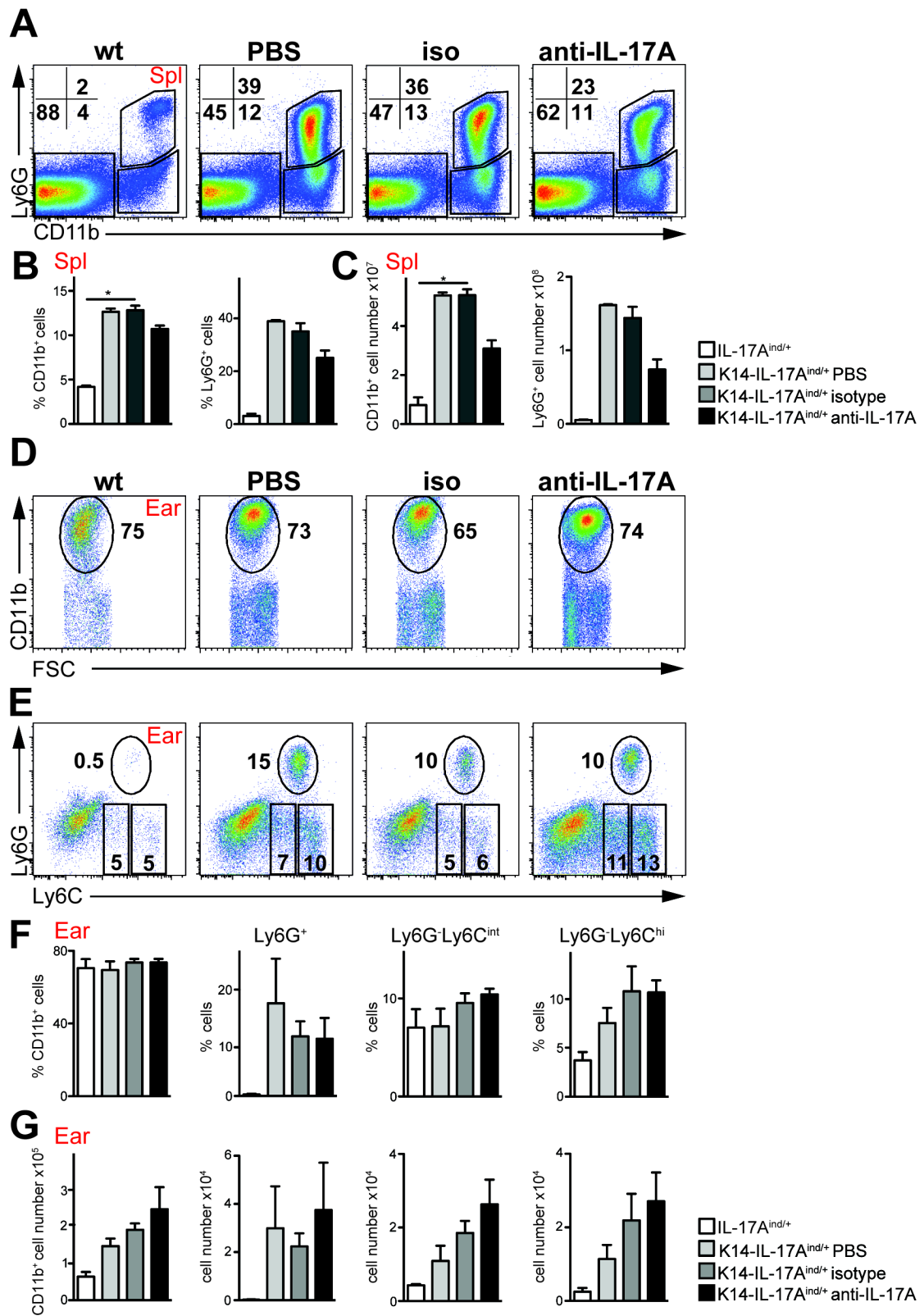


Figure 8: *K14-IL-17A^{ind/+}* mice treated with anti-IL-17A show no effect on infiltrating myelomonocytic cells

(A) Flow cytometric analysis of splenic CD11b⁺ and CD11b⁺Ly6G⁺ cells. Cells are pre-gated on living CD90.2⁺/B220⁺/CD45.2⁺ cells. **(B)** Percentages of CD11b⁺ and CD11b⁺Ly6G⁺ cells of the spleen. Bar graphs are shown with mean and SEM. * $p \leq 0,05$ Significance was calculated using Kruskal-Wallis test (untreated group n=2, PBS group n=2; isotype group n=4; anti-IL-17A group n=5). **(C)** Total cell numbers of CD11b⁺ and CD11b⁺Ly6G⁺ cells of the spleen. Bar graphs are shown with mean and SEM. * $p \leq 0,05$ Significance was calculated using Kruskal-Wallis test (untreated group n=2, PBS group n=2; isotype group n=4; anti-IL-17A group n=5). **(D)** Flow cytometric analysis of CD11b⁺ cells of the ears. Cells are pre-gated on living CD90.2⁺/B220⁺/CD45.2⁺ cells. **(E)** Flow cytometric analysis of neutrophils (Ly6G⁺), pro-inflammatory monocytes (Ly6G⁺Ly6C^{hi}) and resident monocytes (Ly6G⁺Ly6C^{int}) of the ears. Cells are pre-gated on living CD90.2⁺/B220⁺/CD45.2⁺ and CD11b⁺ cells. **(F-G)** Percentages **(F)** and total cell numbers **(G)** of CD11b⁺ cells, neutrophils (Ly6G⁺), pro-inflammatory monocytes (Ly6G⁺Ly6C^{hi}) and resident monocytes (Ly6G⁺Ly6C^{int}) of the ears. Bar graphs are shown with mean and SEM. Significance was calculated using Kruskal-Wallis test (untreated group n=2, PBS group n=2; isotype group n=4; anti-IL-17A group n=5).

Flow cytometric analysis of the spleen revealed increased percentages of infiltrating CD11b⁺ (all myelomonocytic cells) and Ly6G⁺ (neutrophils) cells in *K14-IL-17A^{ind/+}* mice compared to *wt* mice (Fig. 8A and B). Besides this, there was a trend that the anti-IL-17A treated group showed less CD11b⁺ and Ly6G⁺ cells compared to the isotype and PBS treated groups. Moreover, the same result was obvious in total cell numbers (Fig. 8C), where the trend was even more evident than with the percentages. As we wanted to examine whether the anti-IL-17A treatment had an effect on the severity of skin inflammation, we also performed flow cytometric analysis of the ears. Contrary to the spleen, the percentage of infiltrating CD11b⁺ cells was similar in all groups (Fig. 8D and F). In terms of total cell numbers the anti-IL-17A treated group showed even more infiltration compared to the PBS and isotype treated mice (Fig. 8G). Analyzing the sub-populations of CD11b⁺ cells, we differentiated neutrophils (Ly6G⁺), pro-inflammatory monocytes (Ly6G⁺Ly6C^{hi}) and resident monocytes (Ly6G⁺Ly6C^{int}) in the ears (Rose et al., 2012). Surprisingly, all groups of mice showed comparable infiltration of myelomonocytic cells in percentages (Fig. 8E and F) and total cell numbers (Fig. 8G).

In addition, it was already shown that *K14-IL-17A^{ind/+}* have a different proportion of $\gamma\delta$ TCR⁺ and β TCR⁺ cells (Croxford et al., 2014) than *wt* mice, meaning they have less $\gamma\delta$ T cells. We wanted to examine if an anti-IL-17A treatment may have an influence on the distribution of β TCR⁺ cells versus $\gamma\delta$ T cells. For this, we performed flow cytometric analysis of $\gamma\delta$ T cells and β TCR⁺ cells in spleen and

ears. In the spleen, both populations showed no differences in percentages and total cell numbers within all four groups (Fig. 9A-C).

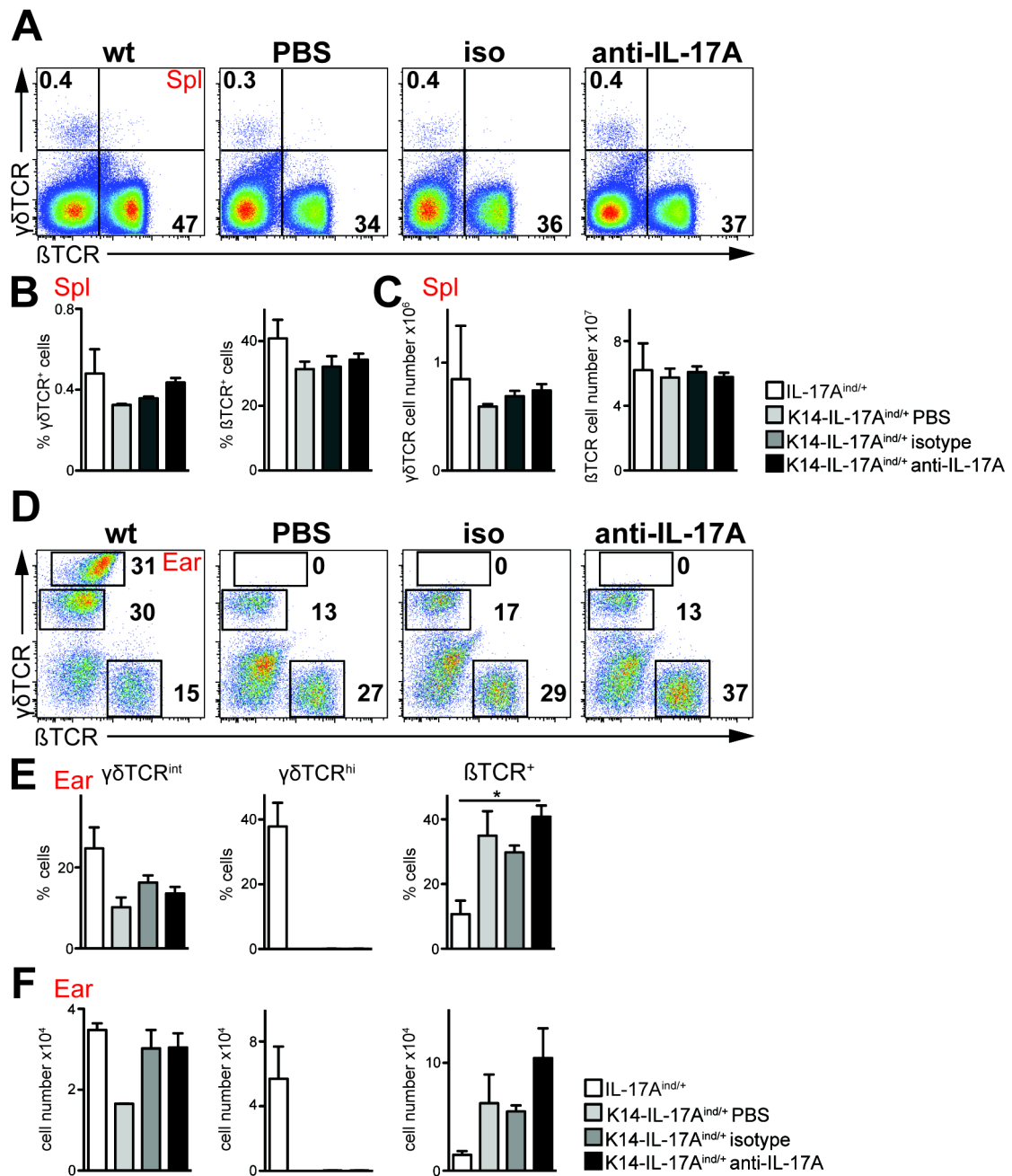


Figure 9: Treatment with anti-IL-17A shows no effect on T cell populations in *K14-IL-17A^{ind/+}* mice

(A) Flow cytometric analysis of splenic $\gamma\delta$ TCR⁺ and β TCR⁺ T cells of indicated experimental groups. Cells are pre-gated on living CD45.2⁺/CD11b⁻/Ly6G⁻ cells. **(B-C)** Percentages **(B)** and total cell numbers **(C)** of $\gamma\delta$ TCR⁺ and β TCR⁺ T cells of the spleen. Bar graphs are shown with mean and SEM. Significance was calculated using Kruskal-Wallis test (untreated group n=2, PBS group n=2; isotype group n=4; anti-IL-17A group n=5). **(D)** Flow cytometric analysis of dermal- ($\gamma\delta$ TCR^{int}), epidermal ($\gamma\delta$ TCR^{hi}) $\gamma\delta$ T cells and β TCR⁺ cells in the ears of indicated experimental groups. Cells are pre-gated on living CD90.2⁺/CD45.2⁺ cells. **(E-F)** Percentages **(E)** and total cell numbers **(F)** of $\gamma\delta$ TCR^{int}, $\gamma\delta$ TCR^{hi} and β TCR⁺ in the ears. Data are shown as bar graphs with mean and SEM. * $p \leq 0,05$ Significance was calculated using Kruskal-Wallis test (untreated group n=2, PBS group n=2; isotype group n=4; anti-IL-17A group n=5).

However, in the ears we could observe that in *K14-IL-17A^{ind/+}* the population of epidermal $\gamma\delta$ T cells ($\gamma\delta$ TCR^{hi}) is completely absent (Fig. 9D). Moreover, while dermal $\gamma\delta$ T cells ($\gamma\delta$ TCR^{int}) are strongly reduced in *K14-IL-17A^{ind/+}* mice compared to the *wt* group, we find more β TCR⁺ in the former group (Fig. 9D and E). This result was also confirmed by the calculation of total cell numbers (Fig. 9F). Conclusively, the treatment with anti-IL-17A antibody had no influence on the original distribution of T cell populations in *K14-IL-17A^{ind/+}* mice.

3.1.3 Repetition of anti-IL-17A treatment in *K14IL17A^{ind/+}* mice shows no improvement in terms of infiltrating myelomonocytic cells and T cells

To prove the results from the first experiment, we performed a repetition of the experiment with the same set up as described above (3.1.1). After six weeks of treatment, pictures of the mice were taken to evaluate the severity of skin inflammation (Fig. 10A). It was obvious that all groups of *K14-IL-17A^{ind/+}* mice still suffered from scaly, red and inflamed back skin, whereas the untreated group seemed to have less psoriatic plaques compared to isotype and anti-IL-17A treated mice (Fig. 10 A). This time the IL-17A ELISA was performed from sera of the six weeks treated mice, but showed a similar result as the first experiment (Fig. 10B): the anti-IL-17A treated mice had 4-5 times less IL-17A in the sera as isotype or untreated mice (Fig. 10B). In addition, the cumulative PASI of the untreated mice was decreased compared to the isotype and anti-IL-17A treated group, but no significant differences could be observed between the latter two groups (Fig. 10C) during the time of treatment. These data are in line with the results of the pictures acquired (Fig. 10A). However, it is important to

mention that the untreated mice were included in the experiment four weeks after the treatment of the other mice started. It has been shown that stress is an environmental factor, which can have an influence on the severity of skin disease (Schwartz et al., 2016). Hence, as the untreated mice were less exposed to stress through the treatment, it is difficult to compare these mice to the other groups.

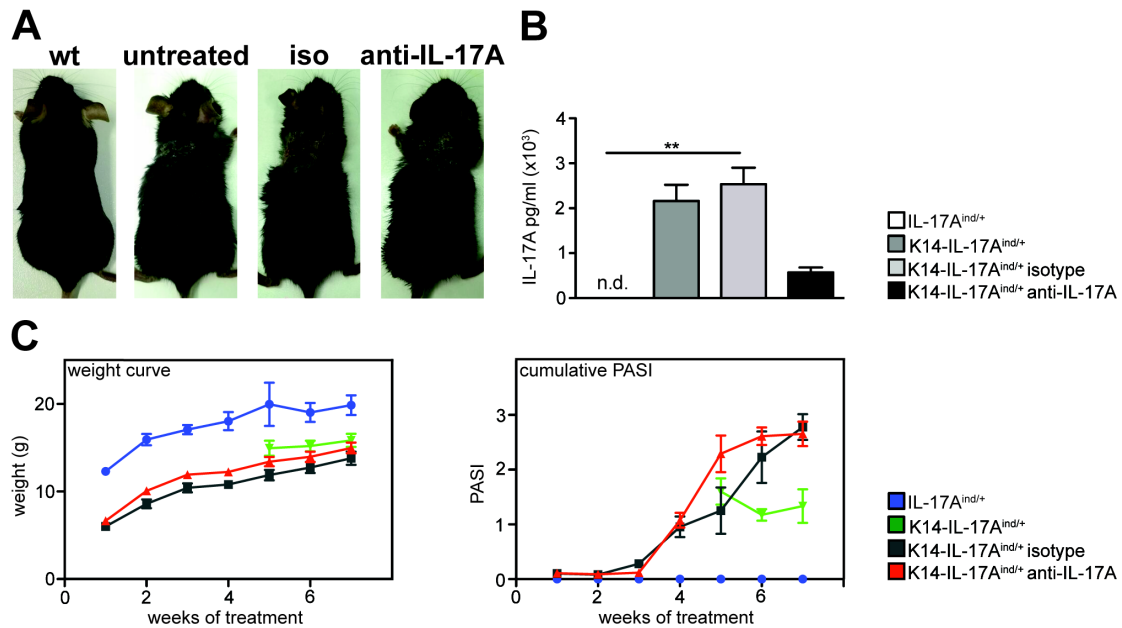


Figure 10: 2nd experiment shows no effect on clinical scores after neutralization of IL-17A in *K14-IL-17A^{ind/+}* mice

A) Pictures of untreated *wt* mice and untreated, isotype- and anti-IL-17A treated *K14-IL-17A^{ind/+}* mice after six weeks. **(B)** Serum Levels of IL-17A in untreated, isotype- or anti-IL-17A treated mice after six weeks of treatment measured by ELISA. Data are shown as bar graphs with mean and SEM. ** $p \leq 0,005$ Significance was calculated using Kruskal-Wallis test (*wt* group $n=3$, untreated group $n=2$; isotype group $n=4$; anti-IL-17A group $n=4$). **(C)** Shown is weight and cumulative PASI (consistent of skin thickness, erythema, scaling and affected area), scored twice a week with a modified PASI from humans (*wt* group $n=3$, untreated group $n=2$; isotype group $n=4$; anti-IL-17A group $n=4$). Isotype and anti-IL-17A treated mice were treated twice a week with a dose of 0.6mg/injection during the time of 6.5 weeks.

3.1.4 Repetition of anti-IL-17A treatment in *K14IL17A^{ind/+}* mice shows no improvement in terms of infiltrating myelomonocytic cells and T cells

To achieve a good comparison to the first experiment, again the distribution of myelomonocytic cells in the spleen and the ears was examined by flow cytometry. In the spleen the untreated mice show the lowest numbers of CD11b⁺ and Ly6G⁺ infiltrating cells within the *K14IL17A^{ind/+}* groups (Fig. 11A-C). The group of anti-IL-17A treated mice had even higher numbers in terms of percentages and total cell numbers in the myelomonocytic cell compartment (Fig. 11A-C), compared to the first experiment (Fig. 8A-C). Furthermore, the distribution of myelomonocytic cells in the ears showed a similar result as observed in the spleen. Surprisingly, the numbers of CD11b⁺ cells are comparable between isotype and anti-IL-17A treated groups, whereas the untreated mice show fewer cells, similar to the numbers of the *wt* group (Fig. 11D and F). Next, we analyzed various sub-populations of CD11b⁺ cells: neutrophils, pro-inflammatory monocytes and resident monocytes. Except for neutrophils, all three groups of *K14IL17A^{ind/+}* mice showed more or less the same amount of infiltrating myelomonocytic cells in percentages (Fig. 11E and F). Anti-IL-17A treated animals showed the highest proportion of infiltrating cells in total cell numbers in all investigated populations; the untreated group was comparable to *wt* (Fig. 11G). This result leads to the assumption that the neutralization of IL-17A had no effect on the myelomonocytic cell compartment, confirming the results of the cumulative PASI (Fig. 10C).

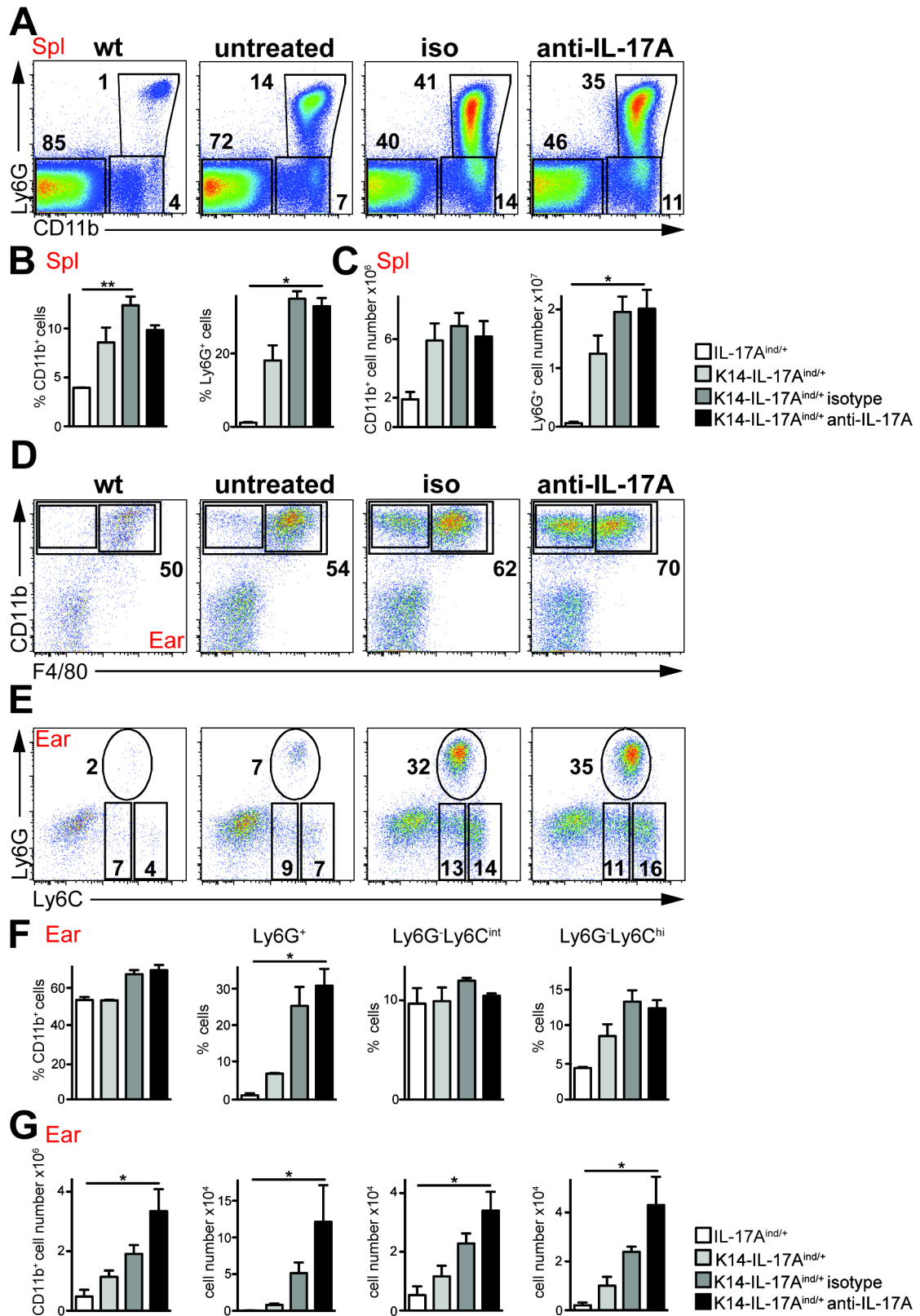


Figure 11: anti-IL-17A treatment of *K14-IL-17A^{ind/+}* mice shows no effect on infiltrating myelomonocytic cells in 2nd experiment

(A) Flow cytometric analysis of splenic CD11b⁺ and CD11b⁺Ly6G⁺ cells of indicated experimental groups. Cells are pre-gated on living CD90.2⁻/B220⁻/CD45.2⁺ cells. **(B-C)** Percentages **(B)** and total cell numbers **(C)** of CD11b⁺ and CD11b⁺Ly6G⁺ cells of the spleen. Bar graphs are shown with mean and SEM. * $p \leq 0,05$, ** $p \leq 0,005$ Significances were calculated using Kruskal-Wallis test (*wt* group $n=3$, untreated group $n=2$; isotype group $n=4$; anti-IL-17A group $n=4$). **(D)** Flow cytometric analysis of CD11b⁺ cells of the ears. Cells are pre-gated on living CD90.2⁻/B220⁻/CD45.2⁺ cells. **(E)** Flow cytometric analysis of neutrophils (Ly6G⁺), pro-inflammatory monocytes (Ly6G⁻Ly6C^{hi}) and resident monocytes (Ly6G⁻Ly6C^{int}) of the ears. Cells are pre-gated on living CD90.2⁻/B220⁻/CD45.2⁺ and CD11b⁺ cells (*wt* group $n=3$, untreated group $n=2$; isotype group $n=4$; anti-IL-17A group $n=4$). **(F-G)** Percentages **(F)** and total cell numbers **(G)** of CD11b⁺ cells, neutrophils (Ly6G⁺), pro-inflammatory monocytes (Ly6G⁻Ly6C^{hi}) and resident monocytes (Ly6G⁻Ly6C^{int}) of the ears. Bar graphs are shown with mean and SEM. * $p \leq 0,05$ Significance was calculated using Kruskal-Wallis test (*wt* group $n=3$, untreated group $n=2$; isotype group $n=4$; anti-IL-17A group $n=4$).

To complete the analysis of infiltrating cells upon anti-IL-17A treatment, we also investigated the distribution of T cell subpopulations by flow cytometry. Again, in the spleen both populations ($\gamma\delta$ T cells and β TCR⁺ cells) showed no differences in percentages and total cell numbers between all four groups (Fig. 12A-C). In addition, the results of the ears are very similar to the results obtained in the first experiment, namely epidermal $\gamma\delta$ T cells were completely absent and the numbers of dermal $\gamma\delta$ T cells were decreased in the groups of *K14-IL-17A^{ind/+}* mice compared to *wt* (Fig. 12D). Moreover, all *K14-IL-17A^{ind/+}* groups show comparable numbers in percentages and total cell numbers of $\gamma\delta$ TCR^{hi}, $\gamma\delta$ TCR^{int} and β TCR⁺ cells (Fig. 12E and F), independently of their treatment. This result indicated that the neutralization of IL-17A has no influence on T cell populations. However, the percentage of $\gamma\delta$ T cells in the ears between the two performed experiments was diverse. The FACS plots of the second experiment showed decreased percentages of $\gamma\delta$ T cells in all groups than the first experiment (Fig. 12D and Fig. 9D). As the same result could be observed in *wt* mice, this result cannot be a consequence of treatment. Nonetheless the result is convincing, as the distribution of percentages and total cell numbers within the groups of both experiments is comparable.

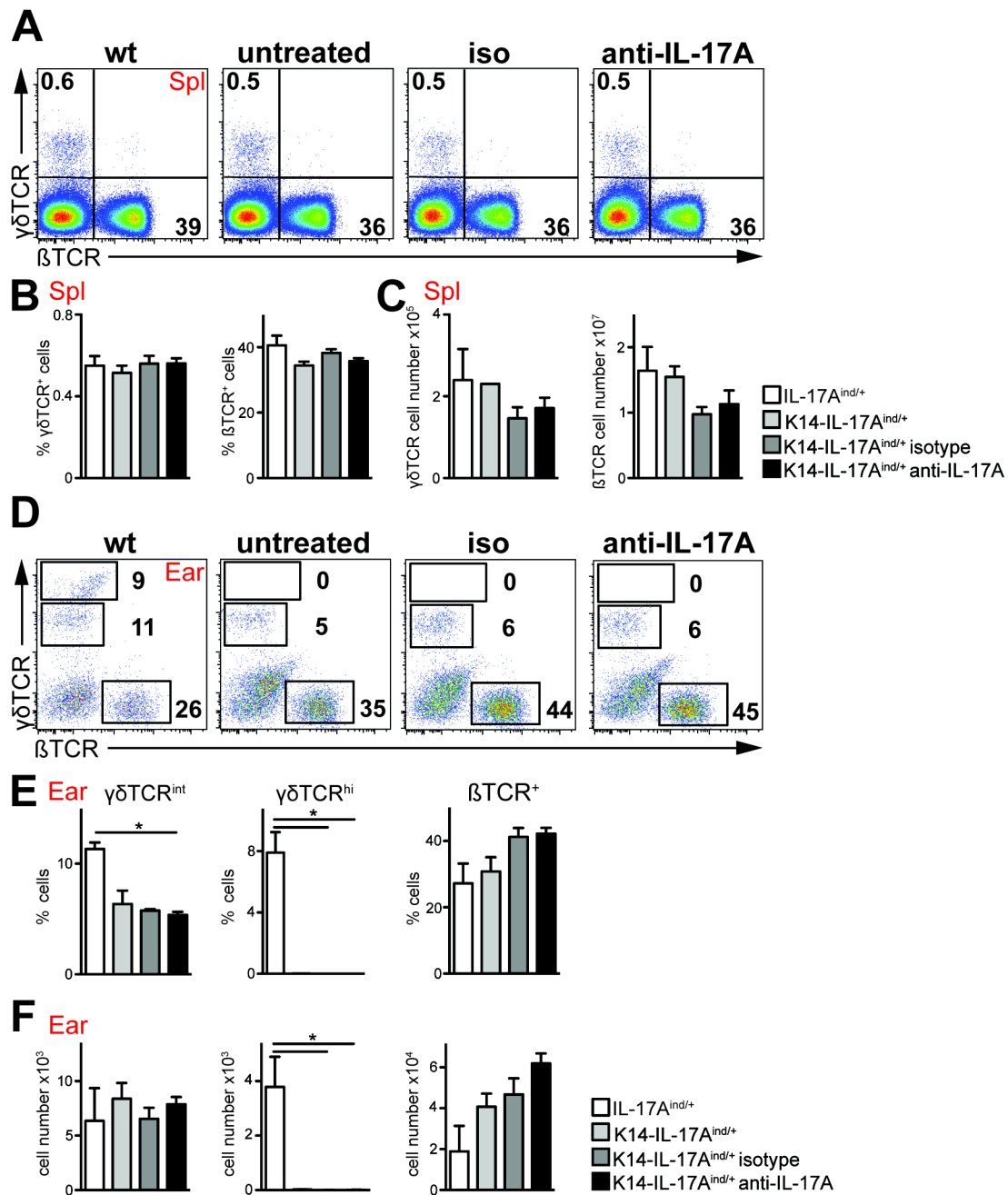


Figure 12: anti-IL-17A treatment of *K14-IL-17A^{ind/+}* mice shows no effect on T cell populations in 2nd experiment

(A) Flow cytometric analysis of splenic $\gamma\delta$ TCR⁺ and β TCR⁺ T cells of the indicated experimental groups. Cells are pre-gated on CD45.2⁺/CD11b⁻/Ly6G⁻ cells. **(B-C)** Percentages **(B)** and total cell numbers **(C)** of $\gamma\delta$ TCR⁺ and β TCR⁺ cells of the spleen. Bar graphs are shown with mean and SEM. Significance was calculated using Kruskal-Wallis test (*wt* group *n*=3, untreated group *n*=2; isotype group *n*=4; anti-IL-17A group *n*=4). **(D)** Flow cytometric analysis of dermal- ($\gamma\delta$ TCR^{int}), epidermal ($\gamma\delta$ TCR^{hi}) $\gamma\delta$ T cells and β TCR⁺ cells in the ears. Cells are pre-gated on living CD90.2⁺/CD45.2⁺ cells. **(E-F)** Percentages **(E)** and total cell numbers **(F)** of $\gamma\delta$ TCR^{int}, $\gamma\delta$ TCR^{hi} and β TCR⁺ in the ears. Data are shown as bar graphs with mean and SEM. * *p* ≤ 0,05 Significance was calculated using Kruskal-Wallis test (*wt* group *n*=3, untreated group *n*=2; isotype group *n*=4; anti-IL-17A group *n*=4).

3.2 Anti-IL-17A treatment of *wt* mice in IMQ-induced psoriasis-like skin disease

3.2.1 Neutralization of IL-17A shows an impact on clinical scores with high dose of 0.6mg/treatment

IMQ-induced psoriasis is a common mouse model of psoriasis like disease. *Aldara*TM cream, which contains 5% Imiquimod (IMQ), is applied to the skin and leads to dermal damage similar to human psoriasis (van der Fits et al., 2009). Furthermore, IL-17 producing cells are also increased in the skin of IMQ-treated mice (Cai et al., 2011; van der Fits et al., 2009). Recently, our group demonstrated that mice with a deletion of IL-17RA still develop a psoriasis-like disease under IMQ treatment, but milder compared to *wt* mice (El Malki et al., 2013).

According to this data, we induced the psoriasis-like disease in *wt* mice by treating the mice with IMQ for 5 or 7 consecutive days. In addition, mice were treated with anti-IL-17A in two different concentrations (0.2mg/injection or 0.6mg/injection) during the application of IMQ, to see whether the treatment might have a dose-dependent effect. As a control, mice were also treated with an isotype in the same concentration as the anti-IL-17A antibody. As expected, the measured parameters such as scaling and erythema and back/ear skin thickness, increased during the time of treatment, except for the weight. However, the clinical scores of the low dose treatment (0.2mg/injection) did not show any differences between the anti-IL-17A and isotype treated group (Fig. 13A). Only the scaling of the anti-IL-17A treated mice was slightly decreased (Fig. 13A).

Besides this, treatment with the higher dose of anti-IL-17A (0.6mg/injection) showed a stronger effect in the clinical scores. Here, right ear thickness and erythema were significantly reduced compared to the isotype and PBS treated groups on day 7 (Fig. 13B). A similar result can be seen in the scaling. Moreover, skin thickness and left ear thickness showed a similar trend (Fig. 13B), indicating that the high dose treatment of anti-IL-17A had a stronger effect on the severity of skin inflammation.

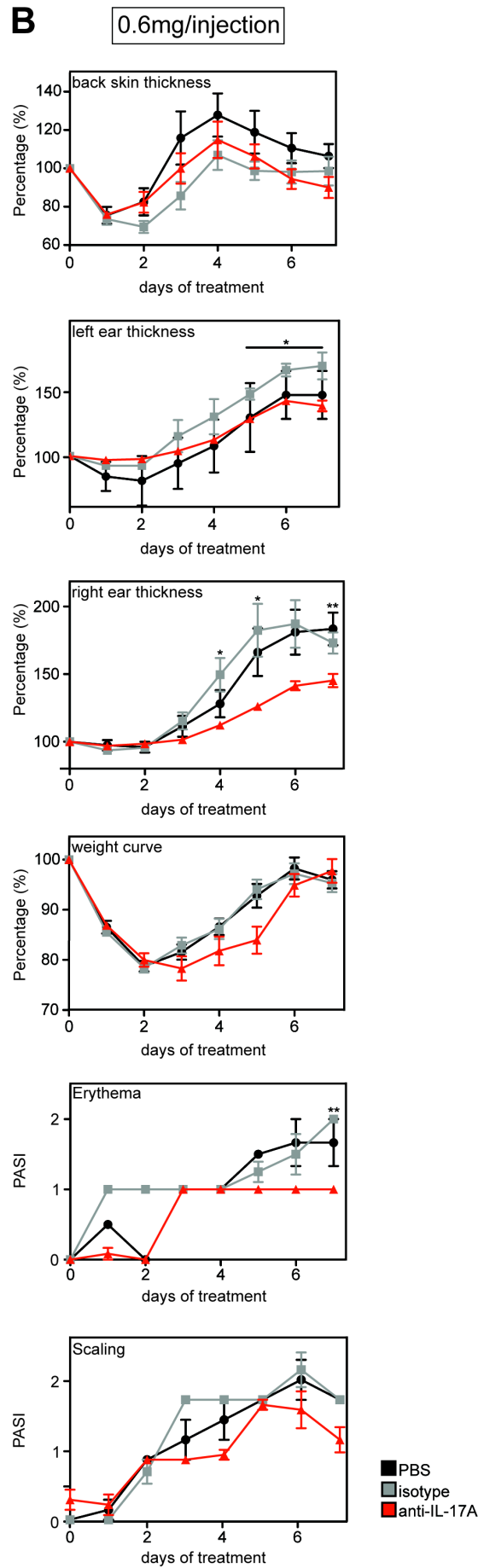
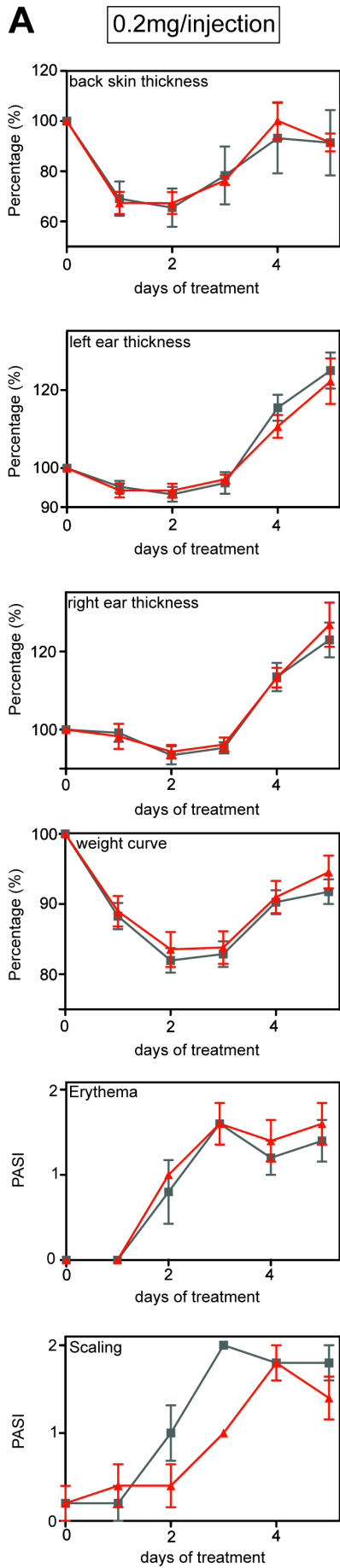


Figure 13: Neutralization of IL-17A with high dose of antibody shows decreased clinical scores in IMQ-induced psoriasis of *wt* mice

wt mice were treated twice with a **(A)** low dose (0.2mg/injection) or **(B)** a high dose (0.6mg/injection) of anti-IL17A during the treatment with IMQ for 5 or 7 consecutive days, respectively. **(A and B)** Modified PASI score from humans (top to bottom) of back skin thickness, left ear thickness, right ear thickness, weight, erythema and scaling. First day of weight- and skin thickness- measurements were set to 100%, values of the consecutive days were calculated accordingly. Erythema and scaling was scored on a scale from 0 to 4. (A: n=5; B: PBS group n=3; isotype group n=4; anti-IL-17A group n=6). As the antibody and the isotype control were dissolved in PBS, a PBS treated group was included in the experiment with the high dose of the antibody.

3.2.2 *Anti-IL-17A treatment with low dose antibody treatment shows a mild effect on infiltrating myelomonocytic cells into the skin*

The application of IMQ to mouse skin is known to recruit neutrophils and other myelomonocytic cells to the site of inflammation and secondary lymphoid organs (Flutter and Nestle, 2013). Due to this, we analyzed different sub-populations of the myelomonocytic cell compartment by flow cytometry.

In the spleen the neutralization of IL-17A showed no effect on any myelomonocytic population, neither in percentages nor total cell numbers (Fig. 14A-D). However, in the ears of the anti-IL-17A treated group less infiltrating CD11b⁺ cells compared to the isotype treated group could be detected (Fig. 14A and B). To have a closer look at the sub-populations of CD11b⁺ cells, we further investigated neutrophils, pro-inflammatory monocytes and resident monocytes. Although in percentages no real differences were obvious (Fig. 14C), total cell numbers showed a trend that there are less neutrophils (Ly6G⁺) and resident monocytes (Ly6G⁺Ly6C^{int}) in anti-IL-17A treated mice than in the isotype treated group (Fig. 14D).

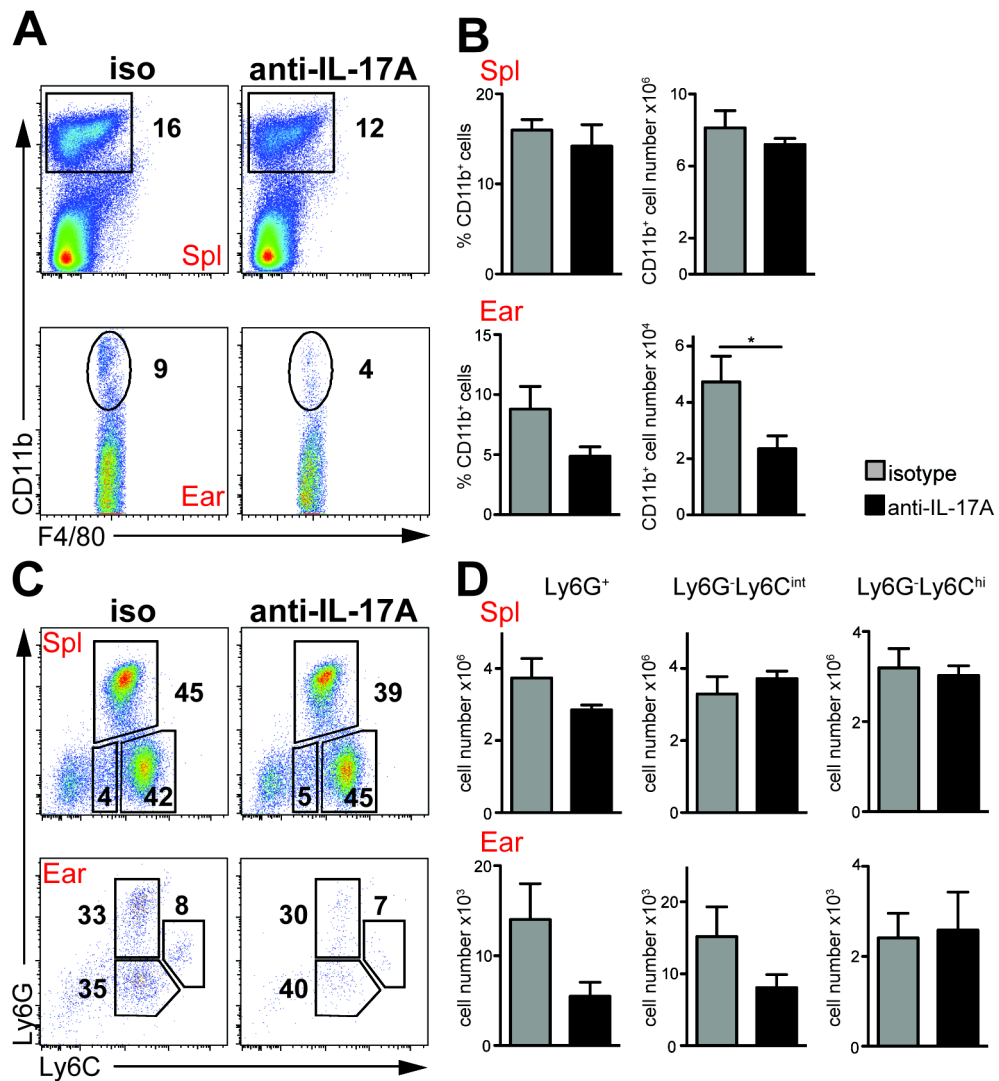


Figure 14: Neutralization of IL-17A with low dose of antibody shows mild effect on infiltrating myelomonocytic cells in the skin of *wt* mice

A) Flow cytometric analysis of CD11b⁺ cells of the indicated organs. Cells are pre-gated on living CD90.2⁻/B220⁻ cells. **(B)** Percentages and total cell numbers of CD11b⁺ cells of the indicated organs. Bar graphs are shown with mean and SEM. * $p \leq 0,05$ Significance was calculated using Student's T-test or Mann Whitney test (n=5), dependent on the results of calculated Gaussian distribution. **(C)** Flow cytometric analysis of neutrophils (Ly6G⁺), pro-inflammatory monocytes (Ly6G-Ly6C^{hi}) and resident monocytes (Ly6G-Ly6C^{int}) in the indicated organs. Cells are pre-gated on living CD90.2⁻/B220⁻ and CD11b⁺ cells. **(D)** Total cell numbers of neutrophils (Ly6G⁺), pro-inflammatory monocytes (Ly6G-Ly6C^{hi}) and resident monocytes (Ly6G-Ly6C^{int}) of the indicated organs. Bar graphs are shown with mean and SEM. Significance was calculated between using Mann Whitney or Student's T-test (n=5), dependent on the results of calculated Gaussian distribution.

3.2.3 *Neutralization of IL-17A with high dose antibody treatment has an impact on myeloid cell populations of skin and secondary lymphoid organs*

While the low dose treatment of anti-IL-17A revealed no differences in the myelomonocytic cell populations in the spleen, the experiment with the applied higher dose of the antibody showed less CD11b⁺ cells in spleen and ear, compared to the isotype and PBS group (Fig. 15A and C). Moreover, total cell numbers of Ly6G⁺ cells show a significant decrease in the spleen of anti-IL-17A treated mice compared to isotype, but the numbers were comparable to the PBS treated group (Fig. 15E, upper row). In the blood the treatment also seemed to have an effect on neutrophils, as there were significantly less Ly6G⁺ in anti-IL-17A treated mice compared to isotype (Fig. 15F). Again, the numbers were similar to the PBS treated group.

Furthermore, all analyzed cell populations in the ears show reduced numbers of cells (in percentages and in total cell numbers), the total cell numbers of Ly6G⁺ cells were even significantly reduced (Fig. 15A-E). However, this reduction was only obvious when compared to the PBS treated group, whereas the isotype treated group showed the same effect in terms of infiltrating cells as the anti-IL-17A treated group (Fig. 15C-E). This strongly indicates, that already the isotype treatment has an effect on the infiltration of myelomonocytic cells into the skin upon IMQ treatment.

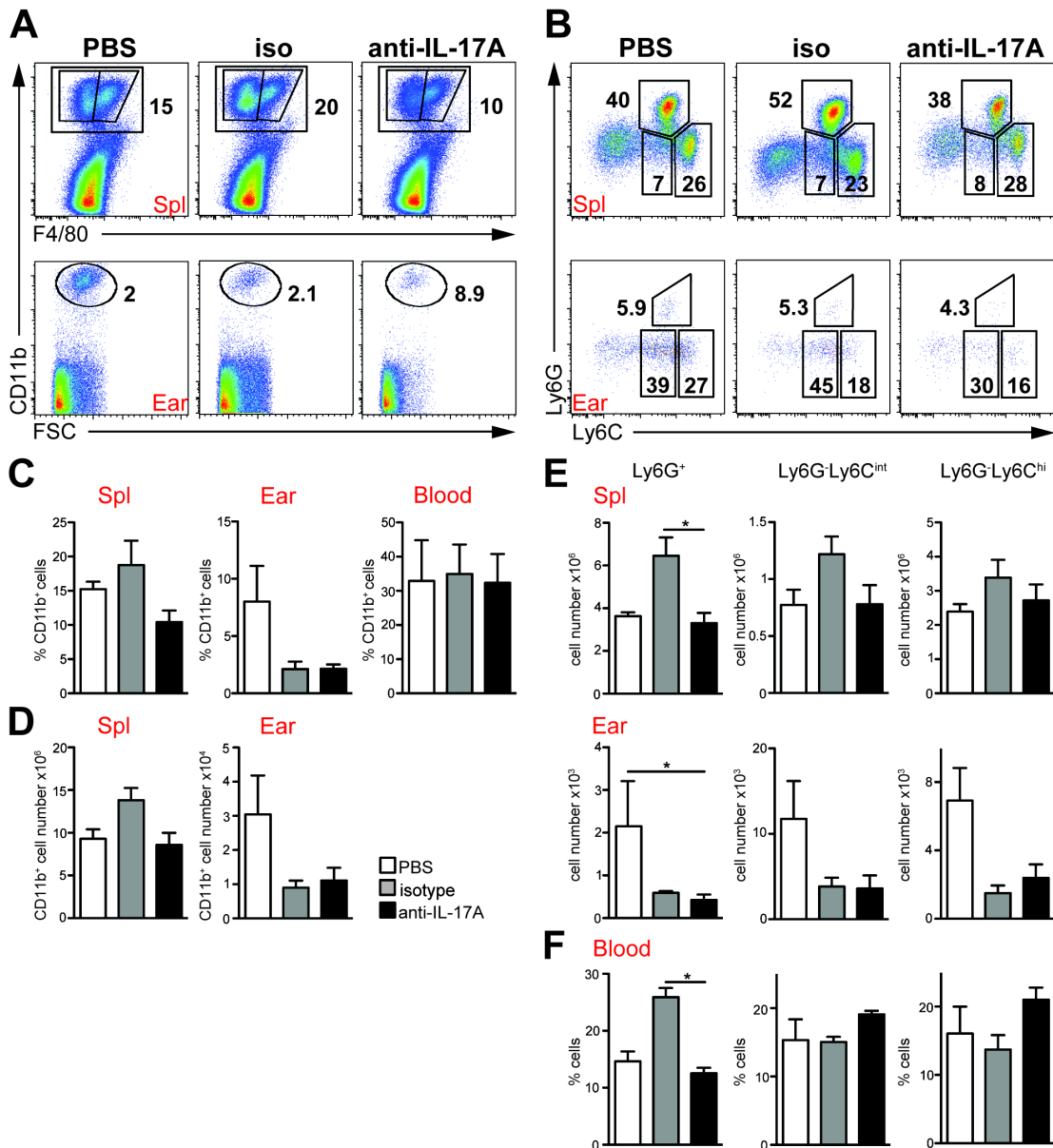


Figure 15: Neutralization of IL-17A with high dose of antibody shows strong effect on infiltrating myelomonocytic cells in the skin and mild effect on secondary lymphoid organs of *wt* mice

(A) Flow cytometric analysis of CD11b⁺ cells of the indicated organs. Cells are pre-gated on living CD90.2⁻/B220⁻ cells (B) Flow cytometric analysis of neutrophils (Ly6G⁺), pro-inflammatory monocytes (Ly6G⁺Ly6C^{hi}) and resident monocytes (Ly6G⁺Ly6C^{int}) of the indicated organs. Cells are pre-gated on living CD90.2⁻/B220⁻ and CD11b⁺ cells. (C) Percentages of CD11b⁺ cells of the indicated organs. (D) Total cell numbers of CD11b⁺ cells of the indicated organs. (E) Total cell numbers of neutrophils (Ly6G⁺), pro-inflammatory monocytes (Ly6G⁺Ly6C^{hi}) and resident monocytes (Ly6G⁺Ly6C^{int}) of the indicated organs. (F) Percentages of neutrophils (Ly6G⁺), pro-inflammatory monocytes (Ly6G⁺Ly6C^{hi}) and resident monocytes (Ly6G⁺Ly6C^{int}) of the blood. Bar graphs are shown with mean and SEM. * $p \leq 0,05$ Significances were calculated using Kruskal-Wallis test (PBS group n=3; Isotype group n=4; anti-IL-17A group n=6).

3.3 IMQ-induced psoriasis-like skin disease in *IL-6Rα^{Δmyel}* mice

3.3.1 *IL-6Rα^{Δmyel}* show reduced expression of *IL-6Rα* in myelomonocytic cells

Our previous analysis showed that the model of IMQ-induced psoriasis has a strong influence on the distribution of myelomonocytic cells in different organs. Furthermore, the neutralization of IL-17A altered this picture, confirming a relevant role for IL-17 in the context of IMQ-induced psoriasis. IL-6 is another pro-inflammatory cytokine strongly connected to IL-17. It acts both up- and down-stream of IL-17. On the one hand, IL-6 stimulates the production of IL-17A and IL-17F by antigen presenting cells (APCs) (Iwakura et al., 2011). On the other hand, IL-17A- and -F activate other immune cells, such as macrophages and keratinocytes, to release IL-6 (Iwakura et al., 2011). Moreover, Lindroos et al showed a connection between Th17 cells and IL-6 in the context of skin diseases. Here, *IL-6^{-/-}* mice produced less IL-17A after IL-23 mediated skin disorder (Lindroos et al., 2011). Also others already demonstrated that IL-6 and its downstream targets (e.g. STAT3) are involved in the development of psoriatic lesions (Croxford et al., 2014; Sano et al., 2005).

Our group demonstrated a role of IL-6 in IMQ-induced psoriasis-like skin disease (El Malki et al., 2013). Besides this, IL-6 is of great importance for general neutrophil recruitment (Fielding et al., 2008). As recently published by our group, we further investigated the role of IL-6 signaling in myelomonocytic cells in the context of IMQ-induced psoriasis-like skin disease (Klebow et al., 2016). For this purpose, we crossed *LysM-Cre* mice (Clausen et al., 1999) with the *IL-6Rα^{FL/FL}* mouse line (Wunderlich et al., 2010), resulting in a mouse line, which lacks the membrane-bound *IL-6Rα* (mIL-6Rα) exclusively in myelomonocytic cells (*IL-6Rα^{Δmyel}* mice) (Fig. 16A).

Clearly, in these mice there is a significant reduction in mIL-6Rα expression in myelomonocytic cells as shown by RT-PCR of CD11b⁺ isolated bone marrow cells (Fig. 16B). We also found a significant reduction in the systemic levels of sIL-6Rα measured in the serum (Fig. 16C), indicating the importance of myelomonocytic cells as source of this molecule (Klebow et al., 2016).

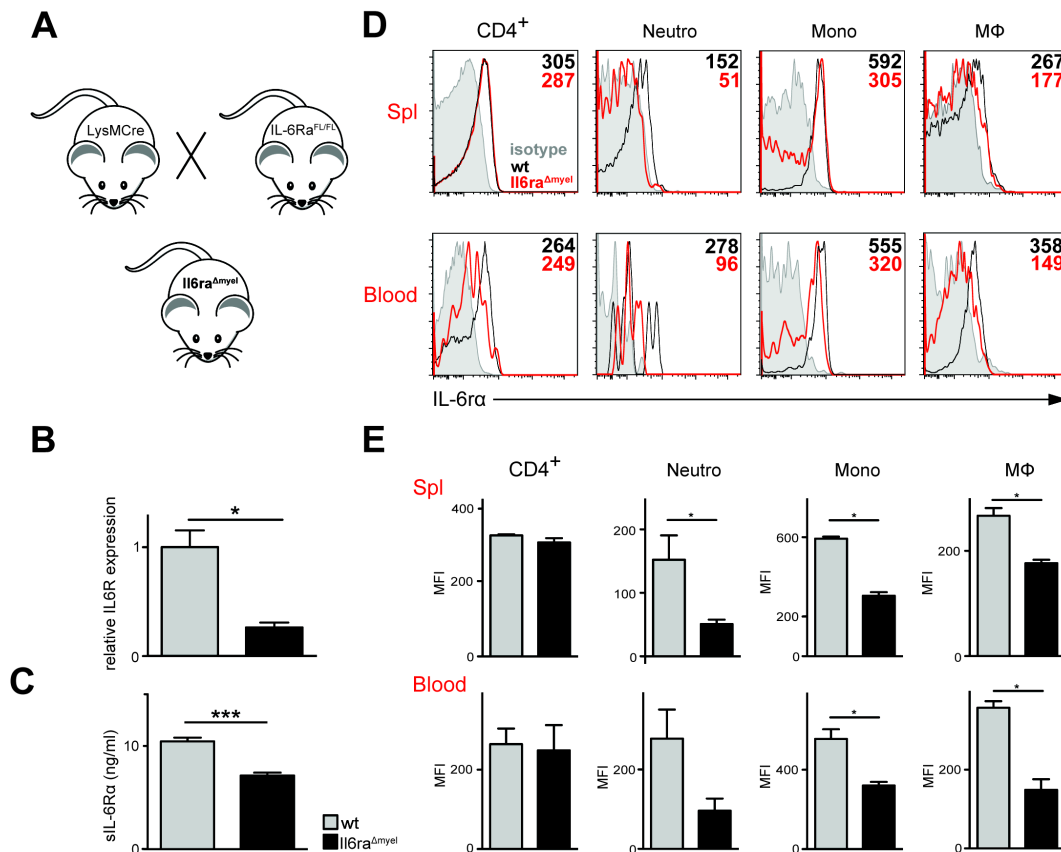


Figure 16: Myelomonocytic cell-specific inactivation of *Il6ra* gene in mice (*Il6ra*^{Δmyel})
(A) Schematic representation of the crossing to obtain *Il6ra*^{Δmyel} mice **(B)** Quantitative RT-PCR for IL-6Rα gene expression from MACS purified CD11b⁺ bone marrow cells in *wt* and *Il6ra*^{Δmyel} mice. Expression levels are shown relative to the housekeeping gene HPRT (n=5). Data are shown as bar graphs with mean and SEM. * p ≤ 0,05 Significance was calculated using Mann Whitney test. **(C)** Serum concentrations of sIL-6Rα from 5 - 30 weeks old *wt* (n=6) and *Il6ra*^{Δmyel} (n=10) mice examined by ELISA. *** p ≤ 0,001 Significance was calculated using Mann Whitney test. **(D)** Flow cytometric analysis of IL-6Rα expression in indicated cell types of different organs. *wt* (n= 7) and *Il6ra*^{Δmyel} (n=8) mice were stained with indicated antibodies. CD4⁺ cells are pre-gated on living CD90.2⁺ cells. Neutrophils (Gr-1^{hi} F4/80⁻), monocytes (Gr-1^{int} F4/80⁺) and macrophages (Gr-1⁻ F4/80⁺) are pre-gated on living CD90.2⁻/B220⁻ and CD11b⁺ cells. Gray histograms represent IgG2b isotype control for the IL-6R staining. Numbers in upper right corner represent mean MFI values of *Il6ra*^{Δmyel} (Mayer et al.) or *wt* (black) cells. Shown are representative histograms of 3 independent experiments. **(E)** Mean Fluorescent Intensity (MFI) of IL-6Rα expression from CD4⁺ cells, neutrophils (Gr-1^{hi} F4/80⁻), monocytes (Gr-1^{int} F4/80⁺) or macrophages (Gr-1⁻ F4/80⁺) in spleen and blood. *p ≤ 0,05 Significance was calculated using Mann Whitney test. **(B, C and E)** Data are shown as bar graphs with mean and SEM.

Moreover, we tested the deletion of IL-6Rα in these mice by flow cytometric analysis of the IL-6Rα expression in spleen and blood for CD4⁺ and myelomonocytic cells (Fig. 16D). Obviously, these mice have a reduced expression of the receptor in the myelomonocytic compartment (neutrophils, monocytes and macrophages) compared to control mice, but no difference in the mean fluorescent intensity (MFI) of IL-6Rα was observed in CD4⁺ cells (Fig. 16E).

3.3.2 Distribution of immune cell populations is similar in *IL-6Rα^{Δmyel}* and *wt* mice

The cytokine IL-6 is important for many different immune cells. For example, T cells need IL-6 for regulating the T_{reg}/Th17 balance (Kimura and Kishimoto, 2010). However, also the production of Th2 cells in CD4⁺ T cells is dependent on IL-6 (Rincon et al., 1997). Moreover, B cells secrete more IL-6 upon stimulation, if the tumor suppressor gene A20 is deleted (Chu et al., 2011). In order to evaluate whether the myelomonocytic deletion of IL-6Rα has an influence on T and B cells in steady state, we performed flow cytometric analysis to see if these populations were altered.

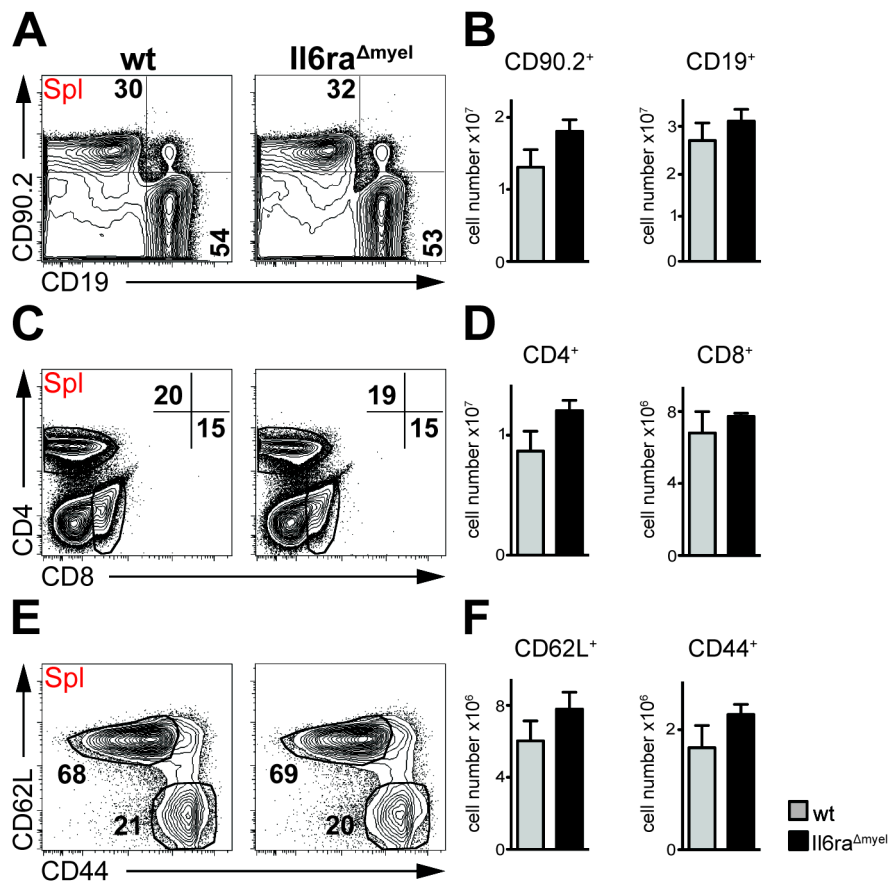


Figure 17: IL-6Rα deletion in myelomonocytic cells has no effect on splenic T cell populations in *Il6ra^{Δmyel}* mice

(A) Flow cytometric analysis of B cells (CD19⁺) and T cells (CD90.2⁺) in the spleen of naïve *wt* and *Il6ra^{Δmyel}* mice. Cells are pre-gated on living lymphocytes. (B) Total cell numbers of CD90.2⁺ and CD19⁺ cells in the spleen of indicated genotypes. (C) Flow cytometric analysis of CD4⁺ and CD8⁺ T cells in the spleen. Cells are pre-gated on living CD90.2⁺CD19⁻ lymphocytes. (D) Total cell numbers of CD4⁺ and CD8⁺ T cells in the spleen. (E) Flow cytometric analysis of naïve (CD4⁺CD62L⁺) and effector (CD4⁺CD44⁺) T cells in the spleen. Cells are pre-gated on living CD19⁻/CD90.2⁺/CD4⁺ lymphocytes. (F) Total cell numbers of CD4⁺CD62L⁺ (naïve) and CD4⁺CD44⁺ (effector) T cells in the spleen. (B, D, F) Data are shown as bar graphs with mean and SEM. Significance was calculated using Student's t-Test (n=5).

First of all, the B:T cell ratio in *IL-6Rα^{Δmyel}* and *wt* mice was comparable (Fig. 17A and B), as was the proportion of CD4⁺ and CD8⁺ (Fig. 17C and D). Also the naïve (CD62L⁺) and effector T cells (CD44⁺) of the CD4⁺ compartment seemed not to be influenced by the deletion of IL-6Rα in myelomonocytic cells (Fig. 17E and F).

Furthermore, all the investigated B cell populations (mature and immature B cells; marginal zone and follicular B cells; follicular type I and follicular type II B cells) showed the same percentages and total cell numbers between *IL-6Rα^{Δmyel}* and *wt* mice (Fig. 18A-F).

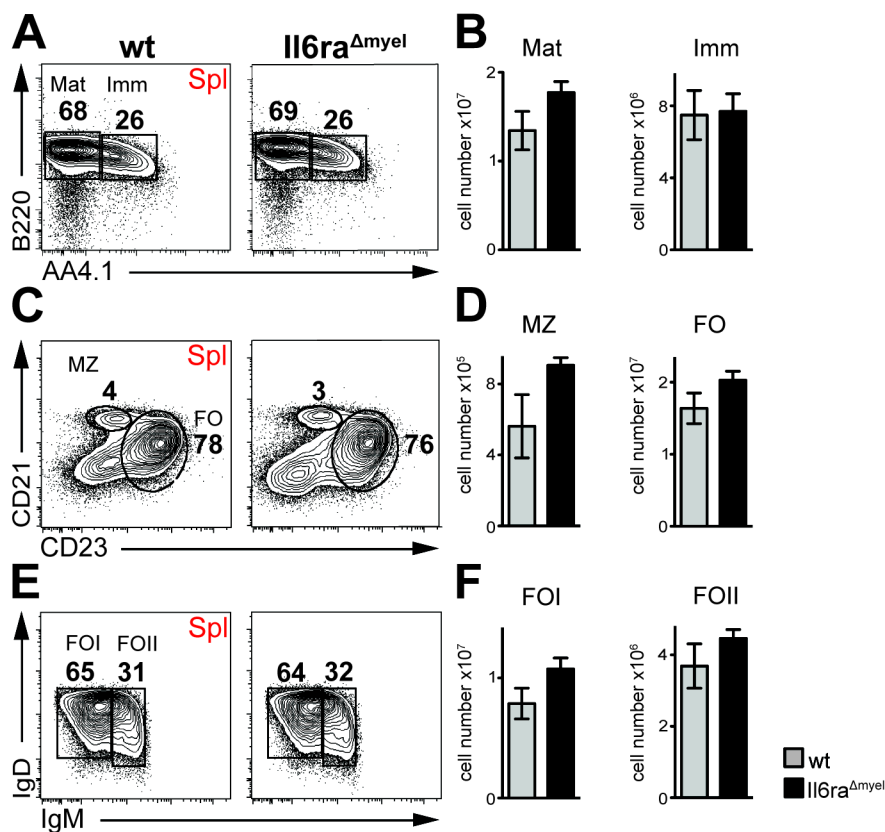


Figure 18: IL-6Rα deletion in myelomonocytic cells has no effect on splenic B cell subpopulations in *Il6ra^{Δmyel}* mice

(A) Flow cytometric analysis of mature (Mat; B220⁺AA4.1⁻) and immature (Imm; B220⁺AA4.1⁺) splenic B cells of indicated genotypes. Cells are pre-gated on living CD19⁺ lymphocytes. (B) Total cell numbers of Mat and Imm B cells in the spleen. (C) Flow cytometric analysis of marginal zone (MZ; CD21⁺CD23⁻) and follicular (FO; CD21⁺CD23⁺) B cells in the spleen. Cells are pre-gated on living CD19⁺ lymphocytes. (D) Total cell numbers of MZ and FO cells in the spleen. (E) Flow cytometric analysis of splenic follicular type I (FOI; IgM^{int}IgD⁺) and follicular type II (FOII; IgM^{hi}IgD⁺) B cells. Cells are pre-gated on living CD19⁺/AA4.1⁻/CD21⁺/IgM⁺ cells. (F) Total cell numbers of splenic FOI and FOII B cells (B, D and F). Data are shown as bar graphs with mean and SEM. Significance was calculated using Student's t-Test (n=5).

Before the *IL-6R α ^{Δmyel}* mice can be analyzed in the model of IMQ-induced psoriasis, immune cell populations, which are influenced in this model, needs to first be examined during steady state.

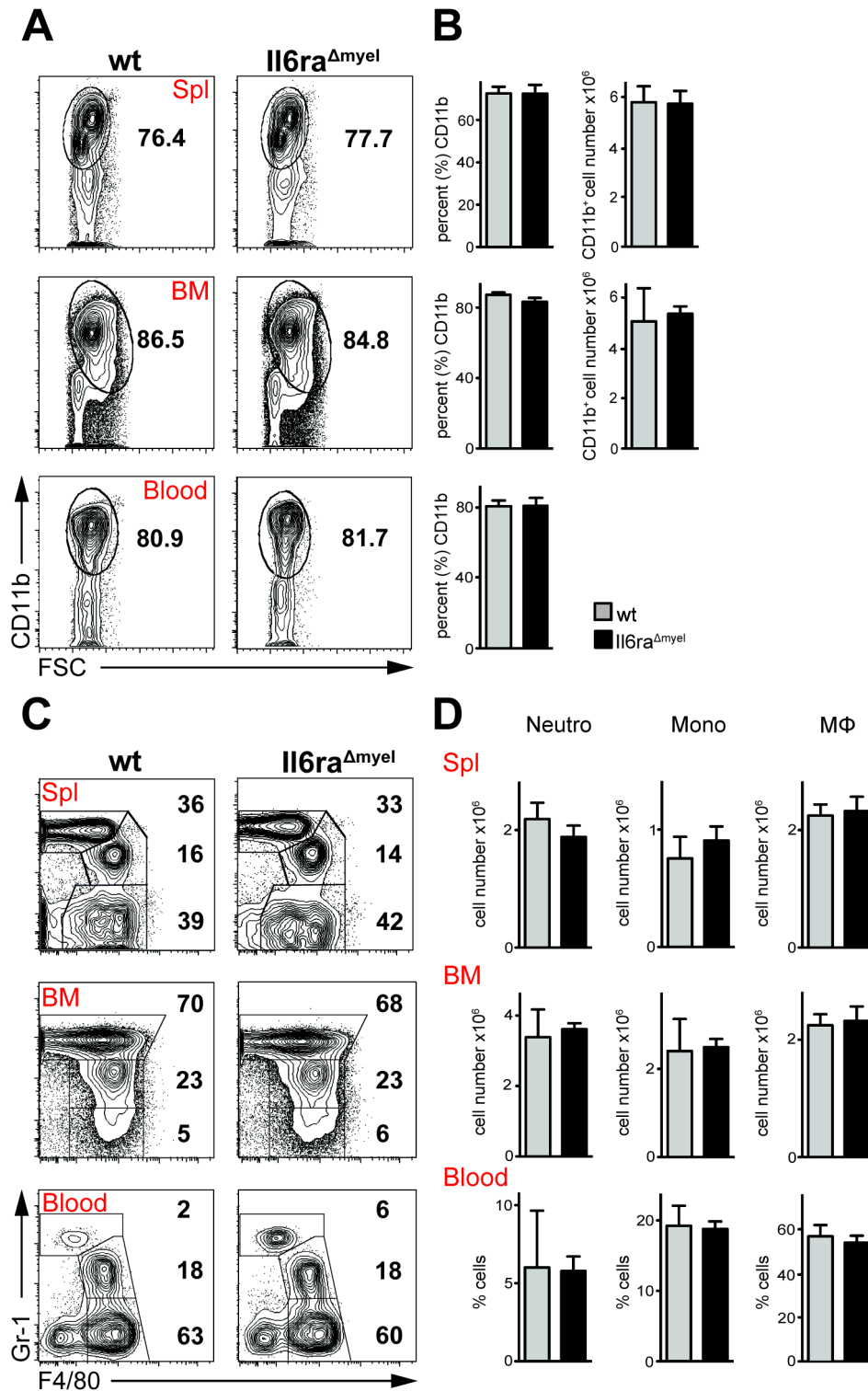


Figure 19: *Il6ra*^{Δmyel} mice show no differences in myelomonocytic cell compartments compared to *wt*

(A) Flow cytometric analysis of CD11b⁺ cells of the indicated organs. Cells are pre-gated on living CD90.2⁻/CD19⁻ cells. **(B)** Percentages and total cell numbers of CD11b⁺ cells in the indicated organs. **(C)** Flow cytometric analysis of neutrophils (GR1^{hi}F4/80⁻), monocytes (GR1^{int}F4/80⁺) and macrophages (GR1⁻F4/80⁺) of the indicated organs in *Il6ra*^{Δmyel} mice and *wt* littermate controls. Cells are pre-gated on living CD90.2⁻/CD19⁻ and CD11b⁺ cells. **(D)** Total cell numbers of neutrophils (Gr-1^{hi} F4/80⁻), monocytes (Gr-1^{int} F4/80⁺) and macrophages (Gr-1⁻ F4/80⁺). **(B, D)** Data are shown as bar graphs with mean and SEM. Significance was calculated using Mann Whitney test (n=5).

Therefore, we evaluated the different populations of myelomonocytic cells. Flow cytometric analysis of spleen, bone marrow and blood revealed the same numbers of CD11b⁺ cells in *IL-6Rα*^{Δmyel} and *wt* mice (Fig. 19A and B). Next, sub-populations of CD11b⁺ cells, like neutrophils, monocytes and macrophages were also investigated. Again, there was no difference visible in ratio or total cell numbers in spleen, bone marrow and blood (Fig. 19C and D).

Besides the myelomonocytic cells, also the $\gamma\delta$ T cells are involved in the pathogenicity of IMQ-induced psoriasis. It was shown that the stimulation of $\gamma\delta$ T cells by TLR agonists had an influence on their effector function. This mechanism is driven by different cytokines, including IL-6 (Dar et al., 2014). Moreover, within the $\gamma\delta$ T cell population, dermal and epidermal $\gamma\delta$ T cells can be distinguished, the former population being the main producer of IL-17A in IMQ-induced psoriasis (Cai et al., 2011; Pantelyushin et al., 2012). To examine whether all populations are distributed equally under steady state conditions, we performed flow cytometric analysis of the spleen and the ears. The $\gamma\delta$ T cells of the spleen showed no differences between the groups of *IL-6Rα*^{Δmyel} and *wt* mice (Fig. 20A and B). In the ears, dermal ($\gamma\delta$ TCR^{int}), epidermal ($\gamma\delta$ TCR^{hi}) and IL-17 producing dermal $\gamma\delta$ T cells ($\gamma\delta$ TCR^{int} IL-17A⁺) were examined. Again, no differences in percentages and total cell numbers were evident when comparing *wt* to *IL-6Rα*^{Δmyel} mice (Fig. 20E-G).

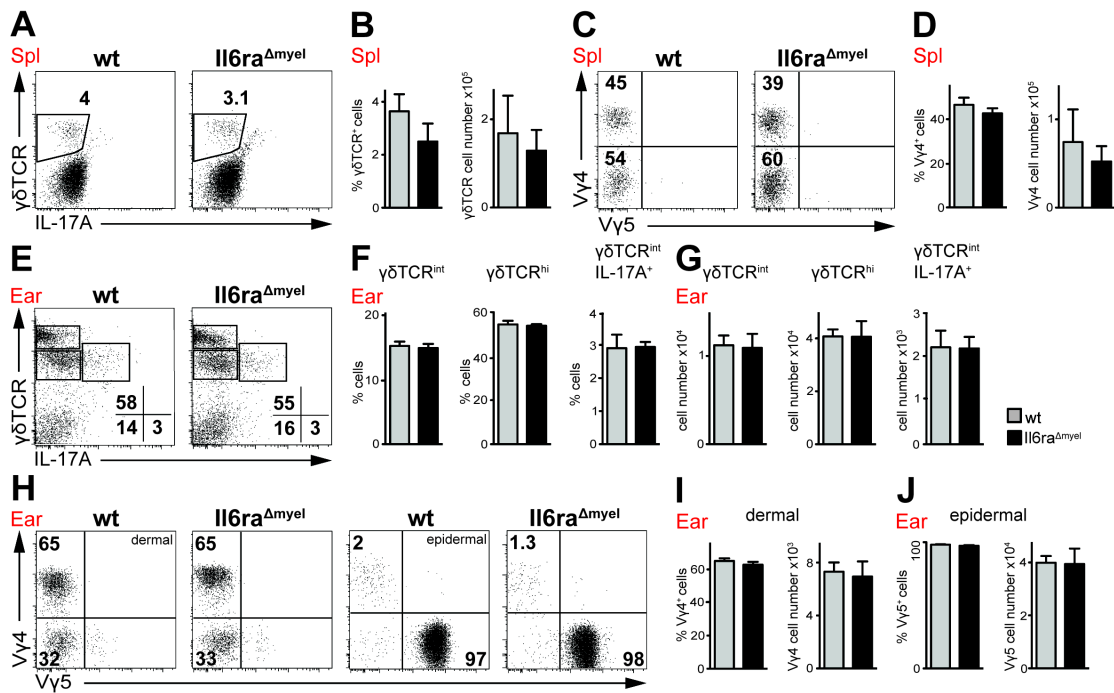


Figure 20: IL-6 α deletion in myelomonocytic cells has no effect on $\gamma\delta$ T cell sub-populations in *Il6ra^{Δmyel}* mice

(A) Flow cytometric analysis of splenic $\gamma\delta$ TCR⁺ T cells of *Il6ra^{Δmyel}* mice and *wt* littermate control animals using indicated antibodies. Cells are pre-gated on living CD45.2⁺/CD3⁺ cells. (B) Percentages and total cell numbers of $\gamma\delta$ TCR⁺ cells in the spleen. (C) Flow cytometric analysis of V γ 4⁺V γ 5⁻ $\gamma\delta$ T cells in the spleen. Cells are pre-gated on living CD45.2⁺/CD3⁺/ $\gamma\delta$ TCR⁺ cells. (D) Percentages and total cell numbers of V γ 4⁺V γ 5⁻ $\gamma\delta$ T cells in the spleen. (E) Flow cytometric analysis of dermal ($\gamma\delta$ TCR^{int}IL-17A⁻) and epidermal ($\gamma\delta$ TCR^{hi}IL-17A⁻) $\gamma\delta$ T cells and IL-17A producing dermal $\gamma\delta$ T cells ($\gamma\delta$ TCR^{int}IL-17A⁺) in the ears of *Il6ra^{Δmyel}* mice and *wt* littermate control animals. Cells are pre-gated on living CD45.2⁺/CD3⁺ cells. (F) Percentages and total cell numbers of dermal, epidermal and dermal IL-17A producing $\gamma\delta$ TCR⁺ cells in the ears. (G) Flow cytometric analysis of dermal (V γ 4⁺V γ 5⁻) and epidermal (V γ 4⁺V γ 5⁺) $\gamma\delta$ TCR sub-populations in the ears. Cells are pre-gated on CD45.2⁺/CD3⁺/ $\gamma\delta$ TCR^{int} (dermal)/ $\gamma\delta$ TCR^{hi} (epidermal) cells. (H) Percentages and total cell numbers of V γ 4⁺V γ 5⁻ and V γ 4⁺V γ 5⁺ $\gamma\delta$ TCR sub-populations cells in the ears. (B, D, F and G) Data are shown as bar graphs with mean and SEM. Significance was calculated using Mann Whitney test (n=4).

Based on the investigation of Cai et al., we wanted to analyze the V γ TCR segments in our *IL-6R α ^{Δmyel}* mice. Dermal $\gamma\delta$ T cells express more V γ 4, whereas epidermal $\gamma\delta$ T cells are V γ 5⁺ (Cai et al., 2011). Besides this, V γ 5⁺ can be exclusively found only in the epidermis (Sumaria et al., 2011). For this, we stained spleen and ears for V γ 4 and V γ 5 segments for analysis by flow cytometry. As expected, none of the evaluated populations from either spleen or ears differed between *IL-6R α ^{Δmyel}* and *wt* mice (Fig. 20C and D, H-J).

3.3.3 Myelomonocytic deletion of *IL-6R α* does not ameliorate IMQ-induced psoriasis-like skin disease

As IL-6 has a central role in the development of psoriasis, this cytokine could serve as a potential target in the treatment of this disease (Saggini et al., 2014). We therefore analyzed IL-6-mediated signaling in myelomonocytic cells in psoriasis and treated *IL-6R α ^{Amyel}* mice and respective control groups with IMQ or sham cream for 5 consecutive days. The treatment of mice with IMQ is a common model to induce psoriasis-like disease (van der Fits et al., 2009).

The severity of disease was documented with the PASI system. Following the treatment with IMQ, the back/ear skin thickness and cumulative PASI of erythema and scaling increased with days of treatment in comparison to sham-treated mice. However, measured parameters between *IL-6R α ^{Amyel}* and *wt* mice were the same (Fig. 21A). In addition, we examined the back skin of the four different groups for infiltrating cells of the myelomonocytic compartment via fluorescent immunohistochemistry after 5 days of treatment (Klebow et al., 2016). Skin thickness of IMQ treated mice seemed to be increased compared to sham treated groups (Fig. 21B and C). IMQ-treatment resulted in more neutrophils (MPO⁺ cells) (Fig. 21B) and macrophages (F4/80⁺ cells) infiltrating the skin (Fig. 21C) in IMQ treated groups compared to sham treated mice. However, there were no visible differences in infiltrating cells within the IMQ-treated groups.

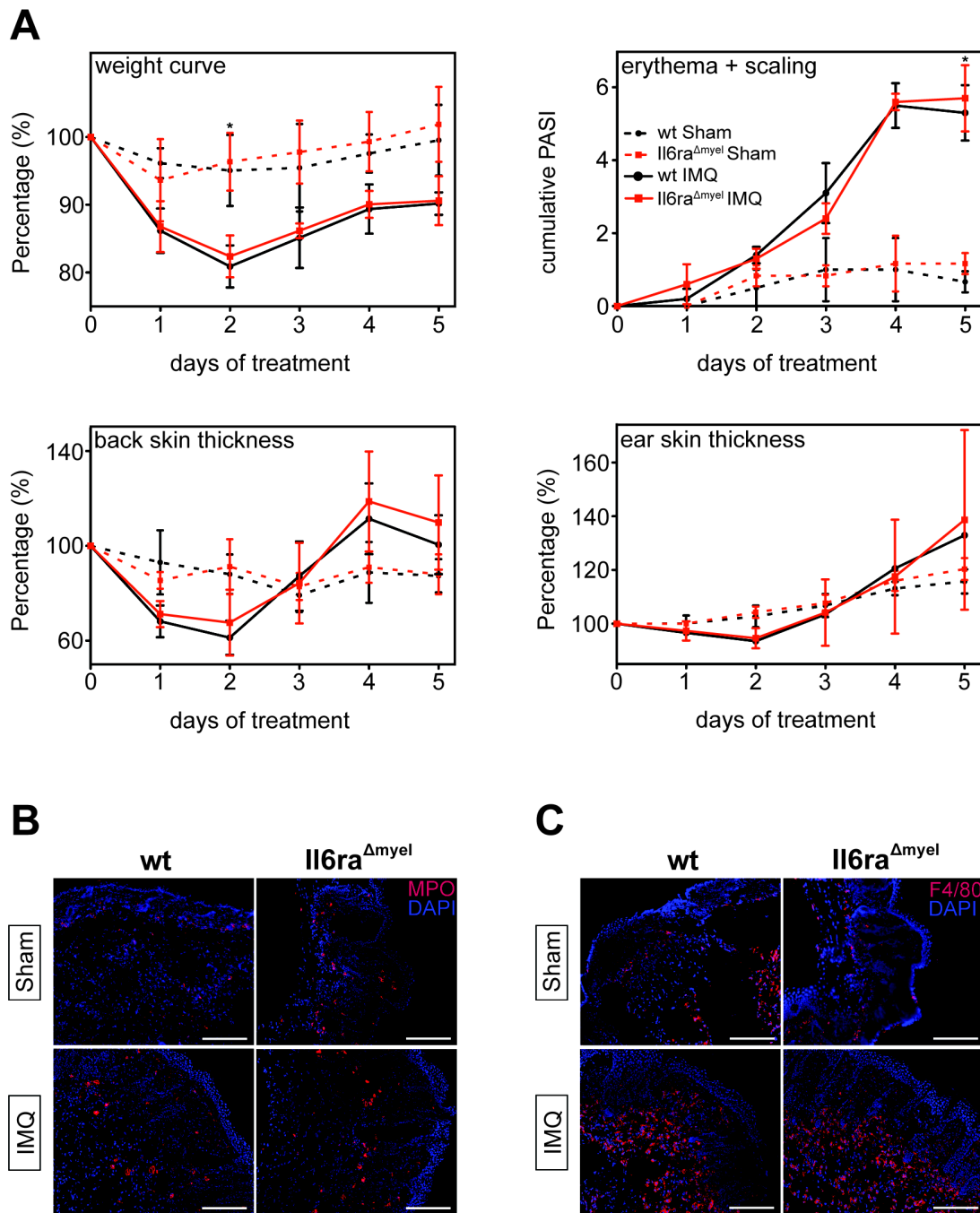


Figure 21: *Il6ra^{Δmyel}* mice show no effect in clinical scores and histology in IMQ-induced psoriasis compared to *wt* mice

Back skin of *Il6ra^{Δmyel}* and *wt* mice was treated either with sham (n=3) or IMQ (n=6) over 5 consecutive days. Weight, ear/back skin thickness and erythema/scaling of IMQ treated group and sham treated group was scored daily on a scale from 0 to 4 with a modified PASI from humans. First day of weight- and skin thickness- measurements were set to 100%, values of the consecutive days were calculated accordingly. **(A)** Shown is the modified PASI score from *Il6ra^{Δmyel}* and *wt* animals of the indicated groups. **(B and C)** Fluorescence-immunohistochemistry for (B) myeloperoxidase (MPO)⁺ cells (Mayer et al.) or (C) F4/80⁺ cells (Mayer et al.) and DAPI (blue) of back skin from *Il6ra^{Δmyel}* and *wt* mice treated with either sham or IMQ. Magnifications are given from representative stainings; white scale bars = 200 μm.

3.3.4 Distribution of myelomonocytic cells in *IL-6Rα^{Δmyel}* mice is not influenced by IMQ treatment

Treatment of murine skin with IMQ results in a different immune profile and increased numbers of infiltrating myelomonocytic cells in the skin and secondary lymphoid organs (El Malki et al., 2013; Flutter and Nestle, 2013; van der Fits et al., 2009). Flow cytometric analysis of spleen and ears revealed more CD11b⁺ cells overall after IMQ treatment compared to sham-treated mice in total cell numbers (Fig. 22D), although ratios of CD11b⁺ populations were comparable (Fig. 22A-C) (Klebow et al., 2016). Analysis of the lymph nodes showed the same result as received for spleen and ears (data not shown). To more closely examine the sub-populations of CD11b⁺ cells in spleen and ears, the surface expression of Ly6G and Ly6C was used to differentiate between neutrophils, pro-inflammatory monocytes and resident monocytes. All of these sub-populations were increased in percentage and total cell numbers under IMQ treatment compared to sham treated groups in the spleen (Fig. 22E and G). In the ears we obtained a different result; here, the sham treated controls seem to have the same amount of monocytes as the IMQ treated groups (Klebow et al., 2016). However, it was already shown that steric acids, a component of the sham cream, can already lead to an infiltration of cells (Walter et al., 2013). There were no differences in invading Ly6G⁺ / Ly6C⁺ cells under IMQ-treatment in *IL-6Rα^{Δmyel}* mice compared to *wt* mice in spleen and ears (Fig. 22F and H) (Klebow et al., 2016). In total, this result fits to the fact that the clinical appearance was not significantly altered in mice exhibiting *IL-6Rα* deletion in myelomonocytic cells – with and without IMQ-treatment.

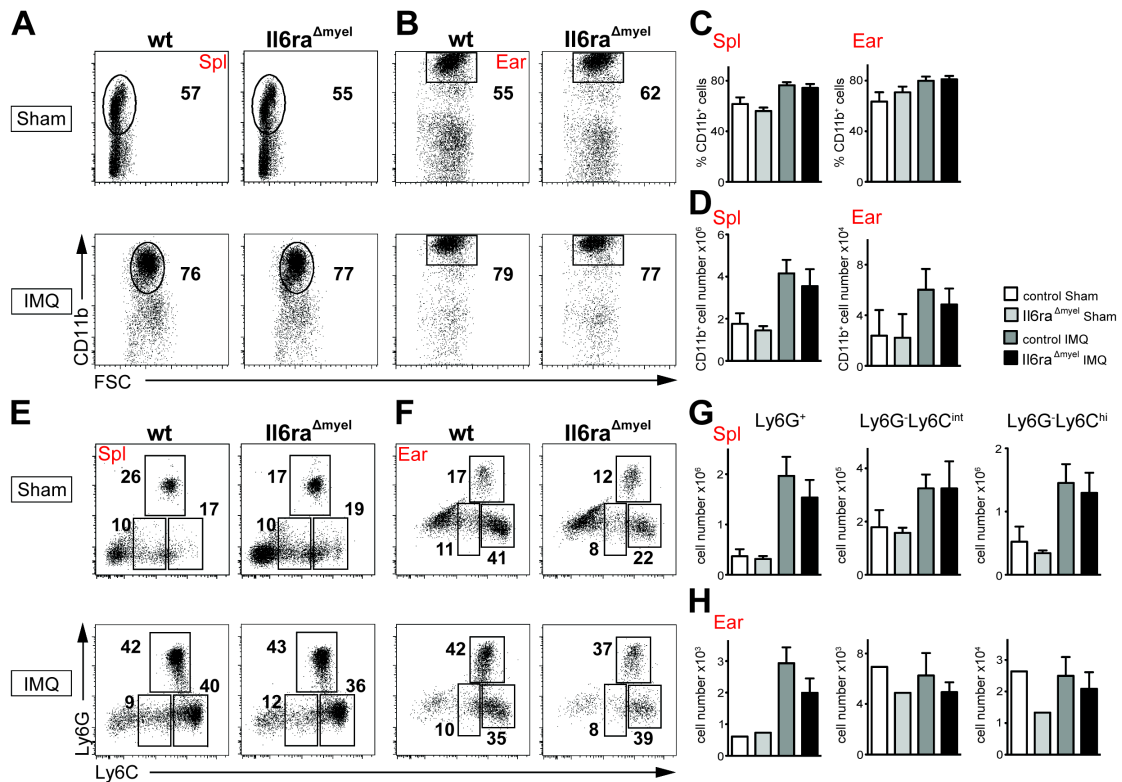


Figure 22: IMQ treatment leads to same differentiation of myelomonocytic cells in *Il6ra^{Δmyel}* and *wt* mice

(A) Flow cytometric analysis of CD11b⁺ cells in the spleen. Cells are pre-gated on living CD90.2⁻/B220⁻ cells. (B) Flow cytometric analysis of CD11b⁺ cells of the ears. Cells are pre-gated on living CD90.2⁻/B220⁻ cells. (C) Percentages and total cell numbers of CD11b⁺ cells of the indicated organs. (D) Flow cytometric analysis of splenic neutrophils (Ly6G⁺), pro-inflammatory monocytes (Ly6G⁺Ly6C^{hi}) and resident monocytes (Ly6G⁺Ly6C^{int}). Cells are pre-gated on living CD90.2⁻/B220⁻ and CD11b⁺ cells. (E) Flow cytometric analysis of neutrophils (Ly6G⁺), pro-inflammatory monocytes (Ly6G⁺Ly6C^{hi}) and resident monocytes (Ly6G⁺Ly6C^{int}) of the ears. Cells are pre-gated on living CD90.2⁻/B220⁻ and CD11b⁺ cells (F) Total cell numbers of neutrophils (Ly6G⁺), pro-inflammatory monocytes (Ly6G⁺Ly6C^{hi}) and resident monocytes (Ly6G⁺Ly6C^{int}) of the indicated organs. (C and F) Bar graphs are shown with mean and SEM. Significances of the spleen were calculated using Kruskal-Wallis test (IMQ groups n=6, sham groups n=3). Significances of the ears were calculated with Student's t-Test between IMQ treated groups (IMQ groups n=6, sham groups n=1).

3.3.5 Diminished IL-6 signaling *IL-6Rα^{Δmyel}* mice has no influence on populations of $\gamma\delta$ T cells during IMQ treatment

Next, we investigated the distribution of $\gamma\delta$ T cells in IMQ-induced psoriasis. Pantelyushin et al. had shown an increase in numbers of IL-17A producing $\gamma\delta$ T cells under IMQ treatment (Pantelyushin et al., 2012). Hence, we also compared the IL-17A production of $\gamma\delta$ T cells between the different groups of mice (Klebow et al., 2016).

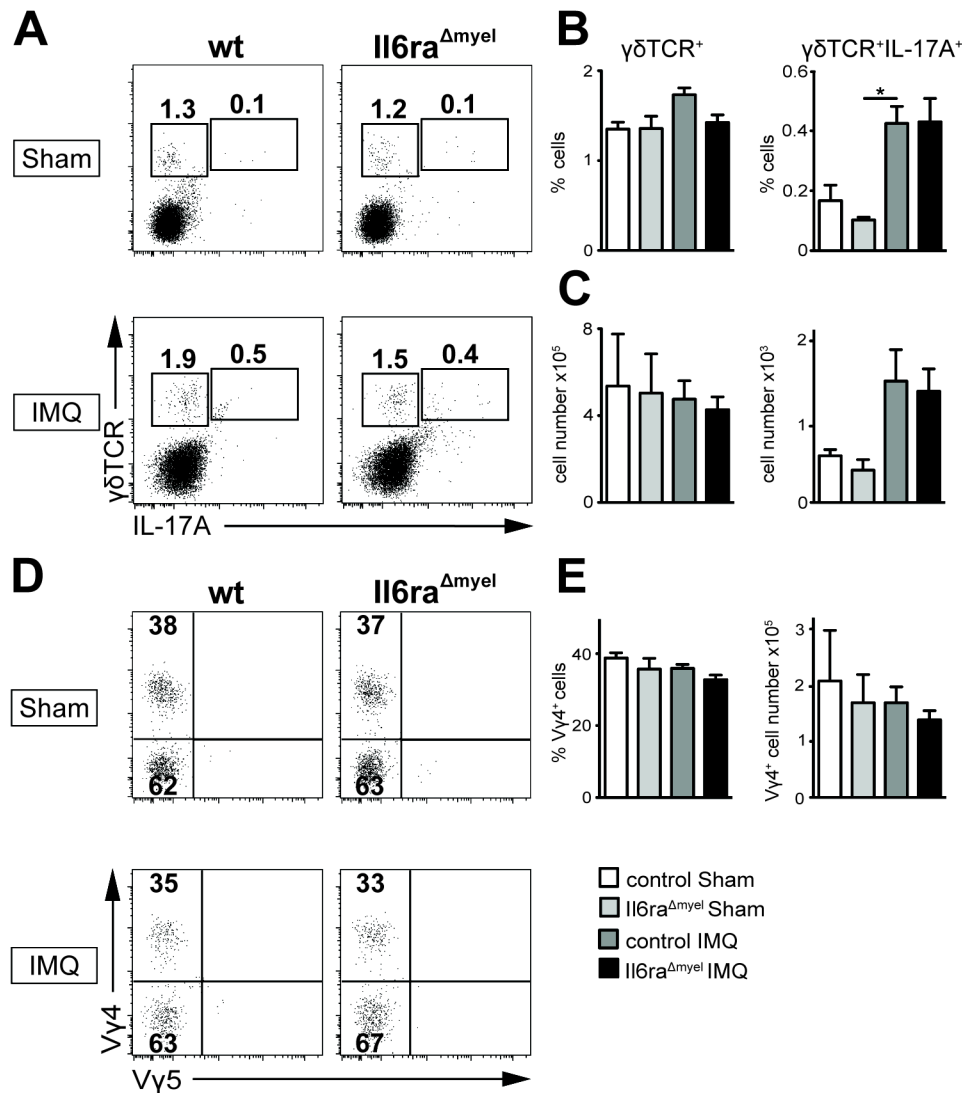


Figure 23: $\gamma\delta$ TCR sub-populations in the spleen of *Il6ra*^{Δmyel} mice and wt are comparable in the model of IMQ-induced psoriasis

(A) Flow cytometric analysis of $\gamma\delta$ TCR⁺IL-17A⁻ and $\gamma\delta$ TCR⁺IL-17A⁺ T cells in the spleen of indicated experimental groups. Cells are pre-gated on living CD45.2⁺/CD3⁺ cells. (B) Percentages (top) and total cell numbers (bottom) of splenic $\gamma\delta$ TCR⁺IL-17A⁻ and $\gamma\delta$ TCR⁺IL-17A⁺ cells. (C) Flow cytometric analysis of splenic V γ 4⁺V γ 5⁻ $\gamma\delta$ T cells of indicated experimental groups. Cells are pre-gated on living CD45.2⁺/CD3⁺/ $\gamma\delta$ TCR⁺ cells. (D) Percentages and total cell numbers of V γ 4⁺V γ 5⁻ $\gamma\delta$ T cells in the spleen. (B and D) Data are shown as bar graphs with mean and SEM. Significance was calculated using Kruskal-Wallis test (IMQ groups n=6, sham groups n=3).

FACS plots and total cell numbers of the spleen showed comparable $\gamma\delta$ TCR⁺ cells in all four groups (Fig. 23A and B). However, total IL-17A - producing $\gamma\delta$ T cells in IMQ-treated mice were increased (Fig. 23C), but within IMQ treated groups, no differences were detectable in the spleen (Klebow et al., 2016). To examine whether the IMQ treatment altered the distribution of V γ TCR segments in *Il6ra*^{Δmyel} mice, we stained for V γ 4 in the spleen. Obviously, the treatment of IMQ had no influence on the population of V γ 4⁺ cells in our mouse model, as in all four

groups the ratios and total cell numbers were comparable (Fig. 23D and E). Moreover, the numbers were almost the same as in steady state conditions of the spleen (Fig. 20C and D). In the ears, percentages of the two $\gamma\delta$ TCR⁺ populations were comparable in all groups (Fig. 24A and B). However, in total cell numbers dermal ($\gamma\delta$ TCR^{int}) and epidermal ($\gamma\delta$ TCR^{hi}) $\gamma\delta$ T cells were elevated in sham treated groups (Fig. 24C) (Klebow et al., 2016). Probably due to more dermal $\gamma\delta$ T cells in sham-treated groups, IL-17A-producing $\gamma\delta$ T cells were comparable in the ears of IMQ-treated mice and sham-treated groups (Fig. 24A and B). Altogether, in the ears the effect was not as intense as expected, due to the fact that $\gamma\delta$ T cells in the skin peak after 7 days of treatment (Flutter and Nestle, 2013; Tortola et al., 2012). Also in the ears we analyzed the distribution of V γ TCR segments, by staining for V γ 4⁺ and V γ 5⁺ cells of dermal and epidermal $\gamma\delta$ T cells. In the V γ 5⁺ population of epidermal $\gamma\delta$ T cells no difference was obvious when comparing all 4 groups (Fig. 24D and F). In contrast, the V γ 4⁺ cells of the dermal $\gamma\delta$ T cell population seemed slightly decreased in IMQ treated groups in total cell numbers (Fig. 24E), probably due to less $\gamma\delta$ TCR^{int} cells in general (Fig. 24B). Cai *et al* reported that the population of V γ 4⁺ cells correlated with IL-17 production, as a V γ 4 depleting mAb led to less IL-17 production of $\gamma\delta$ T cells (Cai et al., 2011). As we didn't see significant differences in any population, we didn't expect to see a difference in the distribution of V γ 4⁺ cells.

Conclusively, inhibition of IL-6 signaling in myelomonocytic cells showed no effect on myelomonocytic cells or $\gamma\delta$ T cells under IMQ treatment.

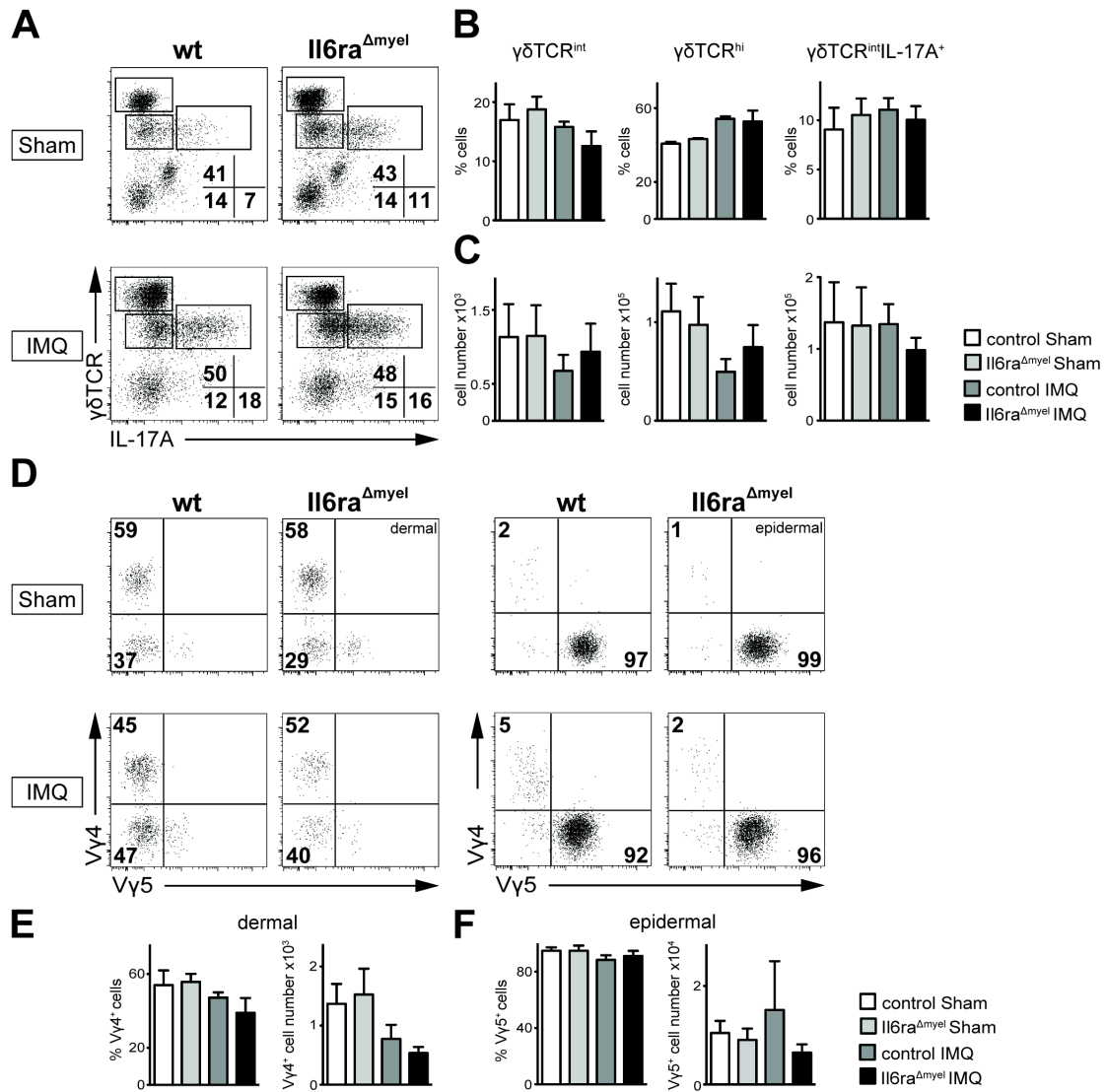


Figure 24: $\gamma\delta$ TCR sub-populations of ears in *Il6ra*^{Amyel} mice are not affected during the treatment with IMQ

A) Flow cytometric analysis of dermal ($\gamma\delta$ TCR^{int}IL-17A⁻), epidermal ($\gamma\delta$ TCR^{hi}IL-17A⁻) $\gamma\delta$ T cells and IL-17A producing dermal $\gamma\delta$ T cells ($\gamma\delta$ TCR^{int}IL-17A⁺) in the ears of indicated experimental groups. Cells are pre-gated on living CD45.2⁺/CD3⁺ cells. **(B)** Percentages (top) and total cell numbers (bottom) of $\gamma\delta$ TCR^{int}IL-17A⁻, $\gamma\delta$ TCR^{hi}IL-17A⁻ and $\gamma\delta$ TCR^{int}IL-17A⁺ cells in the ears. **(C)** Flow cytometric analysis of $\gamma\delta$ TCR sub-populations (left) in the dermis (V γ 4⁺V γ 5⁻) and (Hueber et al.) the epidermis (V γ 4⁺V γ 5⁺) of the ears. Cells are pre-gated on CD45.2⁺/CD3⁺ $\gamma\delta$ TCR^{int} (dermal)/ $\gamma\delta$ TCR^{hi} (epidermal) cells. **(D)** Percentages (left) and total cell numbers (Hueber et al.) of V γ 4⁺V γ 5⁻ and V γ 4⁺V γ 5⁺ $\gamma\delta$ TCR sub-populations in the ears. **(B and D)** Data are shown as bar graphs with mean and SEM. Significance was calculated using Kruskal-Wallis test (IMQ groups n=6, sham groups n=3).

3.3.6 Analysis of STAT3 activation in *IL-6Rα^{Δmyel}* mice compared to *wt* mice

To further confirm the myelomonocytic deletion of the *IL-6Rα*, we investigated the activation of STAT3, which is a downstream target of *IL-6* (Garbers et al., 2015). For this purpose, total splenocytes of *wt* and *IL-6Rα^{Δmyel}* mice were taken and either stimulated with *IL-6* or left unstimulated. As expected, upon *IL-6* stimulation myelomonocytic cells (*Ly6G⁺*, *Ly6G⁺Ly6C^{hi}* and *Ly6G⁺Ly6C^{int}*) display an increased phosphorylation and hence activation of STAT3 compared to unstimulated cells (Fig. 25A and B). Between the stimulated cells of *wt* and *IL-6Rα^{Δmyel}* mice, no difference in pSTAT3 could be detected (Fig. 25A and B). In addition, we performed Western Blot for pSTAT3 to analyze CD11b+ MACS-purified splenocytes, which were either unstimulated or stimulated with *IL-6*. In line with the FACS data, no difference in pSTAT3 between the stimulated groups could be observed (Fig. 25C). Interestingly, RT-PCR revealed a reduction of 50% in STAT3 expression in CD11b MACS purified splenocytes of *IL-6Rα^{Δmyel}* mice compared to cells of *wt* mice treated as before (Fig. 25D). The same trend was obvious in unstimulated cells, but not that strong. Also Oncostatin M (*Osm1*), a gene belonging to the gp130 family was analyzed, showing that the expression was higher in stimulated myelomonocytic cells of *IL-6Rα^{Δmyel}* mice as compared to *wt* mice (Fig. 25D).

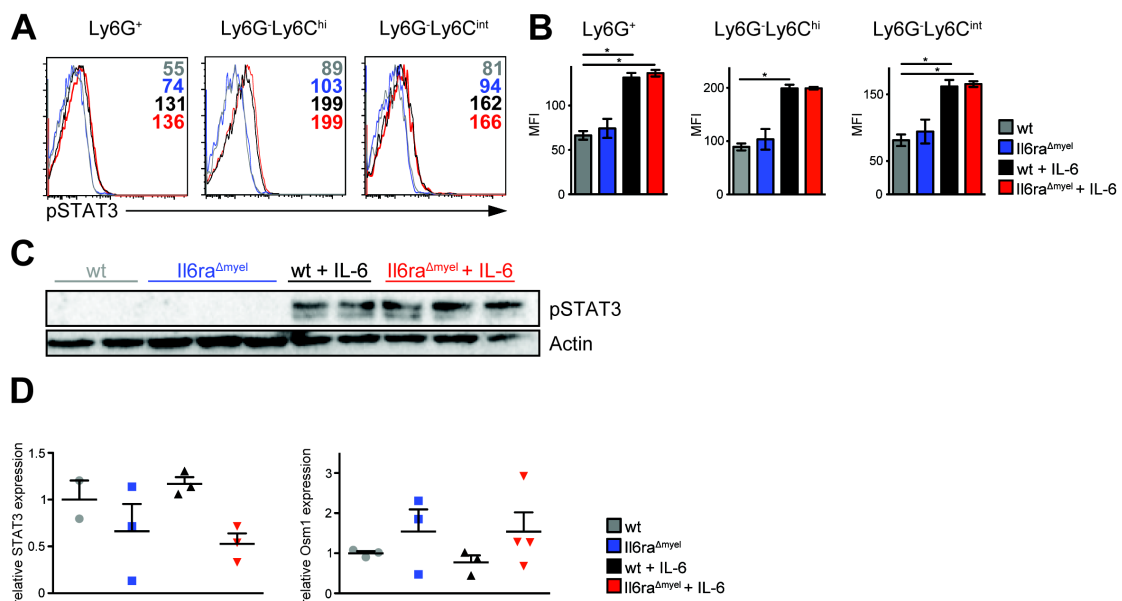


Figure 25: Analysis of STAT3 activation in myelomonocytic cells of *Il6ra*^{Δmyel} mice

(A) Flow cytometric analysis of pSTAT3 in Neutrophils (Ly6G⁺), pro-inflammatory monocytes (Ly6G⁺Ly6C^{hi}) and resident monocytes (Ly6G⁺Ly6C^{int}) of the spleen. Cells are pre-gated on living CD4⁻/B220⁻ cells. Gray (*wt*) and blue (*Il6ra*^{Δmyel}) histograms represent non-stimulated splenocytes. Black (*wt*) and red histograms (*Il6ra*^{Δmyel}) represent splenocytes stimulated with 50ng/ml IL-6 for 30min. Numbers in upper right corner represent the mean MFI values of the different groups. Shown are representative histograms. **(B)** Mean Fluorescent Intensity (MFI) of pSTAT3 expression pre-gated on Neutrophils (Ly6G⁺), pro-inflammatory monocytes (Ly6G⁺Ly6C^{hi}) and resident monocytes (Ly6G⁺Ly6C^{int}). Data are shown as bar graphs with mean and SEM. **p* ≤ 0,05 Significance was calculated using Kruskal-Wallis test. **(C)** Western Blot of total protein lysates from MACS-purified CD11b⁺ splenocytes. Shown are lysates of two *wt* mice and three *Il6ra*^{Δmyel} mice. Cells were either stimulated with 20ng/ml IL-6 for 30min (black and red lanes) or left unstimulated (gray and blue lanes). Anti-pSTAT3 antibody was used to detect phosphorylated STAT3, Actin served as a loading control. **(D)** Quantitative RT-PCR from MACS purified CD11b⁺ splenocytes for the expression of STAT3 and *Osm1* gene in *wt* and *Il6ra*^{Δmyel} mice. Cells were either stimulated with 20ng/ml IL-6 for 30min. (black and red plots) or left unstimulated (gray and blue plots). Expression levels are shown relative to the housekeeping gene HPRT (n=3-4). Data are shown as scatter plots with mean and SEM. Significance was calculated using Mann Whitney test.

3.4 IL-1 signaling in IMQ-induced psoriasis-like skin disease

3.4.1 *Il1r2*^{-/-} mice reveal an impact on myelomonocytic cells in steady state conditions

Besides IL-6 and IL-17, there are also other cytokines involved in the development of IMQ-induced psoriasis. One of these cytokines is IL-1. The IL-1 receptor consists of different components: IL-1R1 is the signal transmitting receptor with its ligands IL-1 α and IL-1 β , where the intracellular Toll-IL-1 receptor domain induces the signaling pathway (Peters et al., 2013). IL-1R2 is the decoy receptor, which is lacking the TIR domain and thus cannot transmit a signal, but can still bind IL-1 α and IL-1 β , although with less affinity (Boraschi and Tagliabue, 2013; Garlanda et al., 2013).

In the context of the skin, it is known that epidermal keratinocytes can secrete large amounts of IL-1 α (Barland et al., 2004; Uribe-Herranz et al., 2013). Mice, which specifically overexpress IL-1 α in keratinocytes, suffer from skin inflammation (Groves et al., 1995). Moreover, IL-1R1 deficient mice, which have less IL-1 signaling, exhibited reduced micro abscess formation in the skin upon IMQ treatment (Uribe-Herranz et al., 2013). Another group confirmed these results and, besides this, could also show that mice, which lack IL-1 α and IL-1 β , develop a milder skin disease under IMQ treatment (Rabeony et al., 2015). This reveals a great importance of this cytokine in the context of IMQ-induced

psoriasis. To further investigate the role of IL-1 in skin inflammation, we crossed CMV-Cre (Schwenk et al., 1995) mice to *IL1r2^{fl/fl}* mice (Taconic Biosciences), to achieve a knock out of the IL-1R2 in all cells (Fig. 26A). Recent analysis by another group showed that neutrophils express the highest levels of IL-1R2 (Martin et al., 2013). According to this, we performed RT-PCR for the *IL1r2* gene expressed by CD11b MACS purified bone marrow cells of *wt* and *Il1r2^{-/-}* mice. Clearly, we could demonstrate a strong reduction (75%) of the *Il1r2* gene in *Il1r2^{-/-}* mice compared to *wt* mice (Fig. 26B). As mentioned above, populations of myelomonocytic cells are strongly influenced by the treatment of IMQ. For this, CD11b⁺ cells and their sub-populations were investigated under steady state conditions in different organs. Interestingly, flow cytometric analysis of CD11b⁺ cells displayed more infiltrating cells in the ears of naïve *Il1r2^{-/-}* mice compared to *wt* mice in both percentages and total cell numbers (Fig. 26C-E). Other organs were not affected (Fig. 26D and E). According to the results of the RT-PCR, we analyzed the IL-1R2 expression of neutrophils on protein level by flow cytometry. A strong reduction of this receptor in spleen, ears and bone marrow of *Il1r2^{-/-}* mice compared to *wt* mice could be observed (Fig. 26F). Moreover, we also analyzed the spleen and blood at steady state for infiltrating myelomonocytic cells by flow cytometry (Fig. 26G). Surprisingly, the spleen contained significantly more neutrophils (Ly6G⁺) and less resident monocytes (Ly6G⁻Ly6C^{int}) in *IL1r2^{-/-}* mice compared to *wt* (Fig. 26H). However, the numbers of infiltrating myelomonocytic cells in the blood were not significantly changed (Fig. 26I).

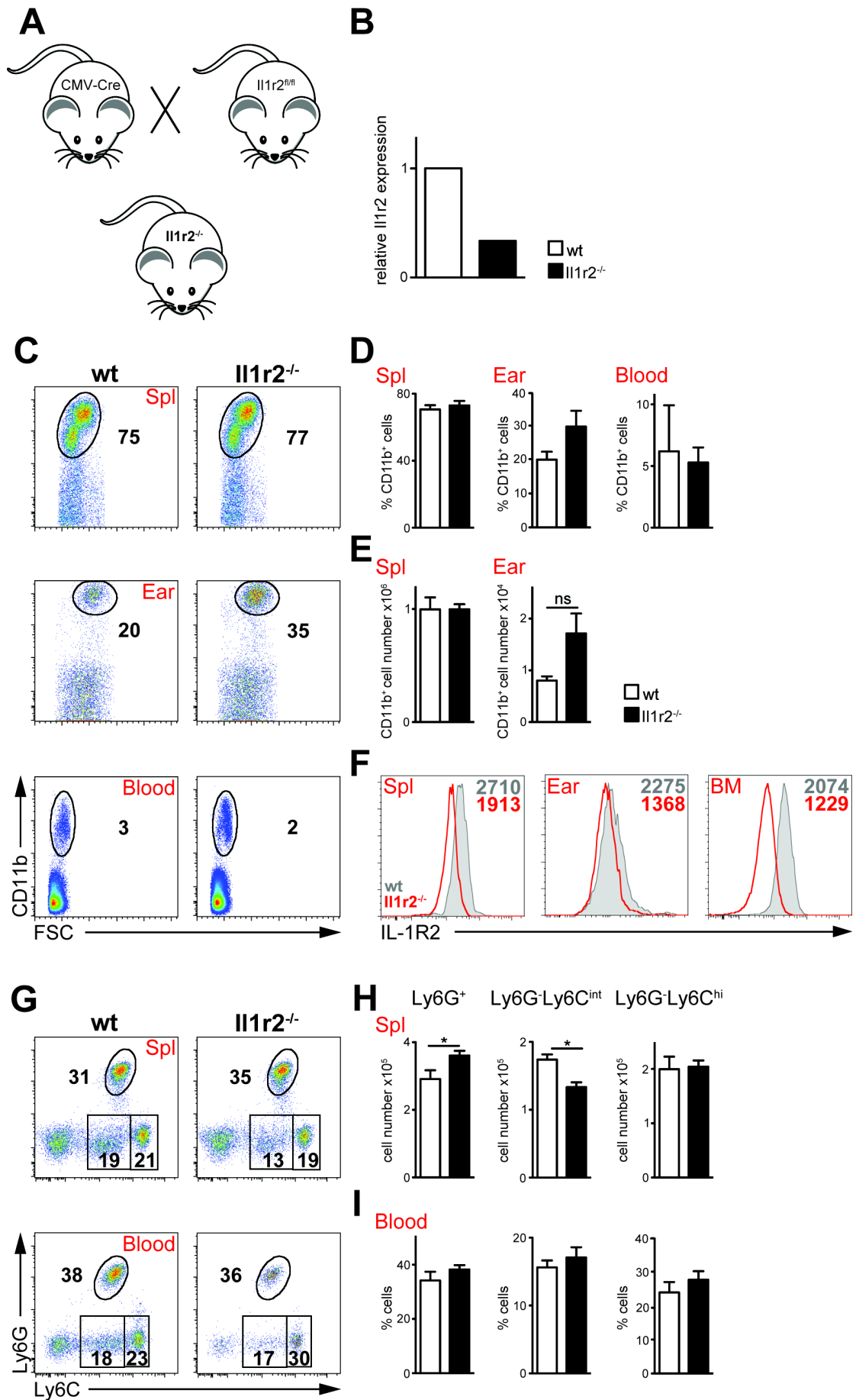


Figure 26: Generation of *Il1r2*^{-/-} mice and distribution of myelomonocytic cells in naïve mice

(A) Schematic representation of the crossing to obtain *Il1r2*^{-/-} mice. CMV-Cre mice were crossed to *Il1r2*^{fl/fl} mice to achieve the complete knockout of IL-1R2 (*Il1r2*^{-/-} mice). **(B)** Quantitative RT-PCR from CD11b MACS purified bone marrow cells for the *Il1r2* gene in *wt* and *Il1r2*^{-/-} mice. Expression levels are shown relative to the housekeeping gene HPRT (n=3 (*wt*); n=1 (*Il1r2*^{-/-})). Data are shown as bar graphs with mean and SEM. **(C)** Flow cytometric analysis of CD11b⁺ cells of the indicated organs. Cells are pre-gated on living CD90.2⁻/B220⁻ cells. **(D-E)** Percentages **(D)** and total cell numbers **(E)** of CD11b⁺ cells of the indicated organs. **(F)** Flow cytometric analysis of IL-1R2 expression on neutrophils (Ly6G⁺) in the indicated organs from *wt* mice (grey) and *Il1r2*^{-/-} mice (Mayer et al.). Numbers in upper right corner represent the mean MFI values of *Il1r2* expression in respective colors. Cells are pre-gated on living CD90.2⁻/CD19⁻/CD11b⁺ cells. Shown are representative histograms (n=3). **(G)** Flow cytometric analysis of neutrophils (Ly6G⁺), pro-inflammatory monocytes (Ly6G⁺Ly6C^{hi}) and resident monocytes (Ly6G⁺Ly6C^{int}) of indicated organs. Cells are pre-gated on living CD90.2⁻/B220⁻ and CD11b⁺ cells. **(H-I)** Total cell numbers of spleen **(H)** and percentages of blood **(I)** of neutrophils (Ly6G⁺), pro-inflammatory monocytes (Ly6G⁺Ly6C^{hi}) and resident monocytes (Ly6G⁺Ly6C^{int}). **(D, E, H and I)** Data are shown as bar graphs with mean and SEM. * p ≤ 0,05 Significances were calculated using Mann Whitney test (n=4).

3.4.2 *Il1r2*^{-/-} mice show higher susceptibility to IMQ-induced psoriasis

IL-1 signaling plays an important role in the development of IMQ-induced psoriasis, as the knock out of *Il1r1*^{-/-} mice showed a decreased susceptibility to psoriasis (Uribe-Herranz et al., 2013). In order to verify these previous results, we treated *Il1r2*^{-/-} mice with IMQ to analyze how the disease develops in mice with enhanced IL-1 signaling.

First, the severity of disease was documented by pictures of the back skin of mice, which were treated with IMQ for five consecutive days. Here, it was already obvious that *IL1r2*^{-/-} suffer from a stronger disease than *wt* mice (Fig. 27A). Documentation of the PASI score confirmed this and showed *IL1r2*^{-/-} mice to have a higher susceptibility to the treatment in all measured parameters, including erythema + scaling and back/ear skin thickness (Fig. 27B).

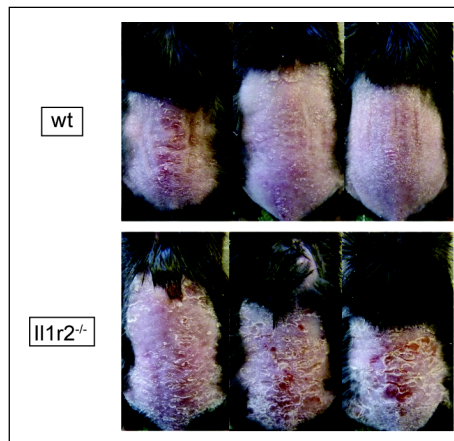
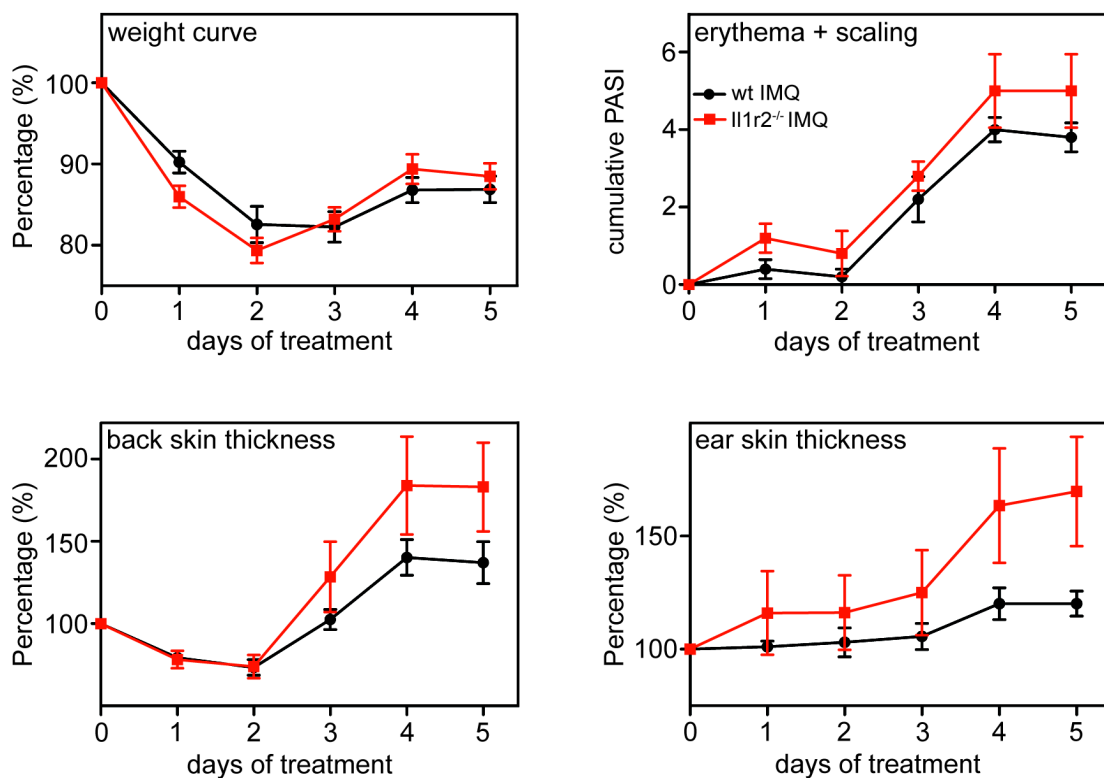
A**B**

Figure 27: *Il1r2*^{-/-} mice show higher clinical scores compared to *wt* mice in IMQ-induced psoriasis

(A) Pictures of the back skin of *wt* and *Il1r2*^{-/-} mice after treatment with IMQ for five consecutive days. **(B)** Modified PASI score of *Il1r2*^{-/-} mice and littermate controls. Weight (upper left), back/ear skin thickness (lower left/ lower right) and erythema/scaling (upper right) was scored daily on a scale from 0 to 4 (n=5). First day of weight- and skin thickness- measurements were set to 100%, values of the consecutive days were calculated accordingly.

Due to the clinical results, we wanted to see which cells infiltrate the skin and secondary lymphoid organs as a consequence of the treatment with IMQ, by flow cytometry. FACS analysis revealed increased numbers of CD11b⁺ cells in the spleen, which was confirmed by total cell counts being significantly increased in

Il1r2^{-/-} compared to *wt* (Fig. 28A and B). Moreover, the same result could be seen in the ears, where *Il1r2*^{-/-} have significantly more CD11b⁺ cells in percentages and total cell counts (Fig. 28C and D).

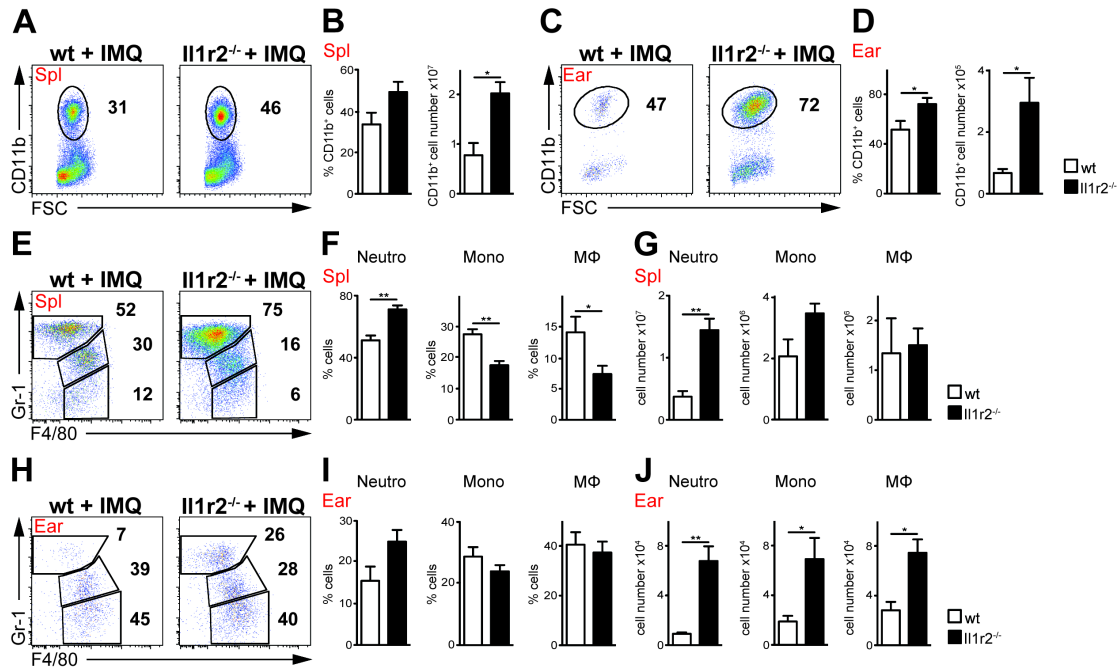


Figure 28: Deletion of *Il1r2* leads to an increase of infiltrating myelomonocytic cells in IMQ-induced psoriasis

(A) Flow cytometric analysis of CD11b⁺ cells of the spleen. Cells are pre-gated on living CD90.2⁻/CD19⁻ cells. (B) Percentages and total cell numbers of splenic CD11b⁺ cells (n=5). (C) Flow cytometric analysis of CD11b⁺ cells of the ears. Cells are pre-gated on living CD90.2⁻/CD19⁻ cells. (D) Percentages and total cell numbers of CD11b⁺ cells of the ears (n=5). (E) Flow cytometric analysis of splenic neutrophils (Gr-1^{hi} F4/80⁻), monocytes (Gr-1^{int} F4/80⁺) and macrophages (Gr-1⁻ F4/80⁺). Cells are pre-gated on living CD90.2⁻/CD19⁻ and CD11b⁺ cells. (F-G) Percentages (F) and total cell numbers (G) of neutrophils (Gr-1^{hi} F4/80⁻) (Neutro), monocytes (Gr-1^{int} F4/80⁺) (Mono) and macrophages (Gr-1⁻ F4/80⁺) (MΦ) of the spleen (n=5). (H) Flow cytometric analysis of neutrophils (Gr-1^{hi} F4/80⁻), monocytes (Gr-1^{int} F4/80⁺) and macrophages (Gr-1⁻ F4/80⁺) of the ears. Cells are pre-gated on living CD90.2⁻/CD19⁻ and CD11b⁺ cells. (I-J) Percentages (I) and total cell numbers (J) of neutrophils (Gr-1^{hi} F4/80⁻) (Neutro), monocytes (Gr-1^{int} F4/80⁺) (Mono) and macrophages (Gr-1⁻ F4/80⁺) (MΦ) of the ears (n=5). (B, D, F, G, I and J) Bar graphs are shown with mean and SEM. * p ≤ 0,05 Significance was calculated using Student's T-test (n=5).

Analyzing the sub-populations of the CD11b⁺ compartment, the IMQ treatment had an influence on all different cell types of the spleen. Neutrophils displayed significantly higher percentages whereas monocytes and macrophages were significantly decreased (Fig. 28E and F). Total cell numbers were also significantly increased in terms of neutrophils, while the numbers of monocytes and macrophages were not affected (Fig. 28G). However, in the ears of *Il1r2*^{-/-} mice, no differences in myelomonocytic cells (neutrophils, monocytes and

macrophages) in percentages could be detected (Fig. 28H and I), but in total numbers all populations were significantly increased in *IL1r2*^{-/-} mice compared to *wt* (Fig. 28J). In order to investigate whether other immune cells might also be influenced by the IMQ treatment, we analyzed the distribution of $\gamma\delta$ T cells in the skin of *Il1r2*^{-/-} mice by flow cytometry which were shown to produce high amounts of IL-17A under IMQ treatment (Pantelyushin et al., 2012). Apparently, neither dermal ($\gamma\delta$ TCR^{int}), epidermal ($\gamma\delta$ TCR^{hi}), nor IL-17A producing dermal $\gamma\delta$ T cells ($\gamma\delta$ TCR^{int}IL-17A⁺) were affected by IMQ treatment in *Il1r2*^{-/-} mice compared to *wt* (Fig. 29A-C). Percentages as well as total cell counts were not significantly changed (Fig. 29A-C). Additionally, V γ TCR segments of dermal (V γ 4⁺V γ 5⁻) and epidermal (V γ 4⁺V γ 5⁺) $\gamma\delta$ T cells were also not altered (Fig. 29D-F) by the IMQ treatment within the analyzed groups.

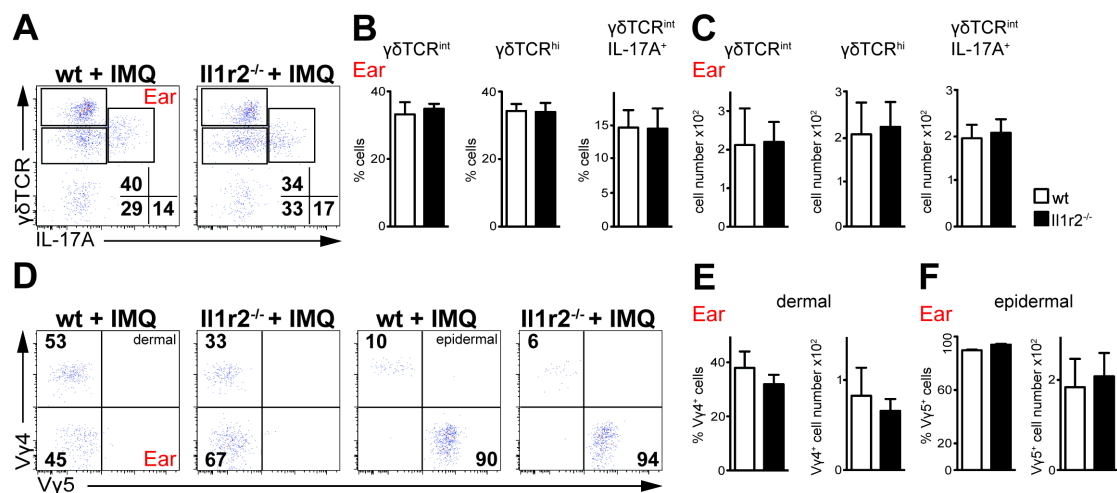


Figure 29: $\gamma\delta$ T cells of *Il1r2*^{-/-} mice are not altered in IMQ-induced psoriasis

(A) Flow cytometric analysis of dermal ($\gamma\delta$ TCR^{int}IL-17A⁻) and epidermal ($\gamma\delta$ TCR^{hi}IL-17A⁻) $\gamma\delta$ T cells and IL-17A producing dermal $\gamma\delta$ T cells ($\gamma\delta$ TCR^{int}IL-17A⁺) in the ears. Cells are pre-gated on living CD45.2⁺/CD3⁺ cells. (B-C) Percentages (B) and total cell numbers (C) of $\gamma\delta$ TCR^{int}IL-17A⁻, $\gamma\delta$ TCR^{hi}IL-17A⁻ and $\gamma\delta$ TCR^{int}IL-17A⁺ cells in the ears (n=4). (D) Flow cytometric analysis of subpopulations of dermal (V γ 4⁺V γ 5⁻) (left) and (Hueber et al.) epidermal (V γ 4⁺V γ 5⁺) (Hueber et al.) $\gamma\delta$ TCR⁺ cells in the ears. Cells are pre-gated on CD45.2⁺/CD3⁺/ $\gamma\delta$ TCR^{int} (dermal)/ $\gamma\delta$ TCR^{hi} (epidermal) cells. (E-F) Percentages (E) and total cell numbers (F) of V γ 4⁺V γ 5⁻ (left) and V γ 4⁺V γ 5⁺ (Hueber et al.) $\gamma\delta$ T cells in the ears. (B, C, E and F) Bar graphs are shown with mean and SEM. Significance was calculated using Mann Whitney test (n=4).

As already mentioned, different cytokines were shown to be involved in the pathogenesis of IMQ-induced psoriasis, like IL-6, IL-17, IL-22, IL-23, IL-1 (El Malki et al., 2013; Uribe-Herranz et al., 2013; Van Belle et al., 2012; van der Fits et al., 2009; Wohn et al., 2013). Next, we wanted to investigate the expression of

those cytokines and performed RT-PCR analysis of the back skin of IMQ-treated mice compared to those of controls (this experiment was performed with the help of Nguyen Thanh Son). IL-22 and IL-17A production were not affected by the treatment (Fig. 30A), whereas IL-17F, IL-6 and IL-1 β were slightly increased in *Il1r2*^{-/-} mice compared to *wt* (Fig. 30A). As it is expected to have increased systemic levels of IL-17A due to the IMQ treatment, an ELISA of blood sera was performed. Here, *Il1r2*^{-/-} IMQ-treated mice displayed a mild increase for IL-17A in the sera of blood compared to *wt* (Fig. 30B). We can say that the knock out of IL-1R2 showed the opposite outcome in the model of IMQ-induced psoriasis compared to the knock out of IL-1R1. The slight up-regulation of cytokines in the skin of *Il1r2*^{-/-} might be related to the distribution of myelomonocytic cells in the skin and other organs.

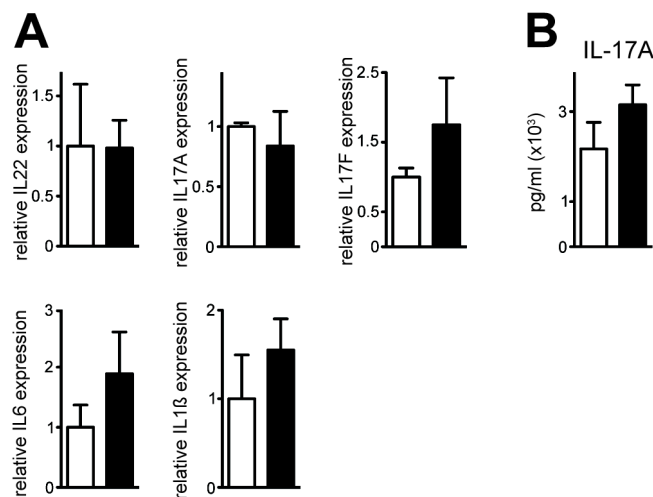


Figure 30: Deletion of *Il1r2* leads to an increase of pro-inflammatory cytokines in IMQ-induced psoriasis.

(A) Quantitative RT-PCR from back skin of IMQ treated mice for *Il22*, *Il17A*, *Il17F*, *Il6* and *Il1 β* gene expression in *wt* and *Il1r2*^{-/-} mice. Expression levels are shown relative to the housekeeping gene *HPRT* (n=3). Data are shown as bar graphs with mean and SEM. Significance was calculated using Mann Whitney test. **(B)** Levels of IL-17A from blood sera of IMQ treated mice measured by ELISA. Data are shown as bar graphs with mean and SEM. Significance was calculated using Mann Whitney test (n=3).

3.4.3 Neutrophil specific deletion of *Il1r2* has no influence on myelomonocytic cells

As the complete deletion of IL-1R2 already showed an impact on the myelomonocytic compartment under steady state conditions, these cells seem to be strongly influenced by IL-1 signaling (3.4.1). Furthermore, the IL-1R2 is

expressed on neutrophils in high numbers (Martin et al., 2013). In order to investigate the role of IL-1 signaling in neutrophils in more detail, we crossed Ly6G-Cre mice (Hasenberg et al., 2015) to *Il1r2^{fl/fl}* (Taconic Biosciences) mice to obtain mice with a deletion of IL-1R2 specifically in neutrophils (Fig. 31A). The Ly6G-Cre mice were generated through a knock-in of a Cre-recombinase and a tdTomato into exon1 of the Ly6G locus (Hasenberg et al., 2015).

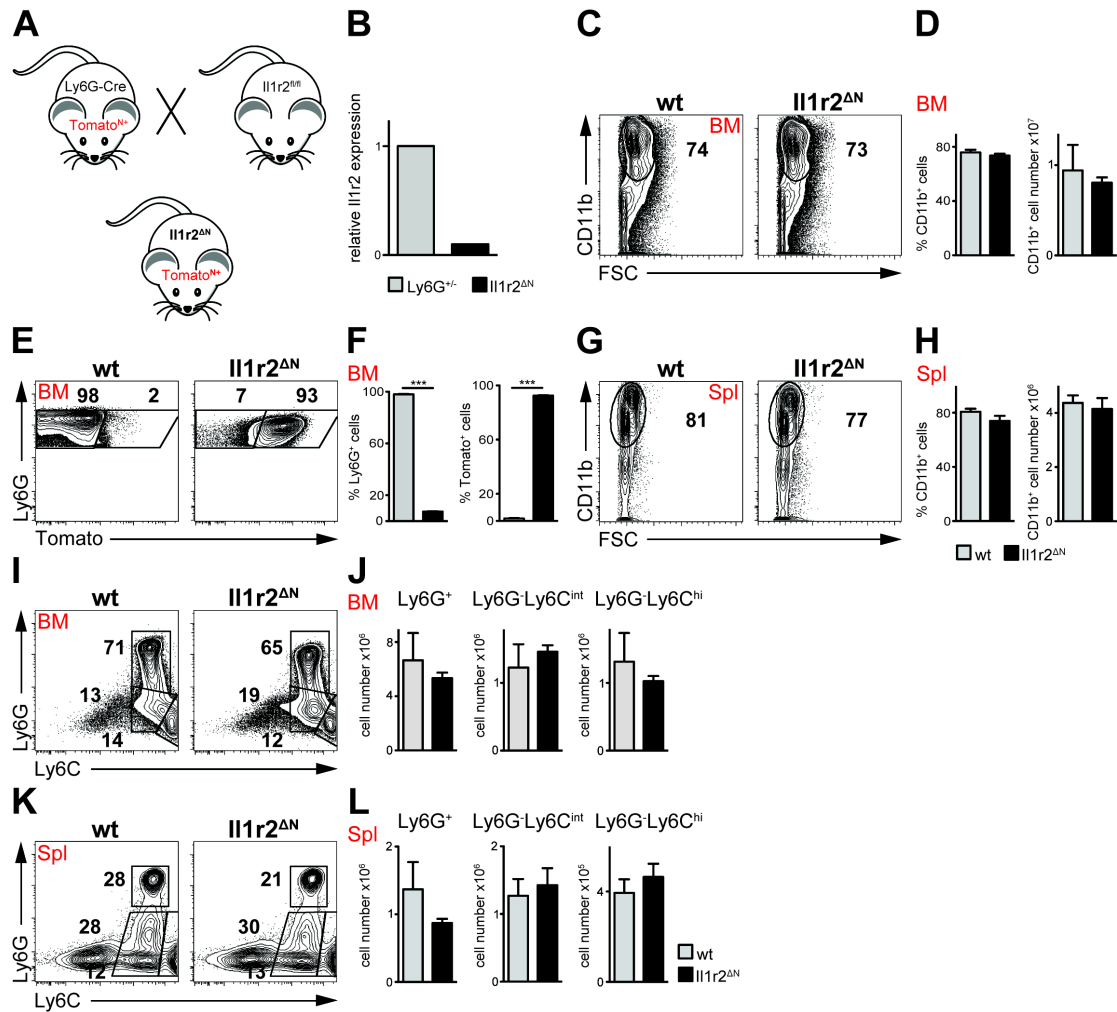


Figure 31: Generation of *Il1r2^{ΔN}* mice and impact of neutrophil specific deletion of IL1r2 on myelomonocytic cells under basal conditions

(A) Schematic representation of the cross to generate *Il1r2^{ΔN}* mice. Ly6G-Cre mice were crossed to *Il1r2^{fl/fl}* mice to achieve a deletion of IL-1R2 specifically in neutrophils (*Il1r2^{ΔN}* mice). Ly6G-Cre were generated as a knock-in into the Ly6G locus, where Ly6G⁺ cells co-express the tdTomato reporter (Hasenberg et al., 2015). **(B)** Quantitative RT-PCR from tomato positive cells for the *Il1r2* gene in *Ly6G^{+/-}* and *Il1r2^{ΔN}* mice. Expression levels are shown relative to the housekeeping gene HPRT (n=1). Data are shown as bar graphs with mean and SEM. **(C)** Flow cytometric analysis of CD11b⁺ cells of the bone marrow. Cells are pre-gated on living CD90.2⁻/B220⁻ cells **(D)** Percentages and total cell numbers of CD11b⁺ cells of the bone marrow. **(E)** Flow cytometric analysis of Ly6G⁺Tomato⁻ and Ly6G⁺Tomato⁺ cells of the bone marrow in *wt* and *Il1r2^{ΔN}* mice, representing the Cre efficiency in *Il1r2^{ΔN}* mice. Cells are pre-gated on living CD90.2⁻/B220⁻/Ly6G⁺ cells. **(F)** Percentages of Ly6G⁺Tomato⁻ and Ly6G⁺Tomato⁺ cells of the bone marrow. Bar graphs are shown with mean and SEM. Significance was calculated using Student's T-test (n=3 (*wt*); n=4 (*Il1r2^{ΔN}*)). **(G)** Flow cytometric analysis of splenic CD11b⁺ cells from *Il1r2^{ΔN}* and littermate control animals. Cells are pre-gated on living CD90.2⁻/B220⁻ cells. **(H)** Percentages and total cell numbers of CD11b⁺ cells of the spleen. **(I)** Flow cytometric analysis of neutrophils (Ly6G⁺ Ly6C^{int}), pro-inflammatory monocytes (Ly6G⁻Ly6C^{hi}) and resident monocytes (Ly6G⁻Ly6C^{int}) in the bone marrow. Cells are pre-gated on living CD90.2⁻/B220⁻ and CD11b⁺ cells. **(J)** Total cell numbers of neutrophils (Ly6G⁺ Ly6C^{int}), pro-inflammatory monocytes (Ly6G⁻Ly6C^{hi}) and resident monocytes (Ly6G⁻Ly6C^{int}) of the bone marrow. **(K)** Flow cytometric analysis of splenic neutrophils (Ly6G⁺Ly6C^{int}), pro-inflammatory monocytes (Ly6G⁻Ly6C^{hi}) and resident monocytes (Ly6G⁻Ly6C^{int}). Cells are pre-gated on living CD90.2⁻/B220⁻ and CD11b⁺ cells. **(L)** Total cell numbers of neutrophils (Ly6G⁺Ly6C^{int}), pro-inflammatory monocytes (Ly6G⁻Ly6C^{hi}) and resident monocytes (Ly6G⁻Ly6C^{int}) of the spleen. **(D, F, G, H, J and L)** Bar graphs are shown with mean and SEM. Significance was calculated using Mann Whitney test (n=3 (*wt*); n=4 (*Il1r2^{ΔN}*)).

To verify the specific deletion in *Il1r2^{ΔN}* mice, RT-PCR for *Il1r2* of tomato positive sorted cells of the bone marrow was performed. For this experiment a *Ly6G^{+/-}* mouse was used as a control. As shown in Fig. 31B, the expression of *Il1r2* is strongly reduced in *Il1r2^{ΔN}* compared to *Ly6G^{+/-}* mice. In addition, the Cre-efficiency of these mice was also examined by flow cytometry in cells of the bone marrow. For this purpose, cells were pre-gated on Ly6G⁺ cells to see how many of the Ly6G⁺ cells also express tomato. In line with our expectations, *Il1r2^{ΔN}* mice showed a Cre-efficiency of almost 100% compared to *wt* mice, as all Ly6G⁺ cells expressed tomato (Fig. 31E and F). In *wt* mice no tomato⁺ cells could be detected (Fig. 31E and F). Next, the distribution of myelomonocytic cells in *Il1r2^{ΔN}* was analyzed by flow cytometry. The bone marrow from *Il1r2^{ΔN}* mice and the respective controls showed the same CD11b⁺ cells in both percentages and total cell numbers (Fig. 31C and D). Similarly, the spleen showed the same numbers of CD11b⁺ cells in *Il1r2^{ΔN}* mice and controls (Fig. 31G and H). Further, neutrophils (Ly6G⁺), resident monocytes (Ly6G⁻Ly6C^{int}) and pro-inflammatory monocytes (Ly6G⁻Ly6C^{hi}) were examined by flow cytometry in spleen and bone marrow. As already expected from the previous results of the CD11b⁺ cells, the deletion of

Il1r2 did not have an impact on cells of the myelomonocytic compartment from either the bone marrow (Fig. 31I and J) or spleen (Fig. 31K and L).

3.4.4 IMQ-induced psoriasis in *Il1r2^{ΔN}* mice has no effect on cells of the myelomonocytic compartment

To continue the analysis of *Il1r2^{-/-}* mice, which were more susceptible to IMQ-induced psoriasis (3.4.2), psoriasis-like disease was also induced in *Il1r2^{ΔN}* mice. *Il1r2^{ΔN}* mice and respective controls were treated with IMQ or sham cream for five consecutive days. As expected, IMQ treated mice showed increased PASI scores in erythema + scaling and back/ear skin thickness during the treatment compared to sham treated groups (Fig. 32). However, within IMQ treated groups no difference was detected (Fig. 32).

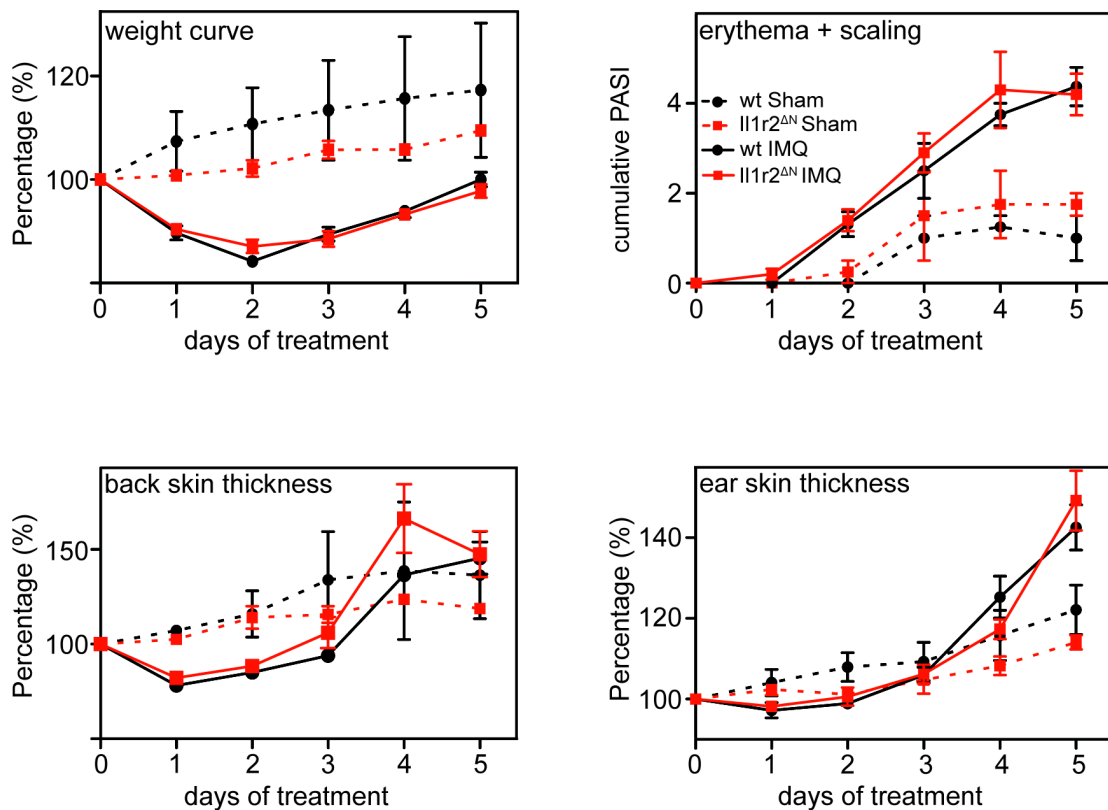


Figure 32: *Il1r2^{ΔN}* mice show no effect in clinical scores in IMQ-induced psoriasis

Modified PASI score of weight (upper left), back/ear skin thickness (lower left/ lower right) and erythema/scaling (upper right) from IMQ treated (n=4-5) and sham treated (n=2) *Il1r2^{ΔN}* mice or littermate controls. First day of weight- and skin thickness- measurements were set to 100%, values of the consecutive days were calculated accordingly.

Moreover, the spleen and ears were analyzed for infiltrating myelomonocytic cells by flow cytometry. Examining the CD11b⁺ cells of spleen and ears, no differences could be detected (Fig. 33A-D).

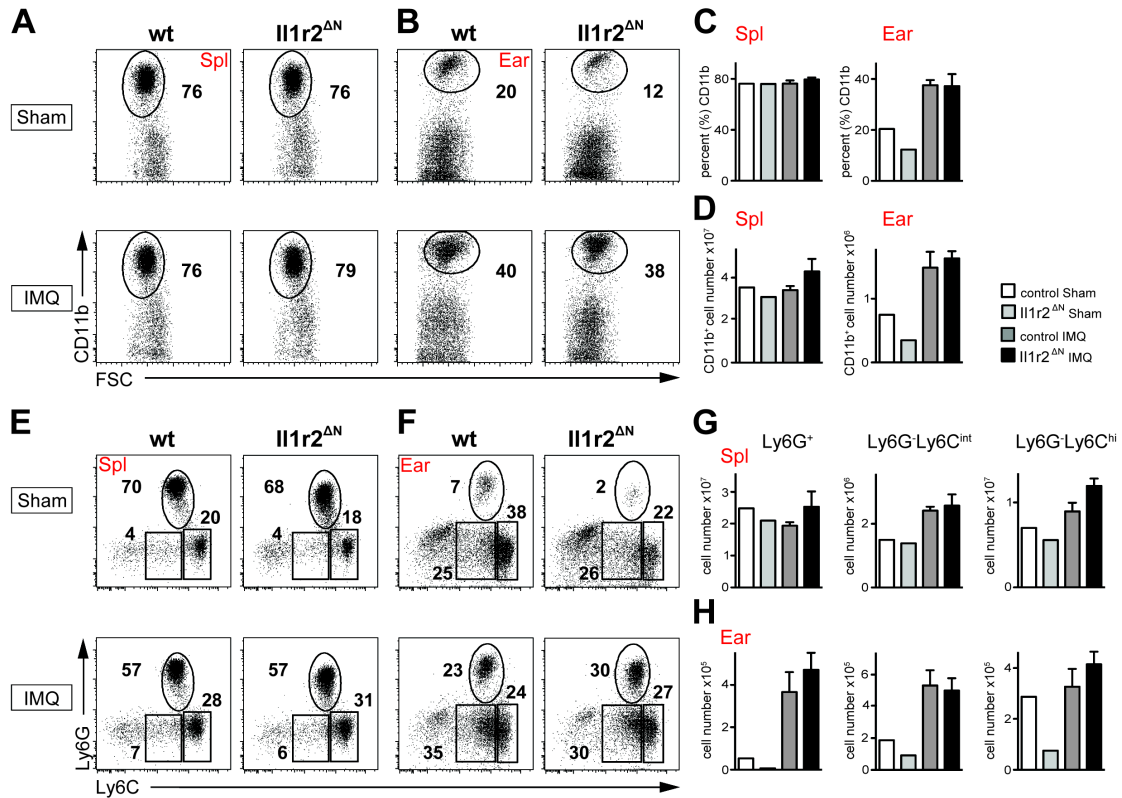


Figure 33: Myelomonocytic cells of *Il1r2*^{ΔN} mice are not altered in IMQ-induced psoriasis

(A) Flow cytometric analysis of splenic CD11b⁺ cells. Cells are pre-gated on living CD90.2⁻/B220⁻ cells. (B) Flow cytometric analysis of CD11b⁺ cells of the ears. Cells are pre-gated on living CD90.2⁻/B220⁻ cells. (C) Percentages of CD11b⁺ cells of the indicated organs. (D) Total cell numbers of CD11b⁺ cells of the indicated organs. (E-F) Flow cytometric analysis of neutrophils (Ly6G⁺Ly6C^{int}), pro-inflammatory monocytes (Ly6G⁻Ly6C^{hi}) and resident monocytes (Ly6G⁻Ly6C^{int}) of (E) spleen and (F) ears. Cells are pre-gated on living CD90.2⁻/B220⁻ and CD11b⁺ cells. (G-H) Total cell numbers of neutrophils (Ly6G⁺Ly6C^{int}), pro-inflammatory monocytes (Ly6G⁻Ly6C^{hi}) and resident monocytes (Ly6G⁻Ly6C^{int}) of (G) spleen and (H) ears. (C, D, G and H) Data are shown as bar graphs with mean and SEM. Significance was calculated between IMQ treated groups using Mann Whitney test (IMQ groups n=3, sham groups n=1).

In the spleen the ratios and total cell numbers of all four groups were comparable (Fig. 33C and D), whereas the infiltration of CD11b⁺ cells to the ears showed differences between IMQ and sham treated groups (Fig. 33C and D). Indeed, also here the IMQ treated mice displayed the same numbers of infiltrates (Fig. 33C and D). A similar picture was obtained from the analysis of neutrophils (Ly6G⁺), resident monocytes (Ly6G⁻Ly6C^{int}) and pro-inflammatory monocytes (Ly6G⁻Ly6C^{hi}) in spleen and ears. The spleen showed similar ratios and total

numbers of all examined populations (Fig. 33E and G), except for total cells of resident and pro-inflammatory monocytes. Here, the IMQ treated groups exhibited a slight increase compared to sham treated mice (Fig. 33G). However, the IMQ treatments lead to the same amount of infiltrates in *Il1r2^{ΔN}* mice and respective controls. Compared to the spleen, the ears showed increased neutrophils in IMQ treated mice compared to the sham groups (Fig. 33F). The total cell numbers display the same picture (Fig. 33H), but once more, within IMQ treated groups no differences were seen.

In conclusion, the neutrophil specific deletion of *Il1r2* (*Il1r2^{ΔN}*) had no impact on the severity of IMQ-induced psoriasis. This clearly shows that the neutrophils are not the immune cells, which are responsible for the more severe IMQ-induced psoriasis we saw with the full knock out of *Il1r2*. Therefore, other cells must be responsible for this effect.

3.4.5 *T cell specific deletion of Il1r2 shows no effect on clinical scores in IMQ-induced psoriasis*

Since the neutrophil specific deletion of *Il1r2* did not show an effect on the model of IMQ-induced psoriasis, we wanted to see if a T cell specific deletion would have an impact on the phenotype. For this purpose we crossed CD4-Cre mice (Wolfer et al., 2001) to *Il1r2^{fl/fl}* mice (Taconic Biosciences), resulting in an IL-1R2 specific knock out on T cells (*Il1r2^{ΔT}*).

Again, we induced a psoriasis-like disease in those mice and documented the severity of disease by the PASI score during the course of treatment. For a better comparison also *Il1r2^{ΔN}* were included into the analysis. Obviously, also the T cell specific deletion had no influence on the severity of disease. No difference between the IMQ treated *Il1r2^{ΔN}*, *Il1r2^{ΔT}* and *wt* mice could be examined in the measured parameters of erythema + scaling and back/ear skin thickness (Fig. 34). Moreover, in terms of skin thickness the sham treated group displayed a similar increase to IMQ-treated groups (Fig. 34). At first appearance it seemed as if also the T cells are not the immune cells, which lead to the strong phenotype in psoriasis-like disease in *Il1r2^{-/-}* mice. However, to make a final conclusion, this

experimental setup would need to be repeated, also including flow cytometric analysis.

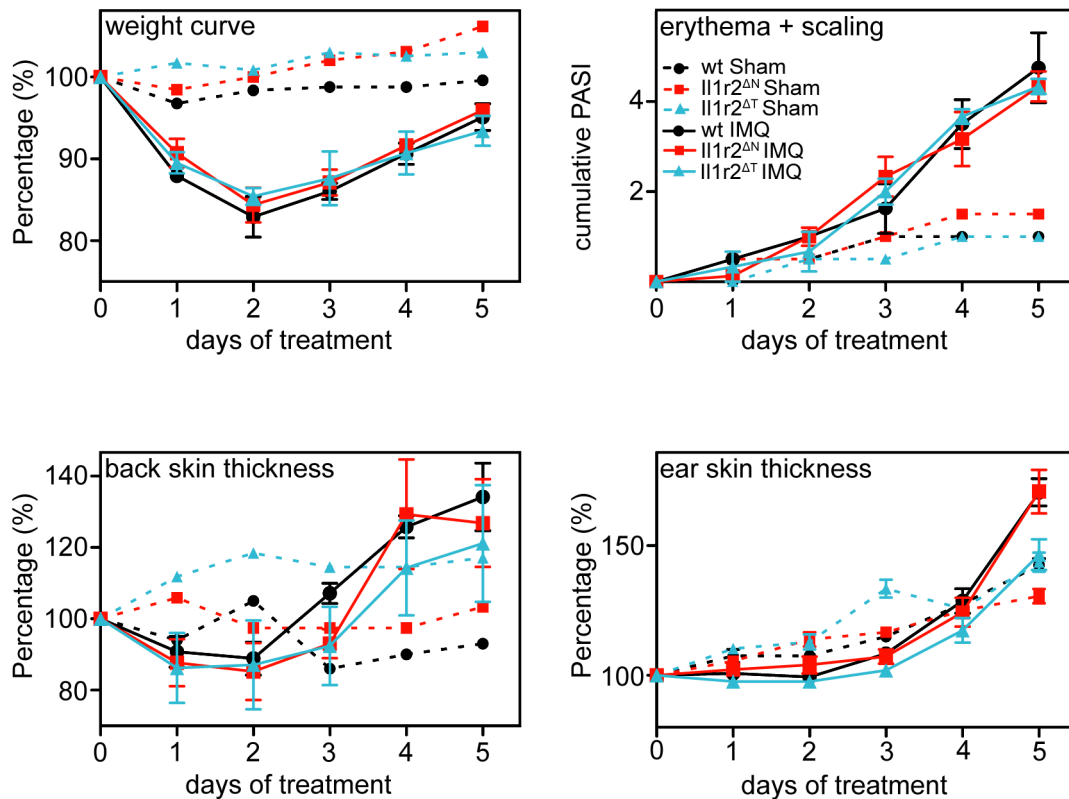


Figure 34: *Il1r2^{ΔN}* and *Il1r2^{ΔT}* mice show no effect in clinical scores in IMQ-induced psoriasis

Modified PASI score of weight (upper left), back/ear skin thickness (lower left/ lower right) and erythema/scaling (upper right) from IMQ treated (n=3-4) and sham treated (n=1) indicated experimental groups and respective littermate controls. First day of weight- and skin thickness-measurements were set 100%, values of the consecutive days were calculated accordingly. T cell specific deletion of IL1r2 was achieved by crossing *Il1r2^{fl/fl}* mice to CD4-Cre mice (*Il1r2^{ΔT}* mice).

3.5 Depletion of neutrophils via the iDTR system

Due to a prominent role of neutrophils in the model of IMQ-induced psoriasis, we wanted to investigate a mouse model with total absence of neutrophils. One possibility to deplete neutrophils in mice is via treatment with Ly6G specific antibodies (Daley et al., 2008).

Considering another approach, Buch et al demonstrated an inducible system where cell lines can be specifically ablated by their expression of the diphtheria toxin receptor (Buch et al., 2005). Here, mice with the inducible diphtheria toxin receptor (iDTR) lack the STOP cassette of the diphtheria toxin receptor (DTR).

Crossing those mice to a specific Cre-line, results in a tissue-specific expression of the DTR. After the injection of diphtheria toxin (DT), only the cells which express the DTR die (Buch et al., 2005). In our case, we crossed the Ly6G-Cre mice (Hasenberg et al., 2015) to iDTR mice to achieve a neutrophil specific ablation after DT injection (Fig. 35A). For the experimental setup, we injected DT on three consecutive days and analyzed the mice at various time points after the last injection (Fig. 35B).

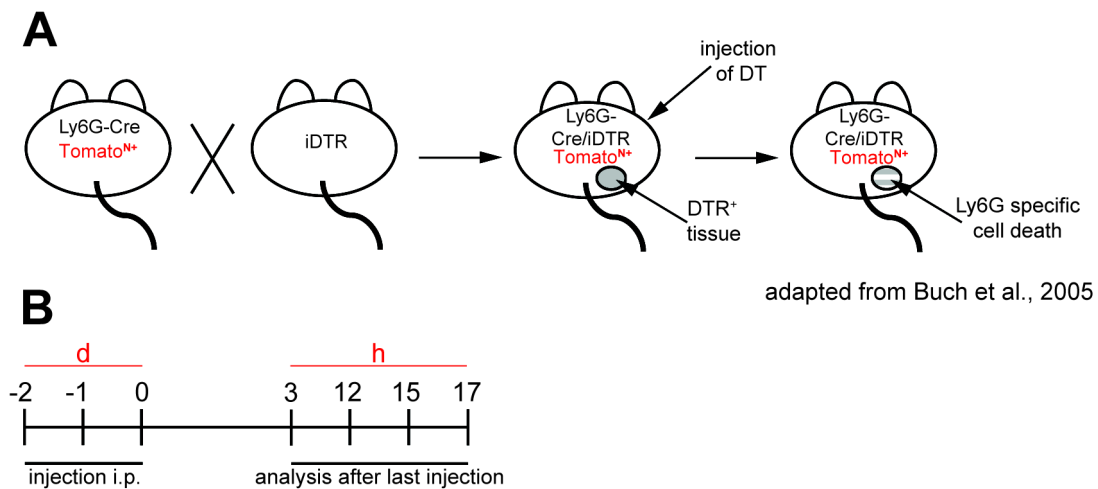


Figure 35: Depletion of Ly6G⁺ via the iDTR system and experimental setup

(A) Schematic representation of the crossing to achieve that Ly6G⁺ cells (neutrophils) express the Diphtheria Toxin receptor. Ly6G-Cre mice were crossed to iDTR mice. Injection of Diphtheria Toxin (DT) into the mice leads to a Ly6G specific cell death. All Ly6G⁺ cells co-express the tdTomato reporter. **(B)** Schematic representation of the experimental setup. Mice were injected on three consecutive days with a dose of 25ng/g mouse weight of DT. Analysis of the mice followed in intervals between 3h-17h after the last injection of DT.

In the first experimental setup, heterozygous *Ly6GiDTR^{+/-}* mice were examined for the depletion efficiency of neutrophils after 3, 12, 15 and 17h of the last DT injection by flow cytometry. Spleen and blood of *Ly6GiDTR^{+/-}* mice showed comparable numbers of Ly6G⁺ cells as the *wt*, 3h hours after depletion (Fig. 36A). Later time points (12, 15 and 17h) presented a depletion efficiency of approximately 50% (Fig. 36A). Percentages and total cell numbers of the mentioned organs gave the same result (Fig. 36B).

In addition, homozygous iDTR mice (*Ly6GiDTR^{-/-}*) were investigated in order to see whether a better depletion could be obtained. These mice were analyzed 15h after the last injection for infiltrating Ly6G⁺ cells in spleen and blood by flow

cytometry (Fig. 36C). Contrary to our expectations, only 50% of the neutrophils could be ablated with homozygous mice (Fig. 36D).

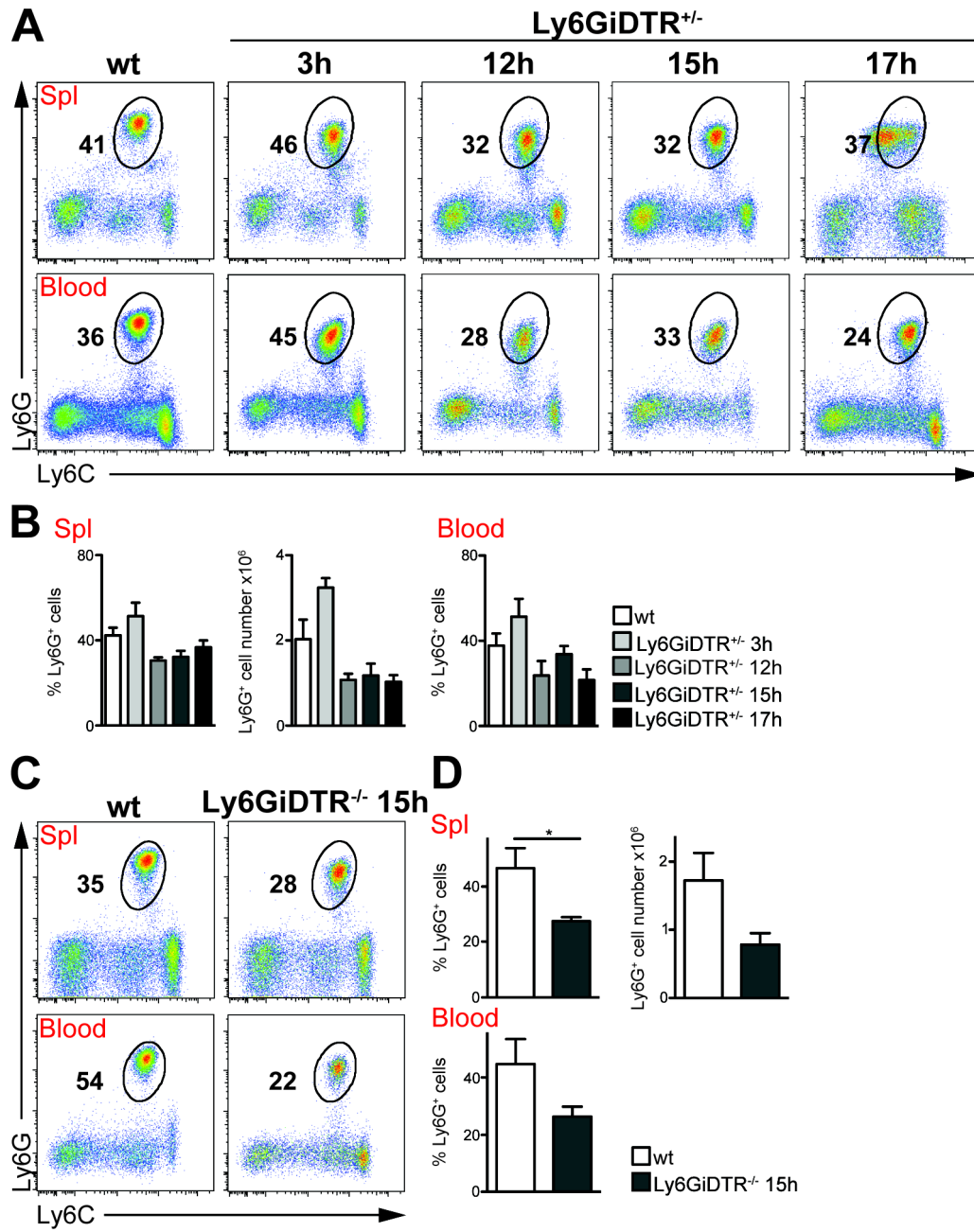


Figure 36: *Ly6GiDTR* mice show a reduction in Ly6G⁺ cells after DT injection

A) Flow cytometric analysis of Ly6G⁺ cells in heterozygous iDTR mice of the indicated organs. Shown are representative FACS plots after 3, 12, 15 or 17h of the last DT injection. Cells are pre-gated on living B220⁻/CD90.2⁻/CD11b⁺ cells. **(B)** Percentages and total cell numbers of Ly6G⁺ cells of the indicated organs. Data are shown as bar graphs with mean and SEM. Significance was calculated using Kruskal-Wallis test (n=3-4 (*Ly6GiDTR*); n=10 (*wt*)). **(C)** Flow cytometric analysis of Ly6G⁺ cells in homozygous iDTR mice of the indicated organs. Shown are representative FACS plots 15h after the last DT injection. Cells are pre-gated on living B220⁻/CD90.2⁻/CD11b⁺ cells. **(D)** Percentages and total cell numbers of Ly6G⁺ cells of the indicated organs. Data are shown as bar graphs with mean and SEM. Significance was calculated using Mann Whitney test (n=4).

Since the deletion efficiency never reached over 50% we did not further investigate this model. An ablation of 50% of neutrophils is not sufficient to study the role of these cells in the model of IMQ-induced psoriasis.

4 Discussion

4.1 Neutralizing antibodies as a treatment option for psoriasis

Psoriasis is an inflammatory disease of the skin, which affects 2-4% of the worldwide population (Danilenko, 2008). There are different treatment approaches, but very successful is the neutralization of cytokines with mAb`s, such as IL-17, IL-23 or TNF α (Campa et al., 2016; Elyoussfi et al., 2016; Farahnik et al., 2016; Jinna and Strober, 2016; Lowes et al., 2013; Waisman, 2012). Recent studies revealed the effectiveness of the human mAb Secukinumab, which targets IL-17A (Elyoussfi et al., 2016; Farahnik et al., 2016; Jinna and Strober, 2016). Secukinumab, has low immunogenicity, indicating that the treatment with this antibody leads to low titers of anti-drug antibodies (ADAs) compared to chimeric mAb`s such as Infliximab and Rituximab (Karle et al., 2016; Lopez-Ferrer et al., 2015). It was developed by Novartis to treat psoriasis, rheumatoid arthritis and uveitis (Hueber et al., 2010). Different phase III clinical studies showed a good efficiency in the treatment of psoriasis (Langley et al., 2014; Paul et al., 2015; Strober et al., 2016) and also in PsA (McInnes et al., 2015). In September 2015 the FDA approved Secukinumab as a drug to treat plaque psoriasis (Campa et al., 2016; Ritchlin and Krueger, 2016).

We used the respective anti-mouse antibody of Secukinumab to treat mice with a strong psoriasis-like phenotype (*K14-IL-17A^{ind/+}*) (Croxford et al., 2014). In two different experiments, where the same dosage of antibody was used, the results varied slightly. In the first experiment we observed a higher reduction of IL-17A in the sera of anti-IL-17A treated mice, already after three weeks of treatment, indicating a better neutralization, when compared to the second experiment. This suggested a more efficient treatment, with less spleen infiltrating myelomonocytic cells. However, the number of infiltrating cells to the skin was comparable in both experiments, possibly due to the high amount of IL-17A in the skin, which was not neutralized by the applied antibody concentration. The treatment was performed twice a week. So the time intervals in between them allowed the production of high amounts of IL-17A, as the removal of the STOP cassette leads to a constant production of the cytokine (Croxford et al., 2014). Due to this, we took into consideration to treat the mice with the same dose of

antibody, but more than twice a week to further improve the psoriasis-like phenotype. The group of untreated mice of the 2nd experiment showed a milder PASI and less infiltrating myelomonocytic cells. Due to weekly scoring and injections, the mice were also subjected to an increased level of stress, which possibly contributes to an impairment of disease (Schwartz et al., 2016; Trojacka et al., 2015). Furthermore, instead of applying the antibody intraperitoneal, subcutaneous injection equivalent to the human treatment (Langley et al., 2014; Paul et al., 2015) could deliver the antibody directly to the source of disease and IL-17 production, possibly leading to a better effect. In addition, this would also go along with not touching the lesional skin, reducing another factor of stress. However, the treatment in general had an effect shown by the results of the 1st experiment, where the spleen of anti-IL-17A treated mice displayed less infiltrating myelomonocytic cells.

These findings were also supported by an anti-IL-17A treatment of *wt* mice in the model of IMQ-induced psoriasis. Here, the clinical scores of the antibody treated mice were decreased compared to isotype and PBS treated groups. Nonetheless, the effect on myelomonocytic cells was reduced. Maybe also here a higher dose of antibody should be considered. The previous experiment, where lower amounts of antibody were applied, showed that the treatment has a dose-dependent effect: no impact on the clinical scores was obvious. As both treatments did not influence the distribution of myelomonocytic cells, but other immune cells can be affected by the anti-IL-17A treatment. Here, for example the $\gamma\delta$ T cells could be considered, as they are claimed to be the main producers of IL-17A in psoriasis (Becher and Pantelyushin, 2012; Cai et al., 2011; Pantelyushin et al., 2012). Certainly, the anti-IL-17A treatment of *K14-IL-17A^{ind/+}* mice had no influence on the distribution of $\gamma\delta$ T cells and β TCR⁺ cells.

Although the anti-IL-17A treatment had only a mild effect on the severity of psoriasis-like disease in *K14-IL-17A^{ind/+}* mice, our group already demonstrated that an anti-IL-6 treatment resulted in a significant reduction of neutrophil microabscesses in the skin (Croxford et al., 2014). Targeting a molecule in the downstream signaling cascade of IL-17A (Iwakura et al., 2011) revealed to be very successful in the treatment of the psoriatic phenotype in those mice. Anti-IL-6 has also been discussed as a treatment option of psoriasis in humans

(Saggini et al., 2014), but stays disputed. Tocilizumab and Siltuximab are the two most common mAb's used to target IL-6. Siltuximab binds the cytokine and is predominantly used to treat Castleman's disease (Davis et al., 2015; Fajgenbaum and Kurzrock, 2016; Mayer et al., 2015), whereas Tocilizumab (produced by Hoffmann-La Roche) is an anti-IL-6R antibody and seems to very efficient in the treatment of Rheumatoid arthritis (RA) (Emery et al., 2008; Genovese et al., 2008). IL-6 is important in B cell maturation by influencing the production of autoantibodies, which are present in RA (Dayer and Choy, 2010). Hence, targeting IL-6 seems to be a good treatment option for RA (Dayer and Choy, 2010). Moreover, IL-6 is highly up regulated in the skin and plasma levels of psoriasis patients (Grossman et al., 1989; Neuner et al., 1991; Zalewska et al., 2006), suggesting Tocilizumab can be used for the treatment of psoriatic lesions. Interestingly, some studies already confirmed an anti-IL-6R treatment in psoriasis, for example it was successfully used to treat plantar pustular psoriasis (Jayasekera et al., 2014). Further, another study reported about completely resolving psoriatic skin lesions by addressing ankylosing spondylitis and chron's disease with the Tocilizumab antibody (Brulhart et al., 2010). However, the application of the anti-IL-6R antibody can induce psoriatic lesions when treating other diseases. Especially patients who suffered from RA and were treated with Tocilizumab developed psoriasis symptoms as side effects (Grasland et al., 2013; Palmou-Fontana et al., 2014; Wendling et al., 2012). Also the treatment of PsA resulted in a more severe psoriasis as a consequence of anti-IL-6R application (Hughes and Chinoy, 2013; Laurent et al., 2010). These observed side effects during the treatment of diseases like RA or PsA were unexpected, as targeting of IL-6 was thought to be successful (Laurent et al., 2010; Palmou-Fontana et al., 2014). Besides this, treatments of diseases with rheumatologic association through the neutralization of TNF α (Wendling et al., 2008) lead to similar observations. Also here, patients developed psoriatic lesions as a consequence of treatment (Collamer et al., 2008; Florent et al., 2010; Markatseli et al., 2009). The phenotype of psoriasis is widely spread (Palmou-Fontana et al., 2014) and thereby it is difficult to find a specific treatment. In contrast to that, it is already known how IL-6 acts systemically and locally in the development of RA (Dayer and Choy, 2010). This indicates not every treatment to be globally successful,

giving a lot of space for different therapy approaches. Certainly, there are other mAb's already mentioned, such as anti-TNF α or anti-IL-23, which serve as treatment options for psoriasis and other diseases.

Conclusively, an anti-IL-17 treatment should be considered for analysis in more detail, as it has a higher potential to serve as the predominant therapy for psoriasis compared to an anti-IL-6R treatment.

4.2 Signaling of IL-6 and its role in (IMQ-induced) psoriasis

Although targeting the IL-6R is not the most successful treatment to improve the psoriatic phenotype in humans, this cytokine has a strong clinical relevance. Besides the knowledge that IL-6 is involved in general recruitment of neutrophils (Fielding et al., 2008), it is also highly expressed in psoriatic skin lesions (Grossman et al., 1989). Furthermore, IL-6 also has an important role in the pathogenesis of IMQ-induced psoriasis-like skin disease (El Malki et al., 2013; van der Fits et al., 2009) and in spontaneous psoriasis (Croxford et al., 2014; Hvid et al., 2008).

As recently published, we deleted the IL-6R α specifically in myelomonocytic cells (*IL-6R α ^{Amyle}*), to investigate the role of IL-6 in the context of IMQ-induced psoriasis-like skin disease (Klebow et al., 2016). In contrast to our expectations, mice lacking the IL-6R α in myelomonocytic cells developed a comparable severity of IMQ-induced psoriasis-like skin disease to *wt* mice. Besides similarity by PASI scores, cell infiltrations of neutrophils, monocytes, macrophages, as well as IL-17A producing $\gamma\delta$ T cells were the same. So, the inflammatory cell invasion to the skin accompanied by the clinical signs of psoriasis was not at all reduced when the IL-6R α in myelomonocytic cells was deleted (Klebow et al., 2016).

One possible explanation for this observed phenotype could be an insufficient Cre-activity. Depletion of the IL-6R α specifically in myelomonocytic cells was achieved by the LysM-Cre. The publication which introduced this LysM-Cre-recombinase initially, showed a very good efficiency in neutrophil granulocytes (nearly 100%), but it was less efficient in macrophages (83%-98%) (Clausen et al., 1999). In our mice we noted a significant reduction of the IL-6R α in all populations of myelomonocytic cells, confirming an efficient recombination of

the LysM-Cre (Klebow et al., 2016). Moreover, other groups could demonstrate a good depletion capacity of this Cre line also in macrophages, as exhibited in the LysM-Cre/iDTR model. Here, the injection of DT led to a macrophage depletion of 95% (Wenzel et al., 2011). Besides this, one group studied the same mouse model as we did (*IL-6R α ^{Δ myel}*) in the context of obesity. They observed no expression of pSTAT3 by Western Blot in bone marrow derived macrophages, underlying a high recombination potential of the LysM-Cre in macrophages (Mauer et al., 2014). As the JAK/STAT3 pathway is activated by signals through the mIL-6R α (Camporeale and Poli, 2012; Neurath and Finotto, 2011), diminished or absent expression of STAT3 concludes less activation of IL-6R α . Analysis of pSTAT3 expression in our mice revealed no difference between *IL-6R α ^{Δ myel}* mice and *wt* mice. This is contrary to the result of Mauer et al., but can be explained by the isolation method. As in our case the cells were MACS purified with CD11b, also other cells (except for the ones with diminished IL-6 signaling), which express CD11b, were included in the suspension, like for example B-1b cells (Yammani and Haas, 2013). Further, also a purity of less than 100% can lead to the observed results, due to the expression of pSTAT3 in other cells.

However, other cytokines of the gp130 family can show redundant activities in cells with reduced IL-6 signaling, as they all share gp130 as a receptor sub-unit (Wolf et al., 2014). We observed a higher expression of Oncostatin M (OSM) in CD11b MACS purified cells in *IL-6R α ^{Δ myel}* mice, leading to the assumption that OSM can compensate for IL-6. OSM activates the same signal cascade as IL-6 (Richards, 2013), which can explain the pSTAT3 expression on protein level. Nevertheless, this has to be verified in more detail also including other members of the gp130 family, like IL-11, CNTF, LIF, CT-1 and CLC (Heinrich et al., 2003; Jones et al., 2011). A repetition of the experiment with sorted cells for the appropriate populations will possibly lead to a definite result. In addition, the analysis of CD11b⁺ stimulated splenocytes revealed a strong reduction of STAT3 in *IL-6R α ^{Δ myel}* mice. This can be probably explained by a feedback loop induced by SOCS proteins (Rawlings et al., 2004; Shuai and Liu, 2003). In particular, SOCS3 can inhibit the phosphorylation of STAT3 (Wang et al., 2013). Interestingly, mice with constitutively active STAT3 in KCs develop a psoriasis-like phenotype (Sano et al., 2005), indicating an important role of IL-6 in the

context of psoriasis. It can be excluded that the observed phenotype during IMQ-induced psoriasis in *IL-6Rα^{Δmyel}* mice was due to an insufficient Cre-activity. So, there must be a different explanation for these results.

Another possibility for our findings (Klebow et al., 2016) is due to the fact that IL-6 has an alternative signaling pathway, which maybe compensate for the classical signaling. Classical IL-6 signaling is restricted to cells, which express the mIL-6Rα, like myelomonocytic cells, hepatocytes and other leukocytes (Rose-John et al., 2007; Wolf et al., 2014). The sIL-6Rα, on the other hand, accrues through proteolytic cleavage of the mIL-6Rα by ADAM 10 or 17 (Schumacher et al., 2015). Like this, all cells expressing the co-receptor gp130, can respond to IL-6 (Wolf et al., 2014). As gp130 is expressed universally, this is the case for all body cells (Rose-John et al., 2007). With the deletion of mIL-6Rα in monocytes/macrophages and granulocytes in our *IL-6Rα^{Δmyel}* mice, the hepatocytes and some leukocytes could still be the source of sIL-6Rα for trans-signaling. Signaling through the mIL-6Rα seems to have anti-inflammatory property, whereas the sIL-6Rα acts pro-inflammatory (Rose-John, 2012; Scheller et al., 2011; Wolf et al., 2014). This theory was supported by experiments with *IL-6^{-/-}* mice in a colon cancer model. Although the mice developed less tumors compared to *wt* mice, they suffered from a stronger inflammation (Grivennikov et al., 2009). This resulted in the assumption that IL-6 in a way was also important for wound healing in the intestine (Grivennikov et al., 2009) and that this process is dependent on the classical signaling of IL-6 (Becker et al., 2004; Scheller et al., 2011). Further, investigations of Barkhausen et al. in a sepsis model revealed that global blocking of IL-6 couldn't improve the survival of the mice (Barkhausen et al., 2011). However, the exclusive depletion of trans-signaling with the application of soluble gp130fc (sgp130fc) resulted in the survival of all mice (Barkhausen et al., 2011), substantiating the theory that the classical IL-6 signaling acts anti-inflammatory. As this was shown already for different inflammatory diseases, these observations maybe also convey the inflammatory processes in psoriasis. We found a reduction of 25% of sIL-6Rα in *IL-6Rα^{Δmyel}* mice (Klebow et al., 2016) compared to *wt* mice. This observed reduction could be due to the depletion of mIL-6Rα on neutrophils. Apoptotic neutrophils strongly contribute to the shedding of mIL-6Rα by inducing trans-

signaling on endothelial cells (Scheller et al., 2011). However, we assume that the remaining 75% are still sufficient to initiate the inflammatory cascades to comparable levels in *IL-6Rα^{Δmyel}* and *wt* mice.

To conclude, the experiments of IMQ-induced psoriasis in our mouse model needs to be repeated with an additional depletion of IL-6 trans signaling. Due to the anti-inflammatory properties of the classical signaling in myelomonocytic cells, *IL-6Rα^{Δmyel}* mice could suffer from a more severe psoriasis-like disease when compared to *wt* mice. Moreover, this shows that the specific inhibition of IL-6 trans-signaling, in form of the soluble gp130Fc (sgp130Fc), has the potential to treat inflammatory diseases. Sgp130 is known to be the inhibitor of trans-signaling by binding only the complex of IL-6/sIL-6Rα (Barkhausen et al., 2011; Rose-John et al., 2006). Jostock et al. generated the sgp130Fc and showed that it only interacts with the soluble form of the IL-6Rα, (Jostock et al., 2001). This allows the specific blocking of IL-6 trans-signaling without affecting the classical signaling. Patients treated with Tocilizumab against RA showed elevated levels of sIL-6Rα in the plasma (Nishimoto et al., 2008). As discussed above (4.1), treatment with the anti-IL-6R antibody is often accompanied by side effects, like evolving psoriatic skin lesions. One explanation here can be the missing anti-inflammatory properties of the classical signaling, where a specific blocking of trans-signaling could be assessed. Interestingly, this protein was already used in different animal models of human inflammatory diseases, like chronic intestinal inflammation or RA. In both studies the treatment of mice with sgp130Fc improved the disease severity (Atreya et al., 2000; Nowell et al., 2003), suggesting this protein as a strong candidate for clinical approaches. The clinical phase I trials for sgp130Fc started in June 2013 (Scheller et al., 2014).

4.3 IL-17 producing cells in (IMQ-induced) psoriasis-like skin disease

The application of IMQ to the skin leads to a strong recruitment of immune cells. Besides myelomonocytic cells, like neutrophils, monocytes and macrophages, also T cells infiltrate to the site of inflammation (Flutter and Nestle, 2013). Furthermore, different cytokines, like IL-17, IL-22 and IL-23 are involved in the

pathogenesis of IMQ-induced psoriasis, (Cho et al., 2012; El Malki et al., 2013; Nakajima et al., 2011; Pantelyushin et al., 2012; Van Belle et al., 2012; van der Fits et al., 2009; Wohn et al., 2013). Experiments with IL-17RA knock out mice revealed a strong ameliorated disease in this model (El Malki et al., 2013; van der Fits et al., 2009).

Besides $\alpha\beta$ T cells, also $\gamma\delta$ T cells are located in the skin (Di Meglio et al., 2011). DETCs which are $\gamma\delta$ TCR⁺ and express V γ 5 exclusively (Gray et al., 2011; Havran and Jameson, 2010) are only located in the epidermis (Sumaria et al., 2011) and are important for the process of wound healing (Havran and Jameson, 2010; MacLeod et al., 2013). Dermal $\gamma\delta$ T cells on the other hand, express V γ 4 instead of V γ 5 (Cai et al., 2011; Sumaria et al., 2011). This could be also confirmed with our observed results, as secondary lymphoid organs, as the spleen of *IL-6R α ^{Δmyel}* mice, did not reveal any V γ 5⁺ cells, but a V γ 4⁺ population. Cai et al. demonstrated that dermal $\gamma\delta$ TCR⁺ T cells produced more IL-17 than $\gamma\delta$ TCR⁻ T cells. Furthermore, this IL-17 production was shown to be dependent on IL-23 and IL-1 β (Cai et al., 2011; Gray et al., 2011; Sutton et al., 2009). Also in the model of IMQ-induced psoriasis, this study detected those dermal V γ 4⁺ $\gamma\delta$ TCR⁺ T cells to be the main producers of IL-17 (Cai et al., 2011). Similar results were shown by Shibata et al. who investigated in adipopectin in the context of IMQ-induced skin inflammation (Shibata et al., 2015). Moreover, also the study of Pantelyushin et al. pictured that V γ 4⁺ cells produce IL-17A in contrast to the V γ 5⁺ population (Pantelyushin et al., 2012). Independent of which mouse model we analyzed in IMQ-induced psoriasis, no differences regarding the distribution of $\gamma\delta$ T cells and the V γ TCR segments could be detected. Possibly, our detected phenotype is due to the time point we analyzed the $\gamma\delta$ T cells during the application of IMQ, as the infiltration of $\gamma\delta$ T cells to the skin peaks on day 7 of IMQ treatment (Flutter and Nestle, 2013; Tortola et al., 2012). We did not expect to see a difference, in analyzing the mice after five days of treatment, as we mainly focused on the infiltration of myelomonocytic cells which peak around day 4-5 (Flutter and Nestle, 2013; Terhorst et al., 2015; Tortola et al., 2012). However, we confirmed dermal V γ 4⁺ $\gamma\delta$ T cells to be the dominant IL-17A producing population in this model. To further investigate the role of $\gamma\delta$ T cells in the context of our mouse strains during IMQ treatment, the experiment would need to be repeated with a

treatment period of 7 consecutive days. It would be interesting to analyze *Il1r2*^{-/-} mice in terms of infiltrating $\gamma\delta$ T cells, as Tortola et al. demonstrated less $\gamma\delta$ T cells in *Il36r*^{-/-} mice during the application of IMQ (Tortola et al., 2012). Since IL-36 belongs to the same family as IL-1 (Garlanda et al., 2013), an impact might also be seen in the *Il1r2*^{-/-} mice. Moreover, it would be also interesting to investigate the $\gamma\delta$ T cell phenotype of the *IL-6R α* ^{Δ myel} mice after a treatment period of 7 days. Dermal $\gamma\delta$ T cells were shown to express the chemokine receptor CCR6 (Becher and Pantelyushin, 2012; Cai et al., 2011; Gray et al., 2011; Pantelyushin et al., 2012) and with its expression these cells can be recruited to the skin by KCs and dendritic cells (Becher and Pantelyushin, 2012). Also an injection of IL-23 to the mouse skin induced CCR6⁺ $\gamma\delta$ TCR^{int} cells to infiltrate the epidermis, which resulted in a production of IL-17 and IL-22 (Mabuchi et al., 2011). However, the application had no influence on the numbers of DETCs in the epidermis (Mabuchi et al., 2011). As *IL-6*^{-/-} mice have been described to develop reduced skin disease after administration of IL-23 (Lindroos et al., 2011), IL-23 seems to be the connection between IL-6 and $\gamma\delta$ T cells in psoriasis. In contrast to mice, there are only few $\gamma\delta$ T cells in human skin and it completely lacks DETCs (Laggner et al., 2011). A recent study revealed an increase of a CCR6⁺ subset of $\gamma\delta$ T cells in human skin (V γ 9V δ 2 T cells), which probably circulates from the blood during psoriasis disease progression and produces IL-17 (Laggner et al., 2011). Also Cai et al. showed that skin samples of psoriasis patients produced more IL-17 upon IL-23 stimulation than healthy controls (Cai et al., 2011). This clearly indicates that $\gamma\delta$ T cells also play a role in human psoriasis and should be further investigated.

Besides IL-17 producing $\gamma\delta$ T cells, also other immune cells with the ability to produce IL-17 may contribute to the pathogenesis of psoriasis. Recent studies investigated in IL-17 producing neutrophils in psoriasis. Lin et al., presented mast cells and neutrophils, but not T cells, as the predominant source of IL-17 in skin biopsies of human psoriasis patients (Lin et al., 2011). Further, they showed that the release of IL-17 was dependent on extracellular trap formations of neutrophils (NETs) (Lin et al., 2011). NETosis is a kind of cell death where granular proteins and chromatin of neutrophils are released into the extracellular space and form kind of a mesh (Grayson and Kaplan, 2016). This

formation of extracellular traps was already observed in different autoimmune diseases (Grayson and Kaplan, 2016). Another study, supporting the findings of Lin et al., reported about two different models of skin irritation (leukotriene B4 (LTB4) treatment and tape stripping), leading to IL-17 production mainly of neutrophils and mast cells in human skin (Keijsers et al., 2014). Besides this, neutrophils also co-expressed the transcription factor ROR γ t and were able to build extracellular traps, in response to the LTB4 treatment (Keijsers et al., 2014). Also in the context of fungal infections, neutrophils of the bone marrow were shown to produce IL-17A in mice and human. Here, it was depicted that IL-6, IL-23 and ROR γ t were necessary for this IL-17 production (Taylor et al., 2014). Linking to the neutralization of IL-17A as a treatment option for psoriasis, Reich et al., confirmed neutrophils and not T cells to contain the largest amount of IL-17 in this disease (Reich et al., 2015). The administration of Secukinumab resulted in a strong neutrophil reduction in the epidermis of human psoriasis patients, by possibly interrupting the neutrophil-KC crosstalk (Reich et al., 2015).

Definitely, the innate cells of the immune system strongly contribute to the IL-17 production in psoriasis, whereby here the neutrophils have to be investigated in more detail, as most of the studies refer to the human disease. Analyzing IL-17 producing neutrophils in *Il1r2*^{-/-} mice would be an interesting approach, as they displayed significantly more myelomonocytic cells during IMQ-induced psoriasis. Further, also the formation of NETs should be investigated by immunohistochemistry of IMQ treated skin sections.

4.4 IL-1 and its family members in (IMQ-induced) psoriasis

IL-1 signaling is strongly involved in the pathogenesis of IMQ-induced psoriasis. IMQ application to mice with diminished IL-1 signaling (*Il1r1*^{-/-} mice), leads to decreased formation of Munro's micro abscesses in the epidermis (Rabeony et al., 2015; Uribe-Herranz et al., 2013), consisting of large numbers of neutrophils (Kaneko et al., 1991). Further, there is evidence that IL-1 signaling is involved in the recruitment of neutrophils to the epidermis, due to lower amounts of secreted CXCL1 and CXCL2 in *Il1r1*^{-/-} mice during IMQ treatment (Uribe-Herranz

et al., 2013). Studies concerning the IL-1 receptor antagonist (IL-1RA) revealed that the depletion of IL-1RA on Balb/c background leads to a psoriasis like dermatitis in mice (Nakajima et al., 2010; Shepherd et al., 2004), confirming an important role of IL-1 in psoriasis. IL-1RA has anti-inflammatory activity and inhibits the binding of IL-1 α and IL-1 β to IL-1R1 (Jensen, 2010). In addition, the combined knock out of IL-1 α and IL-1 β promotes a milder psoriasis-like disease (Rabeony et al., 2015). The study of Nakajima et al. displayed that enhanced IL-1 signaling is accompanied with enhanced expression of TNF α , CXCL1, CXCL2, CXCL10 and CCL20 on KCs. Further, a massive infiltration of myelomonocytic cells to dermis and epidermis was observed (Nakajima et al., 2010). This links to the findings of IMQ treated *Il1r1*^{-/-} mice on Bl6 background (Uribe-Herranz et al., 2013), where similar results could be observed. However, there is also a suggestion that the development of different inflammatory diseases, as cutaneous inflammation, arterial inflammation and arthritis is dependent on the genetic background of the mice (Balb/c or Bl6) (Shepherd et al., 2004).

Besides IL-1R1, the IL-1 receptor also consists of IL-1R2, which is the decoy receptor and can't transmit a signal due to a missing TIR domain (Garlanda et al., 2013). As IL-1 α and IL-1 β can also bind the decoy receptor (Boraschi and Tagliabue, 2013), deletion of IL-1R2 leads to enhanced IL-1 signaling. Our investigations on *Il1r2*^{-/-} mice confirmed the previous findings, that these mice had an increased number of myelomonocytic cells in ears (CD11b⁺) and spleen (Ly6G⁺) at steady state condition. This effect was even more dramatic during the treatment with IMQ, as in spleen and ears all populations of myelomonocytic cells were significantly increased in total numbers. Besides, already the increased PASI scores indicated a higher susceptibility to the psoriasis-like disease, which can be attributed to the increased proliferation of KCs as a consequence of the treatment (Uribe-Herranz et al., 2013). Due to a higher release of IL-1 α by KCs more chemokines are expressed which attract neutrophils to infiltrate the skin (Uribe-Herranz et al., 2013). Further, this is supported by the recent findings that IL-1R2 is highly expressed on neutrophils (Martin et al., 2013; Shimizu et al., 2015). In a model of atherosclerosis, which is a neutrophil driven disease, it was shown that monocytes and macrophages are recruited by neutrophils (Doring et al., 2012). This could explain why IMQ-

induced psoriasis in *Il1r2*^{-/-} mice leads to a strong increase in all populations of myelomonocytic cells, which indicates that both models use the same mechanism. Furthermore, *Il1r2*^{-/-} mice also suffered from a stronger disease in the model of collagen-induced arthritis (Shimizu et al., 2015). Here, it was predicted that IL1-R2 served as a negative regulator of IL-1 by acting on macrophages. Stimulation of macrophages with IL-1 resulted in an up regulation of different inflammatory mediators of arthritis, as IL-6, IL-1 β or CXCL2 on mRNA levels (Shimizu et al., 2015). Interestingly, the mRNA levels of IL-6 and IL-1 β in the IMQ treated skin of our *Il1r2*^{-/-} mice were also increased. Taking this into consideration, it supports the assumption that the induced inflammatory diseases of arthritis and psoriasis follow the same mode of action. The ability of IL-1R2 to have anti-inflammatory properties was confirmed by another study where mice specifically expressed the IL-1R2 on KCs. Here, chronic inflammation was significantly reduced (Rauschmayr et al., 1997). One year earlier the same group showed the contrary effect when IL-1R1 was expressed on KCs (Groves et al., 1996). This clearly indicates that IL-1 signaling on KCs is responsible for the development of an inflammatory disease (Feldmeyer et al., 2010). Further, the strong involvement of IL-1 in IMQ-induced psoriasis was confirmed by investigations concerning the activities of inflammasomes (Flutter and Nestle, 2013), which are responsible for the activation of inflammatory caspases (Martinon and Tschopp, 2007). Caspase-1-deficient mice are resistant to IMQ-induced psoriasis, indicating an involvement of inflammasomes in the pathogenicity of this disease (Cho et al., 2012). Due to suitability of our mouse model this should be investigated in more detail.

Moreover, also other family members of IL-1, like IL-36, affect the severity of IMQ-induced skin inflammation. *Il36r*^{-/-} mice showed no infiltration of dermal $\gamma\delta$ T cells or inflammation of the skin (Tortola et al., 2012). In line with this, the deletion of the receptor antagonist (*Il36rn*^{-/-}) resulted in an increased skin inflammation (Tortola et al., 2012). Another study revealed IL-36 α to be responsible for the formation of neutrophil microabscesses (Milora et al., 2015). Also in humans IL-36 α is upregulated in psoriasis (Boutet et al., 2016) and psoriatic arthritis (Frey et al., 2013). The anti-IL-36R antibody for the treatment of psoriasis was already introduced in one patent (Wolf and Ferris, 2014).

Besides IL-36 α , also a stronger expression of IL-1R1 (Groves et al., 1994), IL-1RA and IL-1 α (Hammerberg et al., 1992) could be shown in psoriatic skin. Intradermal injection of IL-1 α leads to a cutaneous inflammation (Dowd et al., 1988).

Due to the strong impact on IL-1 signaling in psoriasis, Anakinra, an IL-1 receptor antagonist was used as a treatment options for psoriasis, but the efficiency of this treatment is heterogeneous. One clinical study with two female patients showed a decrease in disease severity of generalized pustular psoriasis already after 4 days of treatment (Viguier et al., 2010). However, another study with two patients suffering from severe palmoplantar pustular psoriasis displayed only partially effect on the treatment with Anakinra (Tauber et al., 2014). In both cases the treatment had to be stopped due to strong side effects (Tauber et al., 2014). Moreover, Anakinra treatment had a strong effect on two patients suffering from generalized pustular psoriasis with either a mutation (Huffmeier et al., 2014) or a deletion (Rossi-Semerano et al., 2013) of the IL-36 receptor antagonist gene. In both cases the treatment turned out to be very successful (Huffmeier et al., 2014; Rossi-Semerano et al., 2013), indicating a correlation of IL-1 and IL-36 in psoriasis. However, Anakinra is not the ideal treatment option for all different types of psoriasis. Certainly, IL-1 signaling plays an important role in the pathogenesis of psoriasis and has to be explored in more detail to improve the clinical treatment options.

As we further wanted to investigate which cell type is responsible for the phenotype in the myelomonocytic cells of *Il1r2*^{-/-} mice, we analyzed the conditional deletion of IL-1R2 in neutrophils and T cells. Interestingly, in both cases the mice behaved like *wt* during the treatment with IMQ, indicating that neither the neutrophils, nor the T cells induced this phenotype. This can be explained by a possible shedding of the IL-1R2 on other cells and thereby compensating for the deletion on specific cell types. By now it's only poorly described which cells express IL-1R2, but there is evidence that it is highly expressed on neutrophils (Martin et al., 2013; Shimizu et al., 2015), CD4 T cells and monocytes (Shimizu et al., 2015). ADAM 17 mediates the cleavage of IL-1R2 from the cell surface, to achieve the soluble form of IL-1R2 (Lorenzen et al.,

2012; Uchikawa et al., 2015). However, to make a conclusive statement further analysis will be necessary.

5 Summary

Psoriasis vulgaris is the most common form of the inflammatory skin disease psoriasis and leads to the formation of red, scaly plaques, mainly on the knees, elbows and scalp. Psoriasis affects 2-4% of the population worldwide and is associated with involvement of different immune cells (e.g. T cells and myeloid cells) and proinflammatory cytokines, for example IL-17, IL-6 or IL-1. Here, we used different transgene mouse models to examine the function of these cytokines and the respective receptors in more detail for their role in psoriatic disease.

Our lab recently established a novel mouse model where IL-17A is specifically overexpressed in keratinocytes (*K14-IL-17A^{ind/+}* mice), which leads to skin inflammation showing many hallmarks of human psoriasis. As it was already shown that neutralization of IL-6 in those mice led to an improvement of the psoriatic phenotype, we also investigated the impact of anti-IL-17A treatment in this thesis. We could demonstrate that also the neutralization of IL-17A resulted in a partially improved disease severity. Moreover, the sera of treated *K14-IL-17A^{ind/+}* mice displayed significantly reduced IL-17A levels compared to controls. Further, the treatment did result in an improved PASI score and less spleen-infiltrating myeloid cells. Hence, the results indicate a positive effect of the treatment. This we also confirmed by an anti-IL-17A treatment of *wild type (wt)* mice in the model of IMQ-induced psoriasis where the treatment also reduced the PASI score. IMQ is the active compound of *AldaraTM* cream and serves as a TLR7/8 agonist. Its topical application to the skin leads to a psoriasis-like skin disease, also in terms of the involved cytokines and infiltrating cells.

The role of IL-6 signaling in the psoriasis-like disease was investigated by deleting the membrane-bound IL-6R α specifically in myeloid cells (*IL-6R α ^{Δ myel}*). Treating these mice with IMQ resulted in comparable disease severity as in *wt* mice. These findings could indicate that the effect of the deletion might be compensated by the soluble form of the receptor or by other cytokines of the gp130 family with redundant activities.

Interestingly, IL-1 signaling also seems to have a strong involvement in psoriasis-like disease, as *Il1r2^{-/-}* mice treated with IMQ exhibited significantly more

myeloid cells than *wt* mice. To identify which cells are responsible for the observed phenotype, mice with a tissue specific deletion of IL-1R2 in T cells (*Il1r2^{ΔT}*) and neutrophils (*Il1r2^{ΔN}*) were analyzed in the same model. As none of these mouse strains showed differences compared to *wt* mice during IMQ treatment, neither neutrophils, nor T cells seemed to be responsible for the initial observed findings. Also here compensation by the soluble form of IL-1R2 should be considered.

The results of this thesis underline the neutralization of IL-17A being a promising treatment option for psoriasis. In addition, our findings regarding the role of the cytokines IL-6 and IL-1, could lead to the discovery of new drug targets for the treatment of this inflammatory skin disease.

6 Zusammenfassung

Psoriasis vulgaris ist die häufigste Form der entzündlichen Hautkrankheit Psoriasis und führt zur Bildung von roten schuppigen Plaques hauptsächlich an den Knien, Ellenbogen und der Kopfhaut. Etwa 2-4% der weltweiten Bevölkerung sind von dieser Krankheit betroffen, welche mit der Beteiligung von verschiedenen Immunzellen (z.B. T Zellen und myeloide Zellen) und entzündlichen Zytokinen, wie IL-17, IL-6 und IL-1 einhergeht. In dieser Doktorarbeit wurden verschiedene transgene Mausmodelle verwendet, um die Funktion dieser Zytokine und deren Rezeptoren im Zusammenhang mit der Entwicklung von Psoriasis im Detail zu untersuchen.

Vor einiger Zeit wurde von unserem Labor ein Mausmodell veröffentlicht, in welchem IL-17A spezifisch in Keratinozyten überexprimiert ist (*K14-IL-17A^{ind/+}*). Diese Überexpression führt zu einer entzündlichen Hautreaktion mit vielen Merkmalen der menschlichen Psoriasis. Nachdem eine anti-IL-6 Behandlung dieser Mäuse bereits sehr erfolgreich war, konnten wir in dieser Doktorarbeit zeigen, dass sich auch durch Behandlung mit einem anti-IL-17A Antikörper eine Verbesserung des Hautphänotyps der *K14-IL-17A^{ind/+}* Mäuse eingestellt hat. Dies ging mit einem signifikant reduzierten Serumlevel von IL-17A einher. Außerdem resultierte die Behandlung in einem verbesserten PASI score und reduzierter Infiltration myeloider Zellen in die Milz. Somit deuten die Ergebnisse auf einen positiven Effekt der Behandlung hin. Dies konnte durch eine anti-IL-17A Behandlung von wildtyp (*wt*) Mäusen im IMQ Modell bestätigt werden da auch hier die Behandlung zu einem reduzierten PASI score geführt hat. IMQ ist ein TLR7/8 Agonist und als solcher der Wirkstoff in *Aldara* Creme. Seine Anwendung auf der Haut von Mäusen führt zu Entzündungsreaktionen ähnlich der menschlichen Psoriasis, auch bezüglich der involvierten Zytokine und infiltrierenden Effektorzellen.

Die Funktion von IL-6 im psoriasis-ähnlichen Modell wurde durch die Deletion des membranständigen IL-6R α in myeloiden Zellen (*IL-6R α ^{Δ myel}*) untersucht. Im Vergleich zu *wt* Mäusen resultierte die Behandlung der *IL-6R α ^{Δ myel}* Mäuse mit IMQ in der selben Schwere der Krankheit. Eine mögliche Erklärung hierfür

könnte sein, dass die Deletion durch den löslichen IL-6R oder andere Zytokine der gp130 Familie kompensiert wird.

Interessanterweise hat auch IL-1 einen großen Einfluss auf den Verlauf der psoriasis-ähnlichen Hautkrankheit, da IMQ behandelte *Il1r2*^{-/-} Mäuse signifikant mehr myeloide Zellen in der Haut und Milz aufwiesen als *wt* Mäuse. Um zu ermitteln welche Zellen für den beobachteten Phänotyp verantwortlich sind, wurden auch Mäuse mit einer spezifischen Deletion für den IL-1R2 in T Zellen (*Il1r2*^{ΔT}) und Neutrophilen (*Il1r2*^{ΔN}) im IMQ Modell untersucht. Allerdings zeigte keiner dieser Stämme Unterschiede gegenüber *wt* Mäusen auf. Dies deutet darauf hin, dass weder T Zellen noch Neutrophile für den beobachteten Phänotyp verantwortlich sind. Auch hier sollte aber eine Kompensation durch den löslichen IL-1R2 in Betracht gezogen werden.

Die hier dargestellten Ergebnisse untermauern die Relevanz der Neutralisierung von IL-17A als Behandlungsmöglichkeit für Psoriasis. Des Weiteren könnten die Ergebnisse dieser Arbeit zur Rolle der Zytokine IL-6 und IL-1 im Psoriasismodell den Grundstein für die Entwicklung neuer vielversprechender Behandlungsmöglichkeiten dieser entzündlichen Hautkrankheit legen.

7 References

Aggarwal, S., N. Ghilardi, M.H. Xie, F.J. de Sauvage, and A.L. Gurney. 2003. Interleukin-23 promotes a distinct CD4 T cell activation state characterized by the production of interleukin-17. *The Journal of biological chemistry* 278:1910-1914.

Andres, R.M., M.C. Montesinos, P. Navalon, M. Paya, and M.C. Terencio. 2013. NF-kappaB and STAT3 inhibition as a therapeutic strategy in psoriasis: in vitro and in vivo effects of BTH. *The Journal of investigative dermatology* 133:2362-2371.

Arican, O., M. Aral, S. Sasmaz, and P. Ciragil. 2005. Serum levels of TNF-alpha, IFN-gamma, IL-6, IL-8, IL-12, IL-17 and IL-18 in patients with active psoriasis and correlation with disease severity. *Mediators of inflammation* 5:273-279.

Atreya, R., J. Mudter, S. Finotto, J. Mullberg, T. Jostock, S. Wirtz, M. Schutz, B. Bartsch, M. Holtmann, C. Becker, D. Strand, J. Czaja, J.F. Schlaak, H.A. Lehr, F. Autschbach, G. Schurmann, N. Nishimoto, K. Yoshizaki, H. Ito, T. Kishimoto, P.R. Galle, S. Rose-John, and M.F. Neurath. 2000. Blockade of interleukin 6 trans signaling suppresses T-cell resistance against apoptosis in chronic intestinal inflammation: evidence in crohn disease and experimental colitis in vivo. *Nature medicine* 6:583-588.

Barkhausen, T., T. Tschernig, P. Rosenstiel, M. van Griensven, R.P. Vonberg, M. Dorsch, A. Mueller-Heine, A. Chalaris, J. Scheller, S. Rose-John, D. Seegert, C. Krettek, and G.H. Waetzig. 2011. Selective blockade of interleukin-6 trans-signaling improves survival in a murine polymicrobial sepsis model. *Critical care medicine* 39:1407-1413.

Barland, C.O., E. Zettersten, B.S. Brown, J. Ye, P.M. Elias, and R. Ghadially. 2004. Imiquimod-induced interleukin-1 alpha stimulation improves barrier homeostasis in aged murine epidermis. *The Journal of investigative dermatology* 122:330-336.

Becher, B., and S. Pantelyushin. 2012. Hiding under the skin: Interleukin-17-producing gammadelta T cells go under the skin? *Nature medicine* 18:1748-1750.

Becker, C., M.C. Fantini, C. Schramm, H.A. Lehr, S. Wirtz, A. Nikolaev, J. Burg, S. Strand, R. Kiesslich, S. Huber, H. Ito, N. Nishimoto, K. Yoshizaki, T. Kishimoto, P.R. Galle, M. Blessing, S. Rose-John, and M.F. Neurath. 2004. TGF-beta suppresses tumor progression in colon cancer by inhibition of IL-6 trans-signaling. *Immunity* 21:491-501.

Berking, C., R. Takemoto, R.L. Binder, S.M. Hartman, D.J. Ruiter, P.M. Gallagher, S.R. Lessin, and M. Herlyn. 2002. Photocarcinogenesis in human adult skin grafts. *Carcinogenesis* 23:181-187.

Beutner, K.R., and A. Ferenczy. 1997. Therapeutic approaches to genital warts. *The American journal of medicine* 102:28-37.

Boehncke, W.H., W. Sterry, A. Hainzl, W. Scheffold, and R. Kaufmann. 1994. Psoriasiform architecture of murine epidermis overlying human psoriatic dermis transplanted onto SCID mice. *Archives of dermatological research* 286:325-330.

Boraschi, D., and A. Tagliabue. 2013. The interleukin-1 receptor family. *Seminars in immunology* 25:394-407.

Boutet, M.A., G. Bart, M. Penhoat, J. Amiaud, B. Brulin, C. Charrier, F. Morel, J.C. Lecron, M. Rolli-Derkinderen, A. Bourreille, S. Vigne, C. Gabay, G. Palmer, B. Le Goff, and F. Blanchard. 2016. Distinct expression of interleukin (IL)-36alpha, beta and gamma, their antagonist IL-36Ra and IL-38 in psoriasis, rheumatoid arthritis and Crohn's disease. *Clinical and experimental immunology* 184:159-173.

Boyman, O., H.P. Hefti, C. Conrad, B.J. Nickoloff, M. Suter, and F.O. Nestle. 2004. Spontaneous development of psoriasis in a new animal model shows an essential role for resident T cells and tumor necrosis factor-alpha. *The Journal of experimental medicine* 199:731-736.

Brulhart, L., M.J. Nissen, P. Chevallier, and C. Gabay. 2010. Tocilizumab in a patient with ankylosing spondylitis and Crohn's disease refractory to TNF antagonists. *Joint Bone Spine* 77:625-626.

Buch, T., F.L. Heppner, C. Tertilt, T.J. Heinen, M. Kremer, F.T. Wunderlich, S. Jung, and A. Waisman. 2005. A Cre-inducible diphtheria toxin receptor mediates cell lineage ablation after toxin administration. *Nature methods* 2:419-426.

Buchau, A.S., and R.L. Gallo. 2007. Innate immunity and antimicrobial defense systems in psoriasis. *Clinics in dermatology* 25:616-624.

Cai, Y., X. Shen, C. Ding, C. Qi, K. Li, X. Li, V.R. Jala, H.G. Zhang, T. Wang, J. Zheng, and J. Yan. 2011. Pivotal role of dermal IL-17-producing gammadelta T cells in skin inflammation. *Immunity* 35:596-610.

Campa, M., B. Mansouri, R. Warren, and A. Menter. 2016. A Review of Biologic Therapies Targeting IL-23 and IL-17 for Use in Moderate-to-Severe Plaque Psoriasis. *Dermatology and therapy* 6:1-12.

Camporeale, A., and V. Poli. 2012. IL-6, IL-17 and STAT3: a holy trinity in auto-immunity? *Frontiers in bioscience* 17:2306-2326.

Chamilos, G., J. Gregorio, S. Meller, R. Lande, D.P. Kontoyiannis, R.L. Modlin, and M. Gilliet. 2012. Cytosolic sensing of extracellular self-DNA transported into monocytes by the antimicrobial peptide LL37. *Blood* 120:3699-3707.

Chan, J.R., W. Blumenschein, E. Murphy, C. Diveu, M. Wiekowski, S. Abbondanzo, L. Lucian, R. Geissler, S. Brodie, A.B. Kimball, D.M. Gorman, K. Smith, R. de Waal

Malefyt, R.A. Kastelein, T.K. McClanahan, and E.P. Bowman. 2006. IL-23 stimulates epidermal hyperplasia via TNF and IL-20R2-dependent mechanisms with implications for psoriasis pathogenesis. *The Journal of experimental medicine* 203:2577-2587.

Cho, K.A., J.W. Suh, K.H. Lee, J.L. Kang, and S.Y. Woo. 2012. IL-17 and IL-22 enhance skin inflammation by stimulating the secretion of IL-1beta by keratinocytes via the ROS-NLRP3-caspase-1 pathway. *International immunology* 24:147-158.

Chu, Y., J.C. Vahl, D. Kumar, K. Heger, A. Bertossi, E. Wojtowicz, V. Soberon, D. Schenten, B. Mack, M. Reutelshofer, R. Beyaert, K. Amann, G. van Loo, and M. Schmidt-Supprian. 2011. B cells lacking the tumor suppressor TNFAIP3/A20 display impaired differentiation and hyperactivation and cause inflammation and autoimmunity in aged mice. *Blood* 117:2227-2236.

Clausen, B.E., C. Burkhardt, W. Reith, R. Renkawitz, and I. Forster. 1999. Conditional gene targeting in macrophages and granulocytes using LysMcre mice. *Transgenic Res* 8:265-277.

Collamer, A.N., K.T. Guerrero, J.S. Henning, and D.F. Battafarano. 2008. Psoriatic skin lesions induced by tumor necrosis factor antagonist therapy: A literature review and potential mechanisms of action. *Arthritis Rheum-Arthr* 59:996-1001.

Conrad, C., O. Boyman, G. Tonel, A. Tun-Kyi, U. Laggner, A. de Fougères, V. Kotelianski, H. Gardner, and F.O. Nestle. 2007. Alpha1beta1 integrin is crucial for accumulation of epidermal T cells and the development of psoriasis. *Nature medicine* 13:836-842.

Croxford, A.L., S. Karbach, F.C. Kurschus, S. Wortge, A. Nikolaev, N. Yogev, S. Klebow, R. Schuler, S. Reissig, C. Piotrowski, E. Brylla, I. Bechmann, J. Scheller, S. Rose-John, F.T. Wunderlich, T. Munzel, E. von Stebut, and A. Waisman. 2014. IL-6 regulates neutrophil microabscess formation in IL-17A-driven psoriasiform lesions. *The Journal of investigative dermatology* 134:728-735.

Daley, J.M., A.A. Thomay, M.D. Connolly, J.S. Reichner, and J.E. Albina. 2008. Use of Ly6G-specific monoclonal antibody to deplete neutrophils in mice. *Journal of leukocyte biology* 83:64-70.

Danilenko, D.M. 2008. Review paper: preclinical models of psoriasis. *Veterinary pathology* 45:563-575.

Dar, A.A., R.S. Patil, and S.V. Chiplunkar. 2014. Insights into the Relationship between Toll Like Receptors and Gamma Delta T Cell Responses. *Frontiers in immunology* 5:366.

Davis, C.C., K.S. Shah, and M.J. Lechowicz. 2015. Clinical Development of Siltuximab. *Curr Oncol Rep* 17:29.

Dayer, J.M., and E. Choy. 2010. Therapeutic targets in rheumatoid arthritis: the interleukin-6 receptor. *Rheumatology* 49:15-24.

Di Cesare, A., P. Di Meglio, and F.O. Nestle. 2009. The IL-23/Th17 axis in the immunopathogenesis of psoriasis. *The Journal of investigative dermatology* 129:1339-1350.

Di Meglio, P., G.K. Perera, and F.O. Nestle. 2011. The multitasking organ: recent insights into skin immune function. *Immunity* 35:857-869.

Doring, Y., M. Drechsler, S. Wantha, K. Kemmerich, D. Lievens, S. Vijayan, R.L. Gallo, C. Weber, and O. Soehnlein. 2012. Lack of neutrophil-derived CRAMP reduces atherosclerosis in mice. *Circulation research* 110:1052-1056.

Dowd, P.M., R.D. Camp, and M.W. Greaves. 1988. Human recombinant interleukin-1 alpha is proinflammatory in normal human skin. *Skin pharmacology : the official journal of the Skin Pharmacology Society* 1:30-37.

El Malki, K., S.H. Karbach, J. Huppert, M. Zayoud, S. Reissig, R. Schuler, A. Nikolaev, K. Karram, T. Munzel, C.R. Kuhlmann, H.J. Luhmann, E. von Stebut, S. Wortge, F.C. Kurschus, and A. Waisman. 2013. An alternative pathway of imiquimod-induced psoriasis-like skin inflammation in the absence of interleukin-17 receptor signaling. *The Journal of investigative dermatology* 133:441-451.

Elyoussfi, S., B.J. Thomas, and C. Ciurtin. 2016. Tailored treatment options for patients with psoriatic arthritis and psoriasis: review of established and new biologic and small molecule therapies. *Rheumatology international*

Emery, P., E. Keystone, H.P. Tony, A. Cantagrel, R. van Vollenhoven, A. Sanchez, E. Alecock, J. Lee, and J. Kremer. 2008. IL-6 receptor inhibition with tocilizumab improves treatment outcomes in patients with rheumatoid arthritis refractory to anti-tumour necrosis factor biologicals: results from a 24-week multicentre randomised placebo-controlled trial. *Annals of the rheumatic diseases* 67:1516-1523.

Fajgenbaum, D.C., and R. Kurzrock. 2016. Siltuximab: a targeted therapy for idiopathic multicentric Castleman disease. *Immunotherapy-Uk* 8:17-26.

Fanti, P.A., E. Dika, S. Vaccari, C. Miscial, and C. Varotti. 2006. Generalized psoriasis induced by topical treatment of actinic keratosis with imiquimod. *International journal of dermatology* 45:1464-1465.

Farahnik, B., K. Beroukhim, M. Nakamura, M. Abrouk, T.H. Zhu, R. Singh, K. Lee, T. Bhutani, and J. Koo. 2016. Anti-IL-17 Agents for Psoriasis: A Review of Phase III Data. *Journal of drugs in dermatology : JDD* 15:311-316.

Feldmeyer, L., S. Werner, L.E. French, and H.D. Beer. 2010. Interleukin-1, inflammasomes and the skin. *European journal of cell biology* 89:638-644.

Feng, Y., and W. Chao. 2011. Toll-like receptors and myocardial inflammation. *International journal of inflammation* 2011:170352.

Fielding, C.A., R.M. McLoughlin, L. McLeod, C.S. Colmont, M. Najdovska, D. Grail, M. Ernst, S.A. Jones, N. Topley, and B.J. Jenkins. 2008. IL-6 regulates neutrophil trafficking during acute inflammation via STAT3. *Journal of immunology* 181:2189-2195.

Florent, A., C. Albert, D. Giacchero, C. Roux, and L. Euller-Ziegler. 2010. Reactivation of cutaneous psoriasis during abatacept therapy for spondyloarthritis. *Joint Bone Spine* 77:626-627.

Flutter, B., and F.O. Nestle. 2013. TLRs to cytokines: mechanistic insights from the imiquimod mouse model of psoriasis. *European journal of immunology* 43:3138-3146.

Frey, S., A. Derer, M.E. Messbacher, D.L. Baeten, S. Bugatti, C. Montecucco, G. Schett, and A.J. Hueber. 2013. The novel cytokine interleukin-36alpha is expressed in psoriatic and rheumatoid arthritis synovium. *Annals of the rheumatic diseases* 72:1569-1574.

Fujisawa, H., G.M. Shivji, S. Kondo, B. Wang, M.A. Tomai, R.L. Miller, and D.N. Sauder. 1996. Effect of a novel topical immunomodulator, S-28463, on keratinocyte cytokine gene expression and production. *Journal of interferon & cytokine research : the official journal of the International Society for Interferon and Cytokine Research* 16:555-559.

Gallo, R.L., and T. Nakatsuji. 2011. Microbial symbiosis with the innate immune defense system of the skin. *The Journal of investigative dermatology* 131:1974-1980.

Ganguly, D., G. Chamilos, R. Lande, J. Gregorio, S. Meller, V. Facchinetti, B. Homey, F.J. Barrat, T. Zal, and M. Gilliet. 2009. Self-RNA-antimicrobial peptide complexes activate human dendritic cells through TLR7 and TLR8. *The Journal of experimental medicine* 206:1983-1994.

Garbers, C., S. Aparicio-Siegmund, and S. Rose-John. 2015. The IL-6/gp130/STAT3 signaling axis: recent advances towards specific inhibition. *Curr Opin Immunol* 34:75-82.

Garlanda, C., C.A. Dinarello, and A. Mantovani. 2013. The interleukin-1 family: back to the future. *Immunity* 39:1003-1018.

Geisse, J., I. Caro, J. Lindholm, L. Golitz, P. Stampone, and M. Owens. 2004. Imiquimod 5% cream for the treatment of superficial basal cell carcinoma: results from two phase III, randomized, vehicle-controlled studies. *Journal of the American Academy of Dermatology* 50:722-733.

Gelfand, J.M., A.B. Troxel, J.D. Lewis, S.K. Kurd, D.B. Shin, X. Wang, D.J. Margolis, and B.L. Strom. 2007. The risk of mortality in patients with psoriasis: results from a population-based study. *Archives of dermatology* 143:1493-1499.

Genovese, M.C., J.D. McKay, E.L. Nasonov, E.F. Mysler, N.A. da Silva, E. Alecock, T. Woodworth, and J.J. Gomez-Reino. 2008. Interleukin-6 receptor inhibition with tocilizumab reduces disease activity in rheumatoid arthritis with inadequate response to disease-modifying antirheumatic drugs: the tocilizumab in combination with traditional disease-modifying antirheumatic drug therapy study. *Arthritis and rheumatism* 58:2968-2980.

Gibson, S.J., J.M. Lindh, T.R. Riter, R.M. Gleason, L.M. Rogers, A.E. Fuller, J.L. Oesterich, K.B. Gorden, X. Qiu, S.W. McKane, R.J. Noelle, R.L. Miller, R.M. Kedl, P. Fitzgerald-Bocarsly, M.A. Tomai, and J.P. Vasilakos. 2002. Plasmacytoid dendritic cells produce cytokines and mature in response to the TLR7 agonists, imiquimod and resiquimod. *Cellular immunology* 218:74-86.

Gilliet, M., C. Conrad, M. Geiges, A. Cozzio, W. Thurlimann, G. Burg, F.O. Nestle, and R. Dummer. 2004. Psoriasis triggered by toll-like receptor 7 agonist imiquimod in the presence of dermal plasmacytoid dendritic cell precursors. *Archives of dermatology* 140:1490-1495.

Grasland, A., E. Mahe, E. Raynaud, and I. Mahe. 2013. Psoriasis onset with tocilizumah. *Joint Bone Spine* 80:541-542.

Gray, E.E., K. Suzuki, and J.G. Cyster. 2011. Cutting edge: Identification of a motile IL-17-producing gammadelta T cell population in the dermis. *Journal of immunology* 186:6091-6095.

Grayson, P.C., and M.J. Kaplan. 2016. At the Bench: Neutrophil extracellular traps (NETs) highlight novel aspects of innate immune system involvement in autoimmune diseases. *Journal of leukocyte biology* 99:253-264.

Griffiths, C.E., K. Reich, M. Lebwohl, P. van de Kerkhof, C. Paul, A. Menter, G.S. Cameron, J. Erickson, L. Zhang, R.J. Secrest, S. Ball, D.K. Braun, O.O. Osuntokun, M.P. Heffernan, B.J. Nickoloff, K. Papp, Uncover, and U.-. investigators. 2015. Comparison of ixekizumab with etanercept or placebo in moderate-to-severe psoriasis (UNCOVER-2 and UNCOVER-3): results from two phase 3 randomised trials. *Lancet* 386:541-551.

Grivennikov, S., E. Karin, J. Terzic, D. Mucida, G.Y. Yu, S. Vallabhapurapu, J. Scheller, S. Rose-John, H. Cheroutre, L. Eckmann, and M. Karin. 2009. IL-6 and Stat3 are required for survival of intestinal epithelial cells and development of colitis-associated cancer. *Cancer cell* 15:103-113.

Grossman, R.M., J. Krueger, D. Yourish, A. Granelli-Piperno, D.P. Murphy, L.T. May, T.S. Kupper, P.B. Sehgal, and A.B. Gottlieb. 1989. Interleukin 6 is expressed in high levels in psoriatic skin and stimulates proliferation of cultured human

keratinocytes. *Proceedings of the National Academy of Sciences of the United States of America* 86:6367-6371.

Groves, R.W., H. Mizutani, J.D. Kieffer, and T.S. Kupper. 1995. Inflammatory skin disease in transgenic mice that express high levels of interleukin 1 alpha in basal epidermis. *Proceedings of the National Academy of Sciences of the United States of America* 92:11874-11878.

Groves, R.W., T. Rauschmayr, K. Nakamura, S. Sarkar, I.R. Williams, and T.S. Kupper. 1996. Inflammatory and hyperproliferative skin disease in mice that express elevated levels of the IL-1 receptor (type I) on epidermal keratinocytes. Evidence that IL-1-inducible secondary cytokines produced by keratinocytes in vivo can cause skin disease. *The Journal of clinical investigation* 98:336-344.

Groves, R.W., L. Sherman, H. Mizutani, S.K. Dower, and T.S. Kupper. 1994. Detection of interleukin-1 receptors in human epidermis. Induction of the type II receptor after organ culture and in psoriasis. *The American journal of pathology* 145:1048-1056.

Gudjonsson, J.E., A. Johnston, M. Dyson, H. Valdimarsson, and J.T. Elder. 2007. Mouse models of psoriasis. *The Journal of investigative dermatology* 127:1292-1308.

Gudjonsson, J.E., A. Karason, A. Antonsdottir, E.H. Runarsdottir, V.B. Hauksson, R. Upmanyu, J. Gulcher, K. Stefansson, and H. Valdimarsson. 2003. Psoriasis patients who are homozygous for the HLA-Cw*0602 allele have a 2.5-fold increased risk of developing psoriasis compared with Cw6 heterozygotes. *The British journal of dermatology* 148:233-235.

Hafner, M., J. Wenk, A. Nenci, M. Pasparakis, K. Scharffetter-Kochanek, N. Smyth, T. Peters, D. Kess, O. Holtkotter, P. Shephard, J.E. Kudlow, H. Smola, I. Haase, A. Schippers, T. Krieg, and W. Muller. 2004. Keratin 14 Cre transgenic mice authenticate keratin 14 as an oocyte-expressed protein. *Genesis* 38:176-181.

Haftik, M., J.P. Ortonne, M.J. Staquet, J. Viac, and J. Thivolet. 1981. Normal and psoriatic human skin grafts on "nude" mice: morphological and immunochemical studies. *The Journal of investigative dermatology* 76:48-52.

Hammerberg, C., W.P. Arend, G.J. Fisher, L.S. Chan, A.E. Berger, J.S. Haskill, J.J. Voorhees, and K.D. Cooper. 1992. Interleukin-1 receptor antagonist in normal and psoriatic epidermis. *The Journal of clinical investigation* 90:571-583.

Harrington, L.E., R.D. Hatton, P.R. Mangan, H. Turner, T.L. Murphy, K.M. Murphy, and C.T. Weaver. 2005. Interleukin 17-producing CD4+ effector T cells develop via a lineage distinct from the T helper type 1 and 2 lineages. *Nature immunology* 6:1123-1132.

Hartwig, T., S. Pantelyushin, A.L. Croxford, P. Kulig, and B. Becher. 2015. Dermal IL-17-producing gammadelta T cells establish long-lived memory in the skin. *European journal of immunology* 45:3022-3033.

Hasenberg, A., M. Hasenberg, L. Mann, F. Neumann, L. Borckenstein, M. Stecher, A. Kraus, D.R. Engel, A. Klingberg, P. Seddigh, Z. Abdullah, S. Klebow, S. Engelmann, A. Reinhold, S. Brandau, M. Seeling, A. Waisman, B. Schraven, J.R. Gothert, F. Nimmerjahn, and M. Gunzer. 2015. Catchup: a mouse model for imaging-based tracking and modulation of neutrophil granulocytes. *Nature methods* 12:445-452.

Havran, W.L., and J.M. Jameson. 2010. Epidermal T cells and wound healing. *Journal of immunology* 184:5423-5428.

Heath, W.R., and F.R. Carbone. 2013. The skin-resident and migratory immune system in steady state and memory: innate lymphocytes, dendritic cells and T cells. *Nature immunology* 14:978-985.

Heinrich, P.C., I. Behrmann, S. Haan, H.M. Hermanns, G. Muller-Newen, and F. Schaper. 2003. Principles of interleukin (IL)-6-type cytokine signalling and its regulation. *The Biochemical journal* 374:1-20.

Hemmi, H., T. Kaisho, O. Takeuchi, S. Sato, H. Sanjo, K. Hoshino, T. Horiuchi, H. Tomizawa, K. Takeda, and S. Akira. 2002. Small anti-viral compounds activate immune cells via the TLR7 MyD88-dependent signaling pathway. *Nature immunology* 3:196-200.

Hijnen, D., E.F. Knol, Y.Y. Gent, B. Giovannone, S.J. Beijin, T.S. Kupper, C.A. Bruijnzeel-Koomen, and R.A. Clark. 2013. CD8(+) T cells in the lesional skin of atopic dermatitis and psoriasis patients are an important source of IFN-gamma, IL-13, IL-17, and IL-22. *The Journal of investigative dermatology* 133:973-979.

Hueber, W., D.D. Patel, T. Dryja, A.M. Wright, I. Koroleva, G. Bruin, C. Antoni, Z. Draelos, M.H. Gold, G. Psoriasis Study, P. Durez, P.P. Tak, J.J. Gomez-Reino, G. Rheumatoid Arthritis Study, C.S. Foster, R.Y. Kim, C.M. Samson, N.S. Falk, D.S. Chu, D. Callanan, Q.D. Nguyen, G. Uveitis Study, K. Rose, A. Haider, and F. Di Padova. 2010. Effects of AIN457, a fully human antibody to interleukin-17A, on psoriasis, rheumatoid arthritis, and uveitis. *Science translational medicine* 2:52ra72.

Hueber, W., B.E. Sands, S. Lewitzky, M. Vandemeulebroecke, W. Reinisch, P.D. Higgins, J. Wehkamp, B.G. Feagan, M.D. Yao, M. Karczewski, J. Karczewski, N. Pezous, S. Bek, G. Bruin, B. Mellgard, C. Berger, M. Londei, A.P. Bertolino, G. Tougas, S.P. Travis, and G. Secukinumab in Crohn's Disease Study. 2012. Secukinumab, a human anti-IL-17A monoclonal antibody, for moderate to severe Crohn's disease: unexpected results of a randomised, double-blind placebo-controlled trial. *Gut* 61:1693-1700.

Huffmeier, U., M. Watzold, J. Mohr, M.P. Schon, and R. Mossner. 2014. Successful therapy with anakinra in a patient with generalized pustular psoriasis carrying IL36RN mutations. *The British journal of dermatology* 170:202-204.

Hughes, M., and H. Chinoy. 2013. Successful use of tocilizumab in a patient with psoriatic arthritis. *Rheumatology* 52:1728-1729.

Hvid, H., I. Teige, P.H. Kvist, L. Svensson, and K. Kemp. 2008. TPA induction leads to a Th17-like response in transgenic K14/VEGF mice: a novel in vivo screening model of psoriasis. *International immunology* 20:1097-1106.

Iwakura, Y., H. Ishigame, S. Saijo, and S. Nakae. 2011. Functional specialization of interleukin-17 family members. *Immunity* 34:149-162.

Jayasekera, P., R. Parslew, and A. Al-Sharqi. 2014. A case of tumour necrosis factor-alpha inhibitor- and rituximab-induced plantar pustular psoriasis that completely resolved with tocilizumab. *Brit J Dermatol* 171:1546-1549.

Jensen, L.E. 2010. Targeting the IL-1 family members in skin inflammation. *Current opinion in investigational drugs* 11:1211-1220.

Jinna, S., and B. Strober. 2016. Anti-interleukin-17 treatment of psoriasis. *The Journal of dermatological treatment* 27:311-315.

Johnston, A., Y. Fritz, S.M. Dawes, D. Diaconu, P.M. Al-Attar, A.M. Guzman, C.S. Chen, W. Fu, J.E. Gudjonsson, T.S. McCormick, and N.L. Ward. 2013. Keratinocyte overexpression of IL-17C promotes psoriasiform skin inflammation. *Journal of immunology* 190:2252-2262.

Jones, S.A., J. Scheller, and S. Rose-John. 2011. Therapeutic strategies for the clinical blockade of IL-6/gp130 signaling. *The Journal of clinical investigation* 121:3375-3383.

Jostock, T., J. Mullberg, S. Ozbek, R. Atreya, G. Blinn, N. Voltz, M. Fischer, M.F. Neurath, and S. Rose-John. 2001. Soluble gp130 is the natural inhibitor of soluble interleukin-6 receptor transsignaling responses. *European journal of biochemistry / FEBS* 268:160-167.

Kaisho, T., and S. Akira. 2006. Toll-like receptor function and signaling. *The Journal of allergy and clinical immunology* 117:979-987; quiz 988.

Kaneko, F., N. Itoh, H. Yoshida, M. Suzuki, and I. Ono. 1991. The cell-components and cytokines in the subcorneal microabscess of psoriasis. *Fukushima journal of medical science* 37:103-112.

Kanneganti, T.D., N. Ozoren, M. Body-Malapel, A. Amer, J.H. Park, L. Franchi, J. Whitfield, W. Barchet, M. Colonna, P. Vandenabeele, J. Bertin, A. Coyle, E.P. Grant, S. Akira, and G. Nunez. 2006. Bacterial RNA and small antiviral compounds activate caspase-1 through cryopyrin/Nalp3. *Nature* 440:233-236.

Karbach, S., A.L. Croxford, M. Oelze, R. Schuler, D. Minwegen, J. Wegner, L. Koukes, N. Yogev, A. Nikolaev, S. Reissig, A. Ullmann, M. Knorr, M. Waldner, M.F. Neurath, H. Li, Z. Wu, C. Brochhausen, J. Scheller, S. Rose-John, C. Piotrowski, I. Bechmann, M. Radsak, P. Wild, A. Daiber, E. von Stebut, P. Wenzel, A. Waisman, and T. Munzel. 2014. Interleukin 17 drives vascular inflammation, endothelial dysfunction, and arterial hypertension in psoriasis-like skin disease. *Arteriosclerosis, thrombosis, and vascular biology* 34:2658-2668.

Karle, A., S. Spindeldreher, and F. Kolbinger. 2016. Secukinumab, a novel anti-IL-17A antibody, shows low immunogenicity potential in human in vitro assays comparable to other marketed biotherapeutics with low clinical immunogenicity. *mAbs* 8:536-550.

Kawai, T., and S. Akira. 2006. TLR signaling. *Cell death and differentiation* 13:816-825.

Kawai, T., and S. Akira. 2010. The role of pattern-recognition receptors in innate immunity: update on Toll-like receptors. *Nature immunology* 11:373-384.

Keijsers, R.R., A.G. Hendriks, P.E. van Erp, B. van Cranenbroek, P.C. van de Kerkhof, H.J. Koenen, and I. Joosten. 2014. In vivo induction of cutaneous inflammation results in the accumulation of extracellular trap-forming neutrophils expressing ROR γ and IL-17. *The Journal of investigative dermatology* 134:1276-1284.

Keller, M., A. Ruegg, S. Werner, and H.D. Beer. 2008. Active caspase-1 is a regulator of unconventional protein secretion. *Cell* 132:818-831.

Khavari, P.A. 2006. Modelling cancer in human skin tissue. *Nature reviews. Cancer* 6:270-280.

Kimura, A., and T. Kishimoto. 2010. IL-6: regulator of Treg/Th17 balance. *European journal of immunology* 40:1830-1835.

Klebow, S., M. Hahn, A. Nikoalev, F.T. Wunderlich, N. Hovelmeyer, S.H. Karbach, and A. Waisman. 2016. IL-6 Signaling in Myelomonocytic Cells Is Not Crucial for the Development of IMQ-Induced Psoriasis. *PloS one* 11:e0151913.

Kollisch, G., B.N. Kalali, V. Voelcker, R. Wallich, H. Behrendt, J. Ring, S. Bauer, T. Jakob, M. Mempel, and M. Ollert. 2005. Various members of the Toll-like receptor family contribute to the innate immune response of human epidermal keratinocytes. *Immunology* 114:531-541.

Kono, T., S. Kondo, S. Pastore, G.M. Shivji, M.A. Tomai, R.C. McKenzie, and D.N. Sauder. 1994. Effects of a novel topical immunomodulator, imiquimod, on keratinocyte cytokine gene expression. *Lymphokine and cytokine research* 13:71-76.

Kopp, T., P. Lenz, C. Bello-Fernandez, R.A. Kastelein, T.S. Kupper, and G. Stingl. 2003. IL-23 production by cosecretion of endogenous p19 and transgenic p40 in keratin 14/p40 transgenic mice: evidence for enhanced cutaneous immunity. *Journal of immunology* 170:5438-5444.

Laggner, U., P. Di Meglio, G.K. Perera, C. Hundhausen, K.E. Lacy, N. Ali, C.H. Smith, A.C. Hayday, B.J. Nickoloff, and F.O. Nestle. 2011. Identification of a novel proinflammatory human skin-homing Vgamma9Vdelta2 T cell subset with a potential role in psoriasis. *Journal of immunology* 187:2783-2793.

Lande, R., E. Botti, C. Jandus, D. Dojcinovic, G. Fanelli, C. Conrad, G. Chamilos, L. Feldmeyer, B. Marinari, S. Chon, L. Vence, V. Riccieri, P. Guillaume, A.A. Navarini, P. Romero, A. Costanzo, E. Piccolella, M. Gilliet, and L. Frasca. 2014. The antimicrobial peptide LL37 is a T-cell autoantigen in psoriasis. *Nature communications* 5:5621.

Langley, R.G., B.E. Elewski, M. Lebwohl, K. Reich, C.E. Griffiths, K. Papp, L. Puig, H. Nakagawa, L. Spelman, B. Sigurgeirsson, E. Rivas, T.F. Tsai, N. Wasel, S. Tyring, T. Salko, I. Hampele, M. Notter, A. Karpov, S. Helou, C. Papavassilis, E.S. Group, and F.S. Group. 2014. Secukinumab in plaque psoriasis--results of two phase 3 trials. *The New England journal of medicine* 371:326-338.

Laurent, S., J.M. Le Parc, T. Clerici, M. Breban, and E. Mahe. 2010. Onset of psoriasis following treatment with tocilizumab. *Brit J Dermatol* 163:1364-1365.

Lebre, M.C., A.M. van der Aar, L. van Baarsen, T.M. van Capel, J.H. Schuitemaker, M.L. Kapsenberg, and E.C. de Jong. 2007. Human keratinocytes express functional Toll-like receptor 3, 4, 5, and 9. *The Journal of investigative dermatology* 127:331-341.

Lee, E., W.L. Trepicchio, J.L. Oestreicher, D. Pittman, F. Wang, F. Chamian, M. Dhodapkar, and J.G. Krueger. 2004. Increased expression of interleukin 23 p19 and p40 in lesional skin of patients with psoriasis vulgaris. *The Journal of experimental medicine* 199:125-130.

Leonardi, C.L., A.B. Kimball, K.A. Papp, N. Yeilding, C. Guzzo, Y. Wang, S. Li, L.T. Dooley, K.B. Gordon, and P.s. investigators. 2008. Efficacy and safety of ustekinumab, a human interleukin-12/23 monoclonal antibody, in patients with psoriasis: 76-week results from a randomised, double-blind, placebo-controlled trial (PHOENIX 1). *Lancet* 371:1665-1674.

Levy, D.E., and J.E. Darnell. 2002. STATs: Transcriptional control and biological impact. *Nat Rev Mol Cell Bio* 3:651-662.

Lin, A.M., C.J. Rubin, R. Khandpur, J.Y. Wang, M. Riblett, S. Yalavarthi, E.C. Villanueva, P. Shah, M.J. Kaplan, and A.T. Bruce. 2011. Mast cells and neutrophils release IL-17 through extracellular trap formation in psoriasis. *Journal of immunology* 187:490-500.

Lindroos, J., L. Svensson, H. Norsgaard, P. Lovato, K. Moller, P.H. Hagedorn, G.M. Olsen, and T. Labuda. 2011. IL-23-mediated epidermal hyperplasia is dependent on IL-6. *The Journal of investigative dermatology* 131:1110-1118.

Lopez-Ferrer, A., E. Vilarrasa, and L. Puig. 2015. Secukinumab (AIN457) for the treatment of psoriasis. *Expert review of clinical immunology* 11:1177-1188.

Lorenzen, I., J. Lokau, S. Dusterhoft, A. Trad, C. Garbers, J. Scheller, S. Rose-John, and J. Grotzinger. 2012. The membrane-proximal domain of A Disintegrin and Metalloprotease 17 (ADAM17) is responsible for recognition of the interleukin-6 receptor and interleukin-1 receptor II. *FEBS letters* 586:1093-1100.

Lowes, M.A., A.M. Bowcock, and J.G. Krueger. 2007. Pathogenesis and therapy of psoriasis. *Nature* 445:866-873.

Lowes, M.A., C.B. Russell, D.A. Martin, J.E. Towne, and J.G. Krueger. 2013. The IL-23/T17 pathogenic axis in psoriasis is amplified by keratinocyte responses. *Trends Immunol* 34:174-181.

Lowes, M.A., M. Suarez-Farinas, and J.G. Krueger. 2014. Immunology of psoriasis. *Annual review of immunology* 32:227-255.

Mabuchi, T., T. Takekoshi, and S.T. Hwang. 2011. Epidermal CCR6+ gammadelta T cells are major producers of IL-22 and IL-17 in a murine model of psoriasiform dermatitis. *Journal of immunology* 187:5026-5031.

MacLeod, A.S., S. Hemmers, O. Garijo, M. Chabod, K. Mowen, D.A. Witherden, and W.L. Havran. 2013. Dendritic epidermal T cells regulate skin antimicrobial barrier function. *The Journal of clinical investigation* 123:4364-4374.

Markatseli, T.E., E.S. Kaltsonoudis, P.V. Voulgari, A. Zioga, and A.A. Drosos. 2009. Induction of psoriatic skin lesions in a patient with rheumatoid arthritis treated with rituximab. *Clinical and experimental rheumatology* 27:996-998.

Martin, P., G. Palmer, S. Vigne, C. Lamacchia, E. Rodriguez, D. Talabot-Ayer, S. Rose-John, A. Chalaris, and C. Gabay. 2013. Mouse neutrophils express the decoy type 2 interleukin-1 receptor (IL-1R2) constitutively and in acute inflammatory conditions. *Journal of leukocyte biology* 94:791-802.

Martinon, F., and J. Tschopp. 2007. Inflammatory caspases and inflammasomes: master switches of inflammation. *Cell death and differentiation* 14:10-22.

Mauer, J., B. Chaurasia, J. Goldau, M.C. Vogt, J. Ruud, K.D. Nguyen, S. Theurich, A.C. Hausen, J. Schmitz, H.S. Bronneke, E. Estevez, T.L. Allen, A. Mesaros, L. Partridge, M.A. Febbraio, A. Chawla, F.T. Wunderlich, and J.C. Bruning. 2014. Signaling by IL-6 promotes alternative activation of macrophages to limit endotoxemia and obesity-associated resistance to insulin. *Nature immunology* 15:423-430.

Mayer, C.L., L.Y. Xie, R. Bandekar, M. Qi, H. van de Velde, M. Reddy, X. Qin, H.M. Davis, and T.A. Puchalski. 2015. Dose selection of siltuximab for multicentric Castleman's disease. *Cancer Chemoth Pharm* 75:1037-1045.

McInnes, I.B., P.J. Mease, B. Kirkham, A. Kavanaugh, C.T. Ritchlin, P. Rahman, D. van der Heijde, R. Landewe, P.G. Conaghan, A.B. Gottlieb, H. Richards, L. Pricop, G. Ligozio, M. Patekar, S. Mpofu, and F.S. Group. 2015. Secukinumab, a human anti-interleukin-17A monoclonal antibody, in patients with psoriatic arthritis (FUTURE 2): a randomised, double-blind, placebo-controlled, phase 3 trial. *Lancet* 386:1137-1146.

Medzhitov, R. 2001. Toll-like receptors and innate immunity. *Nature reviews. Immunology* 1:135-145.

Milora, K.A., H. Fu, O. Dubaz, and L.E. Jensen. 2015. Unprocessed Interleukin-36alpha Regulates Psoriasis-Like Skin Inflammation in Cooperation With Interleukin-1. *The Journal of investigative dermatology* 135:2992-3000.

Mullis, K.B., and F.A. Faloon. 1987. Specific synthesis of DNA in vitro via a polymerase-catalyzed chain reaction. *Methods in enzymology* 155:335-350.

Nakajima, A., T. Matsuki, M. Komine, A. Asahina, R. Horai, S. Nakae, H. Ishigame, S. Kakuta, S. Saijo, and Y. Iwakura. 2010. TNF, but not IL-6 and IL-17, is crucial for the development of T cell-independent psoriasis-like dermatitis in *Il1rn*^{-/-} mice. *Journal of immunology* 185:1887-1893.

Nakajima, K., T. Kanda, M. Takaishi, T. Shiga, K. Miyoshi, H. Nakajima, R. Kamijima, M. Tarutani, J.M. Benson, M.M. Elloso, L.L. Gutshall, M.F. Naso, Y. Iwakura, J. DiGiovanni, and S. Sano. 2011. Distinct roles of IL-23 and IL-17 in the development of psoriasis-like lesions in a mouse model. *Journal of immunology* 186:4481-4489.

Nestle, F.O., P. Di Meglio, J.Z. Qin, and B.J. Nickoloff. 2009a. Skin immune sentinels in health and disease. *Nature reviews. Immunology* 9:679-691.

Nestle, F.O., D.H. Kaplan, and J. Barker. 2009b. Psoriasis. *The New England journal of medicine* 361:496-509.

Neuner, P., A. Urbanski, F. Trautinger, A. Moller, R. Kirnbauer, A. Kapp, E. Schopf, T. Schwarz, and T.A. Luger. 1991. Increased IL-6-Production by Monocytes and Keratinocytes in Patients with Psoriasis. *Journal of Investigative Dermatology* 97:27-33.

Neurath, M.F., and S. Finotto. 2011. IL-6 signaling in autoimmunity, chronic inflammation and inflammation-associated cancer. *Cytokine & growth factor reviews* 22:83-89.

Nishimoto, N., K. Terao, T. Mima, H. Nakahara, N. Takagi, and T. Takeuchi. 2008. Mechanisms and pathologic significances in increase in serum interleukin-6 (IL-

6) and soluble IL-6 receptor after administration of an anti-IL-6 receptor antibody, tocilizumab, in patients with rheumatoid arthritis and Castleman disease. *Blood* 112:3959-3964.

Nowell, M.A., P.J. Richards, S. Horiuchi, N. Yamamoto, S. Rose-John, N. Topley, A.S. Williams, and S.A. Jones. 2003. Soluble IL-6 receptor governs IL-6 activity in experimental arthritis: blockade of arthritis severity by soluble glycoprotein 130. *Journal of immunology* 171:3202-3209.

Oppmann, B., R. Lesley, B. Blom, J.C. Timans, Y. Xu, B. Hunte, F. Vega, N. Yu, J. Wang, K. Singh, F. Zonin, E. Vaisberg, T. Churakova, M. Liu, D. Gorman, J. Wagner, S. Zurawski, Y. Liu, J.S. Abrams, K.W. Moore, D. Rennick, R. de Waal-Malefyt, C. Hannum, J.F. Bazan, and R.A. Kastelein. 2000. Novel p19 protein engages IL-12p40 to form a cytokine, IL-23, with biological activities similar as well as distinct from IL-12. *Immunity* 13:715-725.

Palmou-Fontana, N., J.A.S. Gavino, D. McGonagle, E. Garcia-Martinez, and L.I.D. Martin. 2014. Tocilizumab-Induced Psoriasiform Rash in Rheumatoid Arthritis. *Dermatology* 228:311-313.

Pantelyushin, S., S. Haak, B. Ingold, P. Kulig, F.L. Heppner, A.A. Navarini, and B. Becher. 2012. Rorgammat+ innate lymphocytes and gammadelta T cells initiate psoriasiform plaque formation in mice. *The Journal of clinical investigation* 122:2252-2256.

Papp, K.A., C.E. Griffiths, K. Gordon, M. Lebwohl, P.O. Szapary, Y. Wasfi, D. Chan, M.C. Hsu, V. Ho, P.D. Ghislain, B. Strober, K. Reich, P. Investigators, P. Investigators, and A. Investigators. 2013. Long-term safety of ustekinumab in patients with moderate-to-severe psoriasis: final results from 5 years of follow-up. *The British journal of dermatology* 168:844-854.

Papp, K.A., R.G. Langley, M. Lebwohl, G.G. Krueger, P. Szapary, N. Yeilding, C. Guzzo, M.C. Hsu, Y. Wang, S. Li, L.T. Dooley, K. Reich, and P.s. investigators. 2008. Efficacy and safety of ustekinumab, a human interleukin-12/23 monoclonal antibody, in patients with psoriasis: 52-week results from a randomised, double-blind, placebo-controlled trial (PHOENIX 2). *Lancet* 371:1675-1684.

Pasparakis, M., G. Courtois, M. Hafner, M. Schmidt-Supprian, A. Nenci, A. Toksoy, M. Krampert, M. Goebeler, R. Gillitzer, A. Israel, T. Krieg, K. Rajewsky, and I. Haase. 2002. TNF-mediated inflammatory skin disease in mice with epidermis-specific deletion of IKK2. *Nature* 417:861-866.

Pasparakis, M., I. Haase, and F.O. Nestle. 2014. Mechanisms regulating skin immunity and inflammation. *Nature reviews. Immunology* 14:289-301.

Paul, C., J.P. Lacour, L. Tedremets, K. Kreutzer, S. Jazayeri, S. Adams, C. Guindon, R. You, C. Papavassilis, and J.s. group. 2015. Efficacy, safety and usability of secukinumab administration by autoinjector/pen in psoriasis: a randomized,

controlled trial (JUNCTURE). *Journal of the European Academy of Dermatology and Venereology* : JEADV 29:1082-1090.

Perera, G.K., P. Di Meglio, and F.O. Nestle. 2012. Psoriasis. *Annual review of pathology* 7:385-422.

Peters, V.A., J.J. Joesting, and G.G. Freund. 2013. IL-1 receptor 2 (IL-1R2) and its role in immune regulation. *Brain, behavior, and immunity* 32:1-8.

Piskin, G., R.M. Sylva-Steenland, J.D. Bos, and M.B. Teunissen. 2006. In vitro and in situ expression of IL-23 by keratinocytes in healthy skin and psoriasis lesions: enhanced expression in psoriatic skin. *Journal of immunology* 176:1908-1915.

Platt, A.M., and G.J. Randolph. 2013. Dendritic cell migration through the lymphatic vasculature to lymph nodes. *Advances in immunology* 120:51-68.

Prinz, I., and I. Sandrock. 2015. gammadelta T cells come to stay: Innate skin memory in the Aldara model. *European journal of immunology* 45:2994-2997.

Rabeony, H., M. Pohin, P. Vasseur, I. Petit-Paris, J.F. Jegou, L. Favot, E. Frouin, M.A. Boutet, F. Blanchard, D. Togbe, B. Ryffel, F.X. Bernard, J.C. Lecron, and F. Morel. 2015. IMQ-induced skin inflammation in mice is dependent on IL-1R1 and MyD88 signaling but independent of the NLRP3 inflammasome. *European journal of immunology* 45:2847-2857.

Rajan, N., and J.A. Langtry. 2006. Generalized exacerbation of psoriasis associated with imiquimod cream treatment of superficial basal cell carcinomas. *Clinical and experimental dermatology* 31:140-141.

Ratner, M. 2015. IL-17-targeting biologics aim to become standard of care in psoriasis. *Nat Biotechnol* 33:3-4.

Rauschmayr, T., R.W. Groves, and T.S. Kupper. 1997. Keratinocyte expression of the type 2 interleukin 1 receptor mediates local and specific inhibition of interleukin 1-mediated inflammation. *Proceedings of the National Academy of Sciences of the United States of America* 94:5814-5819.

Rawlings, J.S., K.M. Rosler, and D.A. Harrison. 2004. The JAK/STAT signaling pathway. *Journal of cell science* 117:1281-1283.

Raychaudhuri, S.K., E. Maverakis, and S.P. Raychaudhuri. 2014. Diagnosis and classification of psoriasis. *Autoimmunity reviews* 13:490-495.

Raychaudhuri, S.K., and S.P. Raychaudhuri. 2010. Scid mouse model of psoriasis: a unique tool for drug development of autoreactive T-cell and th-17 cell-mediated autoimmune diseases. *Indian journal of dermatology* 55:157-160.

Reich, K., K.A. Papp, R.T. Matheson, J.H. Tu, R. Bissonnette, M. Bourcier, D. Gratton, R.A. Kunyetz, Y. Poulin, L.A. Rosoph, G. Stingl, W.M. Bauer, J.M. Salter,

T.M. Falk, N.A. Blodorn-Schlicht, W. Hueber, U. Sommer, M.M. Schumacher, T. Peters, E. Kriehuber, D.M. Lee, G.A. Wieczorek, F. Kolbinger, and C.C. Bleul. 2015. Evidence that a neutrophil-keratinocyte crosstalk is an early target of IL-17A inhibition in psoriasis. *Experimental dermatology* 24:529-535.

Res, P.C., G. Piskin, O.J. de Boer, C.M. van der Loos, P. Teeling, J.D. Bos, and M.B. Teunissen. 2010. Overrepresentation of IL-17A and IL-22 producing CD8 T cells in lesional skin suggests their involvement in the pathogenesis of psoriasis. *PLoS one* 5:e14108.

Richards, C.D. 2013. The enigmatic cytokine oncostatin m and roles in disease. *ISRN inflammation* 2013:512103.

Rincon, M., J. Anguita, T. Nakamura, E. Fikrig, and R.A. Flavell. 1997. Interleukin (IL)-6 directs the differentiation of IL-4-producing CD4+ T cells. *The Journal of experimental medicine* 185:461-469.

Riol-Blanco, L., J. Ordovas-Montanes, M. Perro, E. Naval, A. Thiriot, D. Alvarez, S. Paust, J.N. Wood, and U.H. von Andrian. 2014. Nociceptive sensory neurons drive interleukin-23-mediated psoriasiform skin inflammation. *Nature* 510:157-161.

Ritchlin, C.T., and J.G. Krueger. 2016. New therapies for psoriasis and psoriatic arthritis. *Current opinion in rheumatology* 28:204-210.

Rose, S., A. Misharin, and H. Perlman. 2012. A novel Ly6C/Ly6G-based strategy to analyze the mouse splenic myeloid compartment. *Cytometry A* 81:343-350.

Rose-John, S. 2012. IL-6 trans-signaling via the soluble IL-6 receptor: importance for the pro-inflammatory activities of IL-6. *International journal of biological sciences* 8:1237-1247.

Rose-John, S., J. Scheller, G. Elson, and S.A. Jones. 2006. Interleukin-6 biology is coordinated by membrane-bound and soluble receptors: role in inflammation and cancer. *Journal of leukocyte biology* 80:227-236.

Rose-John, S., G.H. Waetzig, J. Scheller, J. Grotzinger, and D. Seegert. 2007. The IL-6/sIL-6R complex as a novel target for therapeutic approaches. *Expert opinion on therapeutic targets* 11:613-624.

Rossi-Semerano, L., M. Piram, C. Chiaverini, D. De Ricaud, A. Smahi, and I. Kone-Paut. 2013. First clinical description of an infant with interleukin-36-receptor antagonist deficiency successfully treated with anakinra. *Pediatrics* 132:e1043-1047.

Saggini, A., S. Chimenti, and A. Chiricozzi. 2014. IL-6 as a druggable target in psoriasis: focus on pustular variants. *Journal of immunology research* 2014:964069.

Saiki, R.K., S. Scharf, F. Faloona, K.B. Mullis, G.T. Horn, H.A. Erlich, and N. Arnheim. 1985. Enzymatic amplification of beta-globin genomic sequences and restriction site analysis for diagnosis of sickle cell anemia. *Science* 230:1350-1354.

Sambrook, J., and M.J. Gething. 1989. Protein structure. Chaperones, paperones. *Nature* 342:224-225.

Sano, S., K.S. Chan, S. Carbajal, J. Clifford, M. Peavey, K. Kiguchi, S. Itami, B.J. Nickoloff, and J. DiGiovanni. 2005. Stat3 links activated keratinocytes and immunocytes required for development of psoriasis in a novel transgenic mouse model. *Nature medicine* 11:43-49.

Schauber, J., and R.L. Gallo. 2007. Expanding the roles of antimicrobial peptides in skin: alarming and arming keratinocytes. *The Journal of investigative dermatology* 127:510-512.

Schauber, J., and R.L. Gallo. 2008. Antimicrobial peptides and the skin immune defense system. *The Journal of allergy and clinical immunology* 122:261-266.

Scheller, J., A. Chalaris, D. Schmidt-Arras, and S. Rose-John. 2011. The pro- and anti-inflammatory properties of the cytokine interleukin-6. *Biochimica et biophysica acta* 1813:878-888.

Scheller, J., C. Garbers, and S. Rose-John. 2014. Interleukin-6: from basic biology to selective blockade of pro-inflammatory activities. *Seminars in immunology* 26:2-12.

Scheller, J., and S. Rose-John. 2006. Interleukin-6 and its receptor: from bench to bedside. *Medical microbiology and immunology* 195:173-183.

Schon, M.P., and M. Schon. 2007. Imiquimod: mode of action. *The British journal of dermatology* 157 Suppl 2:8-13.

Schroder, J.M., and J. Harder. 2006. Antimicrobial skin peptides and proteins. *Cellular and molecular life sciences : CMLS* 63:469-486.

Schumacher, N., D. Meyer, A. Mauermann, J. von der Heyde, J. Wolf, J. Schwarz, K. Knittler, G. Murphy, M. Michalek, C. Garbers, J.W. Bartsch, S. Guo, B. Schacher, P. Eickholz, A. Chalaris, S. Rose-John, and B. Rabe. 2015. Shedding of Endogenous Interleukin-6 Receptor (IL-6R) Is Governed by A Disintegrin and Metalloproteinase (ADAM) Proteases while a Full-length IL-6R Isoform Localizes to Circulating Microvesicles. *The Journal of biological chemistry* 290:26059-26071.

Schwartz, J., A.W. Evers, C. Bundy, and A.B. Kimball. 2016. Getting under the Skin: Report from the International Psoriasis Council Workshop on the Role of Stress in Psoriasis. *Frontiers in psychology* 7:87.

Schwenk, F., U. Baron, and K. Rajewsky. 1995. A cre-transgenic mouse strain for the ubiquitous deletion of loxP-flanked gene segments including deletion in germ cells. *Nucleic acids research* 23:5080-5081.

Shepherd, J., M.C. Little, and M.J. Nicklin. 2004. Psoriasis-like cutaneous inflammation in mice lacking interleukin-1 receptor antagonist. *The Journal of investigative dermatology* 122:665-669.

Shibata, S., Y. Tada, C.S. Hau, A. Mitsui, M. Kamata, Y. Asano, M. Sugaya, T. Kadono, Y. Masamoto, M. Kurokawa, T. Yamauchi, N. Kubota, T. Kadowaki, and S. Sato. 2015. Adiponectin regulates psoriasiform skin inflammation by suppressing IL-17 production from gammadelta-T cells. *Nature communications* 6:7687.

Shimizu, K., A. Nakajima, K. Sudo, Y. Liu, A. Mizoroki, T. Ikarashi, R. Horai, S. Kakuta, T. Watanabe, and Y. Iwakura. 2015. IL-1 receptor type 2 suppresses collagen-induced arthritis by inhibiting IL-1 signal on macrophages. *Journal of immunology* 194:3156-3168.

Shuai, K., and B. Liu. 2003. Regulation of JAK-STAT signalling in the immune system. *Nature reviews. Immunology* 3:900-911.

Sims, J.E., and D.E. Smith. 2010. The IL-1 family: regulators of immunity. *Nature reviews. Immunology* 10:89-102.

Stanley, M.A. 2002. Imiquimod and the imidazoquinolones: mechanism of action and therapeutic potential. *Clinical and experimental dermatology* 27:571-577.

Strober, B., B. Sigurgeirsson, G. Popp, R. Sinclair, J. Krell, S. Stonkus, M. Septe, B.E. Elewski, A.B. Gottlieb, Y. Zhao, M.H. Tran, A. Karpov, L.D. McLeod, M. Mordin, C. Papavassilis, J. Nyirady, and M. Lebwohl. 2016. Secukinumab improves patient-reported psoriasis symptoms of itching, pain, and scaling: results of two phase 3, randomized, placebo-controlled clinical trials. *International journal of dermatology* 55:401-407.

Sumaria, N., B. Roediger, L.G. Ng, J. Qin, R. Pinto, L.L. Cavanagh, E. Shklovskaya, B. Fazekas de St Groth, J.A. Triccas, and W. Weninger. 2011. Cutaneous immunosurveillance by self-renewing dermal gammadelta T cells. *The Journal of experimental medicine* 208:505-518.

Sutton, C.E., S.J. Lalor, C.M. Sweeney, C.F. Brereton, E.C. Lavelle, and K.H. Mills. 2009. Interleukin-1 and IL-23 induce innate IL-17 production from gammadelta T cells, amplifying Th17 responses and autoimmunity. *Immunity* 31:331-341.

Suzuki, H., B. Wang, G.M. Shivji, P. Toto, P. Amerio, M.A. Tomai, R.L. Miller, and D.N. Sauder. 2000. Imiquimod, a topical immune response modifier, induces migration of Langerhans cells. *The Journal of investigative dermatology* 114:135-141.

Szeimies, R.M., M.J. Gerritsen, G. Gupta, J.P. Ortonne, S. Serresi, J. Bichel, J.H. Lee, T.L. Fox, and A. Alomar. 2004. Imiquimod 5% cream for the treatment of actinic keratosis: results from a phase III, randomized, double-blind, vehicle-controlled, clinical trial with histology. *Journal of the American Academy of Dermatology* 51:547-555.

Tauber, M., M. Viguier, E. Alimova, A. Petit, F. Liote, A. Smahi, and H. Bachelez. 2014. Partial clinical response to anakinra in severe palmoplantar pustular psoriasis. *The British journal of dermatology* 171:646-649.

Taylor, P.R., S. Roy, S.M. Leal, Jr., Y. Sun, S.J. Howell, B.A. Cobb, X. Li, and E. Pearlman. 2014. Activation of neutrophils by autocrine IL-17A-IL-17RC interactions during fungal infection is regulated by IL-6, IL-23, ROR γ and dectin-2. *Nature immunology* 15:143-151.

Teng, M.W., E.P. Bowman, J.J. McElwee, M.J. Smyth, J.L. Casanova, A.M. Cooper, and D.J. Cua. 2015. IL-12 and IL-23 cytokines: from discovery to targeted therapies for immune-mediated inflammatory diseases. *Nature medicine* 21:719-729.

Terhorst, D., R. Chelbi, C. Wohn, C. Malosse, S. Tamoutounour, A. Jorquera, M. Bajenoff, M. Dalod, B. Malissen, and S. Henri. 2015. Dynamics and Transcriptomics of Skin Dendritic Cells and Macrophages in an Imiquimod-Induced, Biphasic Mouse Model of Psoriasis. *Journal of immunology* 195:4953-4961.

Terui, T., M. Ozawa, and H. Tagami. 2000. Role of neutrophils in induction of acute inflammation in T-cell-mediated immune dermatosis, psoriasis: A neutrophil-associated inflammation-boosting loop. *Experimental dermatology* 9:1-10.

Teunissen, M.B., C.W. Koomen, R. de Waal Malefyt, E.A. Wierenga, and J.D. Bos. 1998. Interleukin-17 and interferon-gamma synergize in the enhancement of proinflammatory cytokine production by human keratinocytes. *The Journal of investigative dermatology* 111:645-649.

Tortola, L., E. Rosenwald, B. Abel, H. Blumberg, M. Schafer, A.J. Coyle, J.C. Renauld, S. Werner, J. Kisielow, and M. Kopf. 2012. Psoriasiform dermatitis is driven by IL-36-mediated DC-keratinocyte crosstalk. *The Journal of clinical investigation* 122:3965-3976.

Trivedi, B. 2012. Microbiome: The surface brigade. *Nature* 492:S60-61.

Trojacka, E., M. Zaleska, and R. Galus. 2015. [Influence of exogenous and endogenous factors on the course of psoriasis]. *Polski merkuriusz lekarski : organ Polskiego Towarzystwa Lekarskiego* 38:169-173.

Turksen, K., T. Kupper, L. Degenstein, I. Williams, and E. Fuchs. 1992. Interleukin 6: insights to its function in skin by overexpression in transgenic mice.

Proceedings of the National Academy of Sciences of the United States of America 89:5068-5072.

Uchikawa, S., M. Yoda, T. Tohmonda, A. Kanaji, M. Matsumoto, Y. Toyama, and K. Horiuchi. 2015. ADAM17 regulates IL-1 signaling by selectively releasing IL-1 receptor type 2 from the cell surface. *Cytokine* 71:238-245.

Uribe-Herranz, M., L.H. Lian, K.M. Hooper, K.A. Milora, and L.E. Jensen. 2013. IL-1R1 signaling facilitates Munro's microabscess formation in psoriasiform imiquimod-induced skin inflammation. *The Journal of investigative dermatology* 133:1541-1549.

Urošević, M., R. Dummer, C. Conrad, M. Beyeler, E. Laine, G. Burg, and M. Gilliet. 2005. Disease-independent skin recruitment and activation of plasmacytoid dendritic cells following imiquimod treatment. *Journal of the National Cancer Institute* 97:1143-1153.

Van Belle, A.B., M. de Heusch, M.M. Lemaire, E. Hendrickx, G. Warnier, K. Dunussi-Joannopoulos, L.A. Fouser, J.C. Renauld, and L. Dumoutier. 2012. IL-22 is required for imiquimod-induced psoriasiform skin inflammation in mice. *Journal of immunology* 188:462-469.

van der Fits, L., S. Mourits, J.S. Voerman, M. Kant, L. Boon, J.D. Laman, F. Cornelissen, A.M. Mus, E. Florencia, E.P. Prens, and E. Lubberts. 2009. Imiquimod-induced psoriasis-like skin inflammation in mice is mediated via the IL-23/IL-17 axis. *Journal of immunology* 182:5836-5845.

Vandanmagsar, B., Y.H. Youm, A. Ravussin, J.E. Galgani, K. Stadler, R.L. Mynatt, E. Ravussin, J.M. Stephens, and V.D. Dixit. 2011. The NLRP3 inflammasome instigates obesity-induced inflammation and insulin resistance. *Nature medicine* 17:179-188.

Viguier, M., P. Guigue, C. Pages, A. Smahi, and H. Bachelez. 2010. Successful treatment of generalized pustular psoriasis with the interleukin-1-receptor antagonist Anakinra: lack of correlation with IL1RN mutations. *Annals of internal medicine* 153:66-67.

Waisman, A. 2012. To be 17 again--anti-interleukin-17 treatment for psoriasis. *The New England journal of medicine* 366:1251-1252.

Walter, A., M. Schafer, V. Cecconi, C. Matter, M. Urošević-Maiwald, B. Belloni, N. Schonewolf, R. Dummer, W. Bloch, S. Werner, H.D. Beer, A. Knuth, and M. van den Broek. 2013. Aldara activates TLR7-independent immune defence. *Nature communications* 4:1560.

Wang, Y., A.H. van Boxel-Dezaire, H. Cheon, J. Yang, and G.R. Stark. 2013. STAT3 activation in response to IL-6 is prolonged by the binding of IL-6 receptor to EGF receptor. *Proceedings of the National Academy of Sciences of the United States of America* 110:16975-16980.

Wen, H., D. Gris, Y. Lei, S. Jha, L. Zhang, M.T. Huang, W.J. Brickey, and J.P. Ting. 2011. Fatty acid-induced NLRP3-ASC inflammasome activation interferes with insulin signaling. *Nature immunology* 12:408-415.

Wendling, D., J.C. Balblanc, D. Briançon, A. Brousse, A. Lohse, P. DepreZ, P. Humbert, and F. Aubin. 2008. Onset or exacerbation of cutaneous psoriasis during TNF alpha antagonist therapy. *Joint Bone Spine* 75:315-318.

Wendling, D., H. Letho-Gyselinck, X. Guillot, and C. Prati. 2012. Psoriasis Onset with Tocilizumab Treatment for Rheumatoid Arthritis. *Journal of Rheumatology* 39:657-658.

Wenzel, P., M. Knorr, S. Kossmann, J. Stratmann, M. Hausding, S. Schuhmacher, S.H. Karbach, M. Schwenk, N. Yogev, E. Schulz, M. Oelze, S. Grabbe, H. Jonuleit, C. Becker, A. Daiber, A. Waisman, and T. Munzel. 2011. Lysozyme M-positive monocytes mediate angiotensin II-induced arterial hypertension and vascular dysfunction. *Circulation* 124:1370-1381.

Wiekowski, M.T., M.W. Leach, E.W. Evans, L. Sullivan, S.C. Chen, G. Vassileva, J.F. Bazan, D.M. Gorman, R.A. Kastelein, S. Narula, and S.A. Lira. 2001. Ubiquitous transgenic expression of the IL-23 subunit p19 induces multiorgan inflammation, runting, infertility, and premature death. *Journal of immunology* 166:7563-7570.

Wohn, C., J.L. Ober-Blobaum, S. Haak, S. Pantelyushin, C. Cheong, S.P. Zahner, S. Onderwater, M. Kant, H. Weighardt, B. Holzmann, B. Reizis, B. Becher, E.P. Prens, and B.E. Clausen. 2013. Langerin(neg) conventional dendritic cells produce IL-23 to drive psoriatic plaque formation in mice. *Proceedings of the National Academy of Sciences of the United States of America* 110:10723-10728.

Wolf, J., and L.K. Ferris. 2014. Anti-IL-36R antibodies, potentially useful for the treatment of psoriasis: a patent evaluation of WO2013074569. *Expert opinion on therapeutic patents* 24:477-479.

Wolf, J., S. Rose-John, and C. Garbers. 2014. Interleukin-6 and its receptors: a highly regulated and dynamic system. *Cytokine* 70:11-20.

Wolfer, A., T. Bakker, A. Wilson, M. Nicolas, V. Ioannidis, D.R. Littman, P.P. Lee, C.B. Wilson, W. Held, H.R. MacDonald, and F. Radtke. 2001. Inactivation of Notch 1 in immature thymocytes does not perturb CD4 or CD8T cell development. *Nature immunology* 2:235-241.

Wunderlich, F.T., P. Strohle, A.C. Konner, S. Gruber, S. Tovar, H.S. Bronneke, L. Juntti-Berggren, L.S. Li, N. van Rooijen, C. Libert, P.O. Berggren, and J.C. Bruning. 2010. Interleukin-6 signaling in liver-parenchymal cells suppresses hepatic inflammation and improves systemic insulin action. *Cell metabolism* 12:237-249.

Yammani, R.D., and K.M. Haas. 2013. Primate B-1 cells generate antigen-specific B cell responses to T cell-independent type 2 antigens. *Journal of immunology* 190:3100-3108.

Zalewska, A., E. Glowacka, J. Wyczolkowska, H. Tchorzewski, J. Narbutt, and A. Sysa-Jedrzejowska. 2006. Interleukin 6 and 8 levels in plasma and fibroblast cultures in psoriasis. *Mediators of inflammation* 81767

Zheng, Y., D.M. Danilenko, P. Valdez, I. Kasman, J. Eastham-Anderson, J. Wu, and W. Ouyang. 2007. Interleukin-22, a T(H)17 cytokine, mediates IL-23-induced dermal inflammation and acanthosis. *Nature* 445:648-651.

8 Acknowledgements

9 Versicherung

10 Lebenslauf

11 Publications

Publikationen

Klebow S.; Hahn M., Nikoalev A.; Wunderlich FT.; Hövelmeyer N.; Karbach SH; Waisman A. IL-6 signaling is not crucial for the development of IMQ-induced psoriasis. Plos One. 2016 Mar 21;11(3):e0151913

Hasenberg A.; Hasenberg M.; Männ L.; Neumann F.; Borkenstein L.; Stecher M.; Kraus A.; Engel D.R.1; Klingberg A.; Seddigh P.; Abdullah Z.; **Klebow S.**; Engelmann S.; Reinhold A.; Brandau S.; Seeling M.; Waisman A.; Schraven B.; Göthert J.R.; Nimmerjahn F.; Gunzer M. Catchup: a mouse model for imaging-based tracking and modulation of neutrophil granulocytes. Nat Methods. 2015 May;12(5):445-52

Struck T.H.; Wey-Fabrizius A.R.; Golombek A.; Hering L.; Weigert A.; Bleidorn C.; **Klebow S.**; Iakovenko N.; Hausdorf B.; Petersen M.; Kück P.; Herlyn H.; Hankeln T. Platyzoan paraphyly based on phylogenomic data supports a noncoelomate ancestry of spiralia. Mol Biol Evol. 2014 Jul;31(7):1833-49

Croxford A.L.; Karbach S.H.; Kurschus F.C.; Wörtge S.; Nikolaev A.; Yogev N.; **Klebow S.**; Schüler R.; Reissig S.; Piotrowski C.; Brylla E.; Bechmann I.; Scheller J.; Rose-John S.; Wunderlich F.T.; Münzel T.; von Stebut E.; Waisman A. IL-6 regulates neutrophil microabscess formation in IL-17A-driven psoriasiform lesions. J. Invest. Dermatol. 2014 Mar;134(3):728-35

Jolivel V.; Luessi F.; Masri J.; Kraus S.H.; Hubo M.; Poisa-Beiro L.; **Klebow S.**; Paterka M.; Yogev N.; Tumani H.; Furlan R.; Siffrin V.; Jonuleit H.; Zipp F.; Waisman A. Modulation of dendritic cell properties by laquinimod as a mechanism for modulating multiple sclerosis. Brain. 2013 Apr;136(Pt 4):1048-66

Vorträge

Klebow S., Karbach S., Waisman A.

Overview of inflammatory cytokines in IMQ-induced psoriasis
Retreat 2015, June 17th-20th, 2015, Löffingen, Germany

Klebow S., Karbach S., Waisman A.

Overview of inflammatory cytokines in IMQ-induced psoriasis
Retreat 2014, June 11th-14th, 2014, Löffingen, Germany

Klebow S., Karbach S., Waisman A.

The role of IL-6 and IL-17A in IMQ induced psoriasis-like skin disease
43. Annual Meeting of the German Society for Immunology September 11th-14th,
2013, Mainz, Germany

Klebow S., Karbach S., Waisman A.

The role of Th-17 related cytokines in IMQ induced psoriasis-like skin disease
Retreat 2013, July 10th-13th, 2013, Menzenschwand, Germany

Klebow S., Karbach S., Waisman A.

The role of CXCR2-ligands for neutrophil mobilization from the bone marrow to
peripheral sites
Immunobone Meeting, June 23rd-25th, 2013, Garmisch-Partenkirchen, Germany

Klebow S., Jolivel V., Waisman A.

The effect of Laquinimod on dendritic cells
Retreat 2012, May 16th-19th, 2012, Chateau du Liebfrauenberg, Frankreich

Poster

Klebow S., Karbach S., Mufazalov I., Waisman A.

The role of IL-1 signaling in IMQ-induced psoriasis-like skin disease

2015 Keystone Symposia Conference: Mechanisms of Pro-Inflammatory Diseases

April

19th-24th, 2015, Olympic Valley, California USA

Klebow S., Karbach S., Waisman A.

The role of Th-17 related cytokines in IMQ-induced psoriasis- like skin disease

43. Annual Meeting of the German Society for Immunology September 11th-14th,

2013, Mainz, Germany

Klebow S., Karbach S., Waisman A.

The role of Th-17 related cytokines in IMQ-induced psoriasis- like skin disease

8th ENII Immunology Summer School May 27th – June 3rd, 2013, Sardinia, Italy